SHATIS'17
4th International Conference on
Structural Health Assessment of Timber Structures
20-22 September 2017 Istanbul, Turkey

EFFECT OF QUETI-INCLINATION ON MECHANICAL PROPERTIES OF TYPICAL TIBETAN TIMBER BEAM-COLUMN JOINT

Qin Shujie and Yang Na

School of Civil Engineering, Beijing Jiaotong University, Beijing 100044, China

Keywords: Queti-inclination, Beam-column joint, Tibetan timber building, Mechanical properties

Abstract

Tibetan heritage buildings have a high historical and cultural value. Many of these buildings have experienced different degree of damage after hundreds of years. "Queti" is an important connecting part of Tibetan timber beam-column joint, which plays a vital role for structure to resist different kinds of load. The Queti-inclination, a relative out-of-plane rigid body deformation of Queti, is a typical type of damage influencing the stability and safety of traditional Tibetan timber structures.

Four finite element models of Tibetan beam-column joint are examined including one normal joint and three damaged joints with Queti-inclination angle of 0, 3, 6 and 9 degree, respectively. The stress state of different components, load-displacement relationship and failure modes of joints under the vertical load are analyzed.

The distribution of compressive stress of components of normal joint is even along the width direction, while it becomes uneven with increasing angle of Queti-inclination with higher stress at the front face and lower stress at the back face. The compressive stiffness of the joint decreases with the increase of angle of Queti-inclination. The failure of joint should be caused by the yielding of timber components when the Queti-inclination angle is small, and it should fail with lower ultimate load due to the loss of stability caused by eccentric moment when the Queti-inclination angle is increasing and large enough. This study provides a reference for the safety evaluation of Tibetan heritage structures.

1 INTRODUCTION

Traditional Tibetan timber buildings are mainly found in the Tibetan area and Mongolian area in China. Some excellent buildings with high historical, religious and artistic values are world-renowned national treasures, such as the Potala Palace, Norbulingka Summer Palace and Jokhang Temple [1]. However, these heritage buildings have experienced different degree of damage over the past hundreds of years [2], especially with the increasing growth of tourist industry in recent years [3].

A typical Tibetan timber beam-column joint is composed of two beams, a Gongmu, a Dianmu and a column from top to down, as illustrated in Figure 1. The beams are connected by tenon-mortise form, and other components are overlaid vertically and fixed by dowels. The combination of Gongmu and Dianmu is called "Queti" in traditional naming system, and it is special connecting part between beam and column in Tibetan timber structure. The Queti-inclination, a relative out-of-plane rigid body deformation of Queti (Figure 2), is a typical type of damage influencing the structural stability and safety and often encountered in Tibetan historical timber buildings. The beam-column joints have been playing a vital role for the ancient timber structures to resist severe winds, earthquake and even human-induced load for hundreds of years. To evaluate the safety of these heritage buildings, it is, therefore, imperative to investigate the mechanical properties of Tibetan beam-column joints.

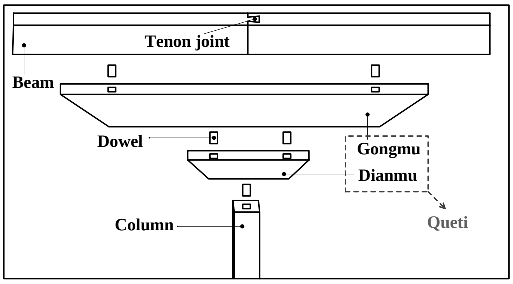

Figure 1: Construction of typical Tibetan timber beam-column joint

Figure 2: Queti-inclination of Tibetan joint

The research on Tibetan buildings, in the point of structural analysis, is relatively limited due to the remoteness of Tibet. Li et al. [2] summarized the structural damage types of ancient Tibetan buildings based on fieldwork and the damage reasons were analyzed. The physical material properties of the old and new Tibetan Populus cathayana were obtained by tests and the time-dependent law of strength degradation was discussed [4]. An experimental study on seismic performance of Tibetan timber beam-column joint was conducted by Zhu [5] with focus on the stiffness, moment-resisting capacity, energy-dissipation and failure modes of the joints under lateral load. Based on the refined FEM, three typical deformation characteristics of Tibetan joint including the excessive deflection of beam, torsion of components and Queti-inclination were analyzed, and a method was proposed to determine the location of deformation damage [6]. Lyu et al. [7] proposed a temperature-based response sensitivity method to identify the connection stiffness of Tibetan beam-column joint with Queti modeled as two rotation springs and one compressive spring. Existing research achievements can provide valuable reference for protection of ancient Tibetan timber structures. However, research has not yet been undertaken to evaluate the damage effect of Queti-inclination on the mechanical properties of Tibetan beam-column joint.

In this paper, four finite element models of typical Tibetan timber beam-column joint are examined including one normal joint and three damaged joints with Queti-inclination angle of

0, 3, 6 and 9 degree, respectively. The stress state of components, load-displacement relationship, failure mode of the joints, and the damage effect of Queti-inclination are studied. This paper can provide a reference for the safety evaluation of Tibetan heritage buildings.

2 TYPICAL TIBETAN TIMBER BEAM-COLUMN JOINT

2.1 Analytical unit

Actually, an ancient Tibetan building is usually an architectural complex. Each room in the building is a separate structural unit with rectangular or square floor. Full height walls are built from the first floor to top with the plane layout of the shape of “#”, and the timber frame system is within the enclosed space. A sketch on the layout of Tibetan timber frame is shown in Figure 3. The timber frame is composed of several beams and columns laid in one direction. There may be several framed bents in a large room. The upper and lower columns are aligned vertically. The analytical unit of beam-column joint with half of beam length is determined according to the symmetry of timber framework, as shown in Figure 4.

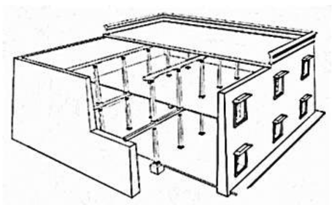

Figure 3: Layout of Tibetan timber frame

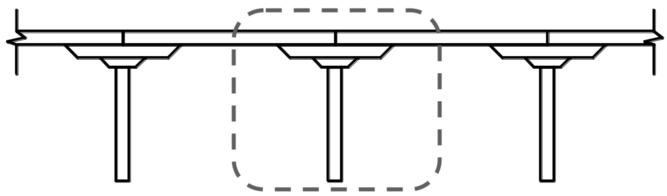

Figure 4: Analytical unit of beam-column joint

2.2 Simplification of load condition

The vertical loads carried by the beam-column joint mainly include two parts (Figure 5a): the load from upper floor transferred by beams and the load from upper column foot on the center of the joint. The simplification of load condition is shown in Figure 5b.

(1) The Tibetan floor system is composed of logs, tree trunks, pebbles, clay and Agatu (a kind of local soil mixture commonly used in Tibet for floor construction). The floor is closely placed on timber beams so that it can be regarded as the uniform load.

(2) The load from upper column foot is on the center of beam-column joint and it is regarded as a concentrated load, which accumulates from the top storey to the ground storey with respect to the configuration of Tibetan timber structures.

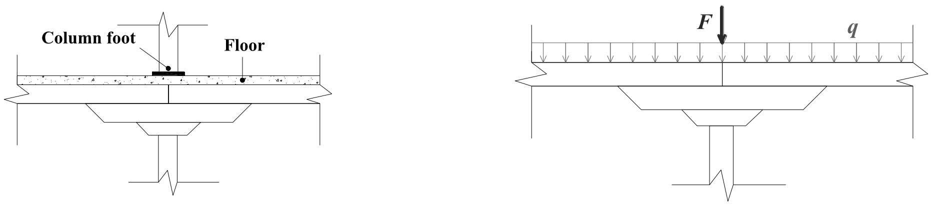

(a) Load condition (b) Simplification of load

Figure 5: Load condition of joint and its simplification

2.3 Boundary constraints

The force diagram of a whole beam is shown in Figure 6. The upper surface of beam is subjected to the uniform load q from the floor, and the lower surface bears the supporting force q' from the Gongmu. The beams are connected each other by the form of mortise-tenon so that the beam-ends can resist a certain moment M. It can be seen, from the diagrams of shear force and bending moment, the shear force at the mid-span of a whole beam, i.e. the two ends of beams of the analytical unit (Figure 4), equals to zero while the bending moment is the largest.

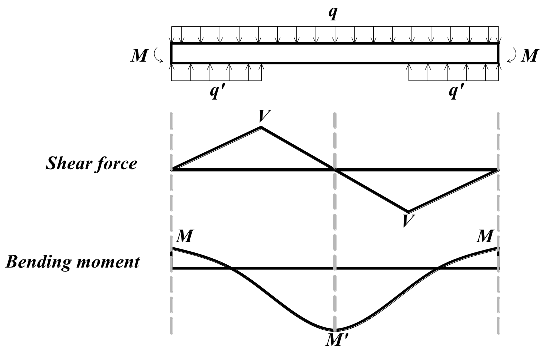

Figure 6: Force diagram of a whole beam

The column in Tibetan timber building is usually placed directly on top of a stone base without any physical connection. The column footing joint can bear the compressive force only but has no tensile capacity.

Based on the above analysis, the simplification of load condition and boundary constraints of the analytical unit of beam-column joint is shown in Figure 7. The top surface of beams is subjected to a uniform load and a concentrated load. The two ends of beams can bear moment but have no capacity to resist the shear force.

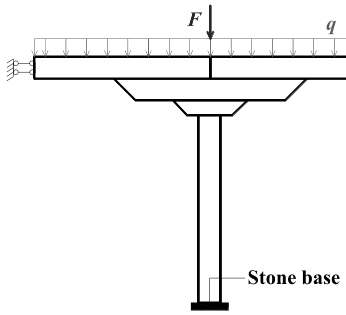

Figure 7: Simplification of load condition and boundary constraints

3 FINITE ELEMENT MODEL OF JOINT

For the Tibetan architectures, there is no a specified dimension module to fabricate the timber components, of which the height, length and cross-sectional dimensions are often changed with the space size of rooms [1]. The dimensions of different components of the joint in this paper are determined with reference to some related literatures [1, 5, 6], as shown in Table 1.

Table 1: Dimensions of components of beam-column joint (mm)

Components	Bottom surface (Length×Width)	Top surface (Length×Width)	Height
Beam (half of beam length)	1100×190	1100×190	190
Gongmu	1300×140	1680×140	190
Dianmu	300×165	500×165	100
Column	190×190	190×190	1630
Dowel	40×40	40×40	100

The angle of Queti-inclination of beam-column joint in ancient Tibetan timber buildings commonly ranges from 0 to 5 degree based on an on-site survey in the city of Lhasa by authors. Few severe damaged joints also can be seen (Figure 2), which influences the stability and safety of structures. In order to evaluate the damage effect of Queti-inclination on the mechanical properties of joints under vertical load, four three-dimensional finite element models including one normal joint and three damaged joints (Figure 8b), marked as BCJM*i* (*i*=1, 2, 3 and 4) with Queti-inclination angle θ equal to 0, 3, 6 and 9 degree respectively (Table 2), are established by ABAQUS software, as shown in Figure 8.

Table 2: Queti-inclination angles of different FE models

Test model	BCJM1	BCJM 2	BCJM 3	BCJM 4
Angle of Queti-inclination (degree)	0	3	6	9

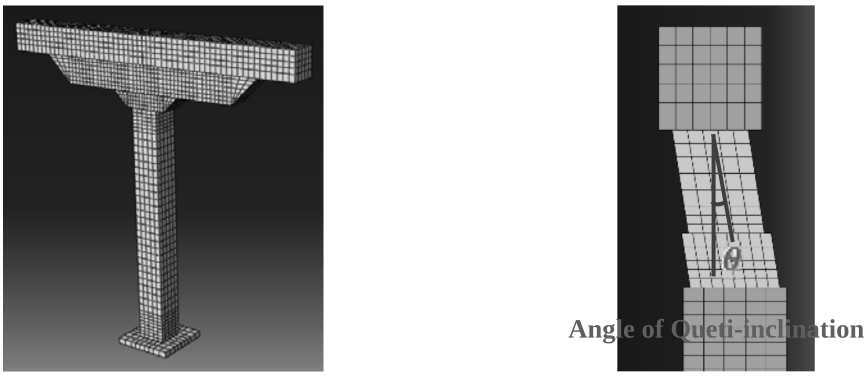

(a) Beam-column joint (b) Queti-inclination

Figure 8: FE model of joint

The joint is modeled with eight-node brick elements with reduced integration (C3D8R). The timber is defined as orthotropic material with material parameters as shown in Table 3. It is noted that, since the plastic characteristic of orthotropic material cannot be simulated by ABAQUS now, the timber components are assumed to be linearly elastic during the loading process.

Table 3: Material parameters

E_L/MPa	E_R/MPa	E_T/MPa	G_{LR}/MPa	G_{LT}/MPa	G_{RT}/MPa	μ_{LR}	μ_{LT}	μ_{RT}
14345	593	702	1075	878	89	0.380	0.532	0.643

Note: *E*, *G* and μ denote the modulus of elasticity, shear modulus and Poisson's ratios, respectively; *L*, *R* and *T* denote the grain, radial and chordwise directions, respectively.

The bottom of stone base is fixed and the column is directly placed on the top of stone base. The friction coefficient is adopted as 0.35 [6]. The beam ends at two ends of the joint are restricted from longitudinal displacement and torsional deformation while the vertical displacement is free.

Loading program is divided into two parts: the uniform load q = 15.91 kN/m (the estimated floor load) is first applied on the top surface of beams, and then the concentrated load F is gradually applied at the center of joint until the F reaches 200 kN or the joint fails.

4 RESULTS AND ANALYSIS

4.1 Stress state of components

Three longitudinal paths on the Gongmu, Dianmu and column are defined, respectively, as shown in Figure 9. The Path-1 and Path-3 are on the front face and back face of each component, respectively, while the Path-2 is in the middle of Path-1 and Path-3.

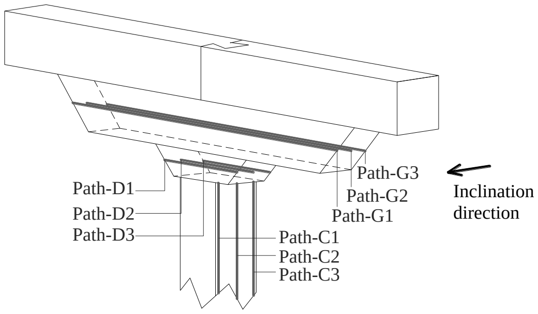

Figure 9: Paths setting

(1) Gongmu

Figure 10 shows the variation of distribution of compressive stress perpendicular to grain of Gongmu with increasing angle of Queti-inclination under the uniform load (q = 15.91 kN/m). It can be seen that: 1) The distribution of compressive stress is uneven along the longitudinal direction with higher values at the middle and lower values at the two ends; 2) The compressive stress of normal Gongmu is even along the width direction, while the stress of Gongmu with Queti-inclination is uneven with high stress at the front face (Path-G1) and lower stress at the back face (Path-G3). 3) The stress at the front face increases and the stress at the back face decreases with the increase of angle of Queti-inclination. The stress at the back face is almost zero when the Queti-inclination angle equals to 9 degree. The maximum stress of Gongmu with Queti-inclination angle of 9 degree is 1.27 MPa, about two times of that of normal Gongmu.

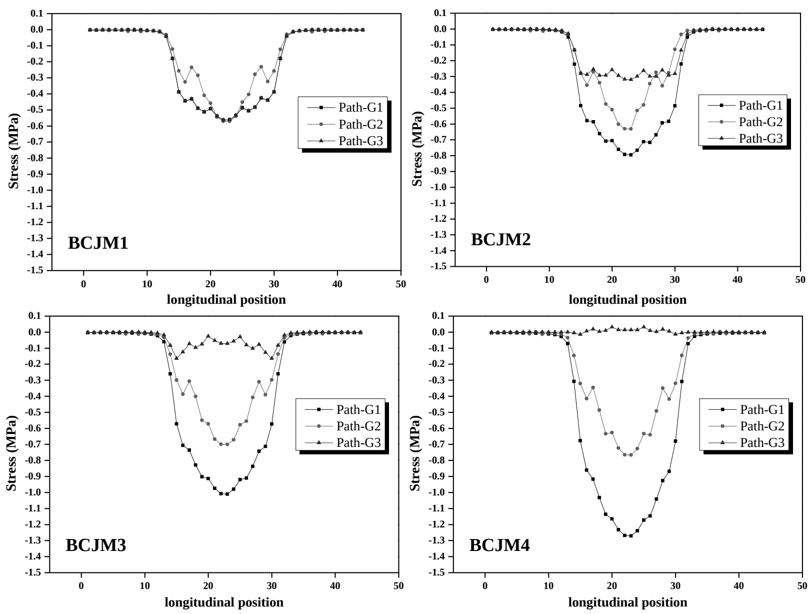

Figure 10: Distribution of compressive stress perpendicular to grain of Gongmu

(2) Dianmu

The variation of stress state of Dianmu along the longitudinal and width direction under the uniform load (q = 15.91 kN/m), as shown in Figure 11, is similar to that of Gongmu. The maximum compressive stress along the longitudinal direction is not at the middle of Dianmu but rather at the two sides close to the middle, i.e. the positions of dowels. This is because the size of Dianmu is relatively small and the stress concentration due to the dowels has a distinct influence on its stress state. The maximum stress of Dianmu with Queti-inclination angle of 9 degree is 3.21 MPa, more than two times of that of normal Dianmu.

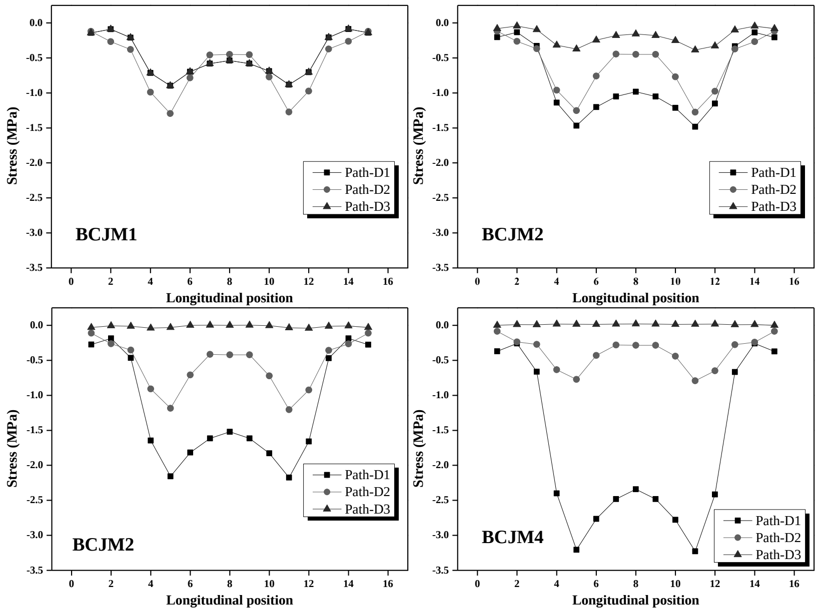

Figure 11: Distribution of compressive stress perpendicular to grain of Dianmu

(3) Column

Figure 12 shows the variation of distribution of compressive stress parallel to grain of column with increasing angle of Queti-inclination under the uniform load (q = 15.91 kN/m). It can be seen that: 1) The compressive stress at the head of column is higher than that of the others due to the stress concentration at the contact surface between Dianmu and column. 2) The distribution of compressive stress of normal column is even along the width direction, while it becomes uneven with the increase of angle of Queti-inclination with higher stress at the front face and lower stress at the back face. 3) The maximum stress of column with Queti-inclination angle of 9 degree is 3.85 MPa, higher than that of Dianmu. However, since the compressive strength parallel to grain of timber is much larger than that perpendicular to grain, the column should be in elastic state and will not yield generally before the Dianmu yields.

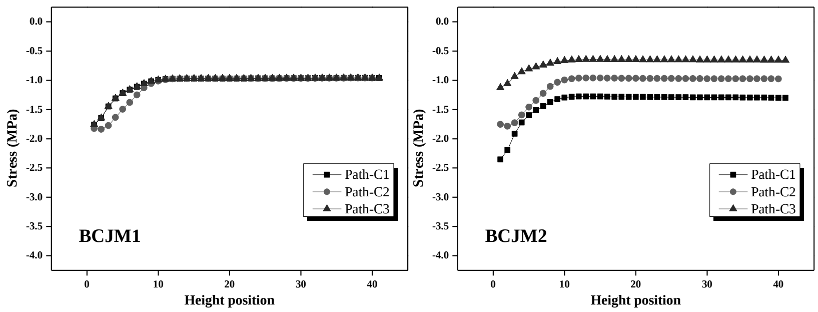

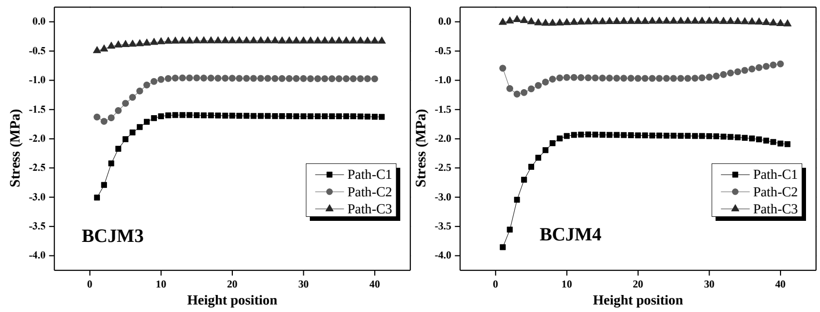

Figure 12: Distribution of compressive stress parallel to grain of column

4.2 Load-displacement relationship

The load-displacement relationship of beam-column joints with different angle of Queti-inclination under the combination of uniform load and concentrated load is shown in Figure 13. The timber components are assumed to be linearly elastic during the load process as mentioned in Section 2.

The simulated results show that, both the normal joint and the joint with Queti-inclination angle of 3 degree do not fails during the loading process and their displacements keep increasing with load. However, it can be conceivable that, if the plastic characteristic of material is considered in the finite element analysis, the yielding of timber perpendicular to grain will occur when the vertical load is large enough, and then the joint fails.

For the joints with Queti-inclination angle of 6 and 9 degree, the simulated ultimate loads decrease. Actually, the column is transformed from the compression state (for normal joint) to the compression-flexure state (for joints with Queti-inclination) under the vertical load. The eccentric moment on the head of column increases with the increase of angle of Queti-inclination. The column will lose its stability and collapse when the eccentric moment reaches a certain value, resulting in the failure of joints under the vertical load. Namely, the larger angle of Queti-inclination leads to the poorer stability and lower ultimate load of joints.

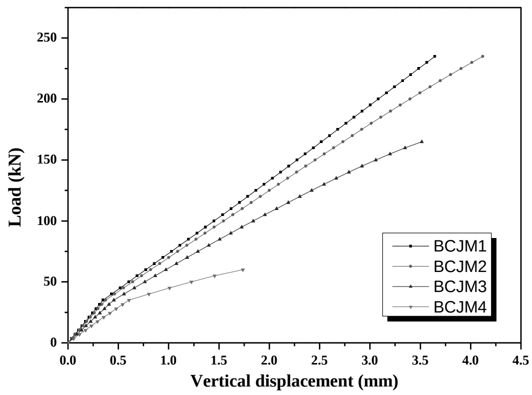

Figure 13: Load-displacement curves

For the joints with different angle of Queti-inclination, the variation of compressive stiffness K_1 under uniform load and compressive stiffness K_2 under concentrated load are shown in Table 4. It can also be clearly seen that, both K_1 and K_2 decrease with the increase of angle of Queti-inclination. The compressive stiffness K_1 and K_2 of joint with Queti-inclination angle of 9 degree are 58.9 kN/mm and 38.0 kN/mm, reduced by 41.4% and 35.5%, respectively, of those of normal joint.

Table 4: Compressive stiffness of joints with different Queti-inclination angle (kN/mm)

Angle of Queti-inclination (degree)	0	3	6	9
K_1	100.5	93.8	77.7	58.9
K_2	58.9	56.1	48.7	38.0

5 CONCLUSIONS

(1) When under vertical load, both of the distribution of compressive stress of Gongmu and Dianmu along the longitudinal direction exhibit higher stress at the middle and lower stress at the two ends. The stress at the head of column is higher than that of the others.

(2) The distribution of compressive stress of components of normal joint is even along the width direction, while it becomes uneven with increasing angle of Queti-inclination with higher stress at the front face and lower stress at the back face.

(3) The failure of joint should be caused by the yielding of timber components perpendicular to grain when the angle of Queti-inclination is small. The joint should fail with lower ultimate load due to the loss of stability caused by the eccentric moment when the angle of Queti-inclination is increasing and large enough.

(4) The compressive stiffness K_1 under uniform load and compressive stiffness K_2 under concentrated load decrease with the increase of angle of Queti-inclination.

ACKNOWLEDGEMENTS

This work described in this paper was financially supported by the Beijing Natural Science Foundation of China (Key Program) (8151003), National Natural Science Foundation of China for Excellent Young Scholars (51422801), National Natural Science Foundation of China (Key Program) (51338001) and National Key Technology R&D Program (2015BAK01B02).

REFERENCES

[1] Ngawang, R. 2007. “Tibetan architecture overview”. Sichuan Fine Arts Publishing House, Chengdu.

[2] Li, P., Yang, N., and Wang, Y. 2013. “Research on structural present state and damage reasons of ancient Tibetan buildings”. *Appl. Mech. Mater.,* 351-352, Pp:1652-1656.

[3] Lyu, M. N., Yang, Q.S., Yang, N., and Law, S.S. 2015. “Tourist number prediction of historic buildings by Singular Spectrum Analysis”. *J. Appl. Statistics,* 43(5), Pp:1-20.

[4] Yang, N., Li, P., Law, S. S., and Yang, Q. S. 2012. “Experimental research on mechanical properties of timber in ancient Tibetan building”. *J. Mater. Civ. Eng.,* 24, Pp:635-643.

[5] Zhu, L. 2016. “Study on the seismic performance of ancient Tibetan timber structure”. M.S. thesis, Beijing Jiaotong Univ., Beijing, China.

[6] Zhang, Y. and Yang, N. 2013. “Deformation characteristics and relationships of timber frame in typical Tibetan architecture”. *J. Beijing Jiaotong Univ.,* 37(1), Pp:145-151.

[7] Lyu, M. N., Zhu, X. Q., and Yang, Q. S. 2017. “Connection stiffness identification of historic timber buildings using Temperature-based sensitivity analysis”. *Eng. Struct.,* 131, Pp:180-191.

SHATIS'17
4th International Conference on
Structural Health Assessment of Timber Structures
20-22 September 2017 Istanbul, Turkey

SEISMIC BEHAVIOR OF A TWO-STORY HOUSE FROM THE HISTORICAL CENTER OF LIMA – A MIXED SYSTEM ADOBE MASONRY AND QUINCHA SYSTEM

Daniel E. Torrealva[1], Arturo E. Santa-Maria[1],

[1] Catholic University of Peru

Keywords: Traditional Peruvian House, Dynamic Analysis, Stiffness Comparison, Experimental Test Comparison

Abstract

The Historical Center of Lima, a World Heritage city owes its survival to earthquakes, in great part to a timber construction system called "quincha". This lightweight construction system was used for the construction of second and third stories in an attempt to cope with the frequent destructive earthquakes that devastated the city. The "quincha" system is similar to those found in other parts of the world and consists of timber posts, a bottom and top timber girders and a combination of woven cane and mud as infill. It is widely accepted that this system is earthquake resistant in spite of being old and poorly maintained.

A two degree of freedom system was modeled to represent the structural system and a sensitivity analysis was performed using a modal spectral analysis and time history analysis. The variable was the relative stiffness of the first story versus the second story. The results of the sensitivity analysis showed that when the ratio of the lateral stiffness of the first story to the lateral stiffness of the second story is between five and eight, there is a reduction of 15% in the base shear and for higher ratios the reduction increases asymptotically to 25%. These results were then compared with the data from shaking table tests on a two story full scale specimen adobe-quincha.

When having this type of structure stiffer first level and soft second level, it is advisable not to stiffen the second level since it causes more base shear and more damage in the adobe masonry of the first story.

1 INTRODUCTION

Peru has hosted cultures with earth-building traditions although the fact that the country is located in one of the seismic zones of South America, the prevailing technologies have been, adobe masonry and quincha [1] and many of these constructions have endured different telluric movements by more than 100 years.

The adobe presents great static stability, excellent thermal and acoustic properties, besides being economical [2]; however, it presents a poorly dynamic behavior, because it is a very fragile material and prone to collapse. An important step in the development of earthquake resistant structures was the replacement of heavy adobe walls in the second floor by a lighter and more flexible material, a combination of timber, cane and mud called “quincha”. As the acting load of an earthquake is proportional to the weight of the structure, the use of quincha allowed to build more resistant buildings that have survived up to now [3], [4].

Research on structures with adobe and quincha has been poorly developed, and this system remains a traditional knowledge obtained only from experience without an adequate investigation. Most of the buildings in the historical center of Lima are composed of this structural system; therefore, it is extremely important to carry out adequate research that allows an efficient structural analysis against seismic loads.

2 TRADITIONAL CONSTRUCTION SYSTEM OF ADOBE AND QUINCHA

The structures with adobe masonry on both floors have shown poor behavior during earthquakes due to the weight of their walls and the poor mechanical behavior of the material. [5].

The alternative for these two-story adobe constructions was the use of a light second story as “quincha”. This constructive system uses, mainly, timber and reed, and forms a framework with a finish of clay or plaster (Figure 1). The construction system of quincha consists of a timber frame with posts that are secured with horizontal elements. Its wooden framework carries a cane fabric and mud as infill and forms a vertical surface that supports the wooden ceilings [6]. Quincha is very useful as an earthquake resistant material; because the lateral displacement capacities that can absorb the vibrations raised in the earthquake and prevent these vibrations spread to the entire structure.

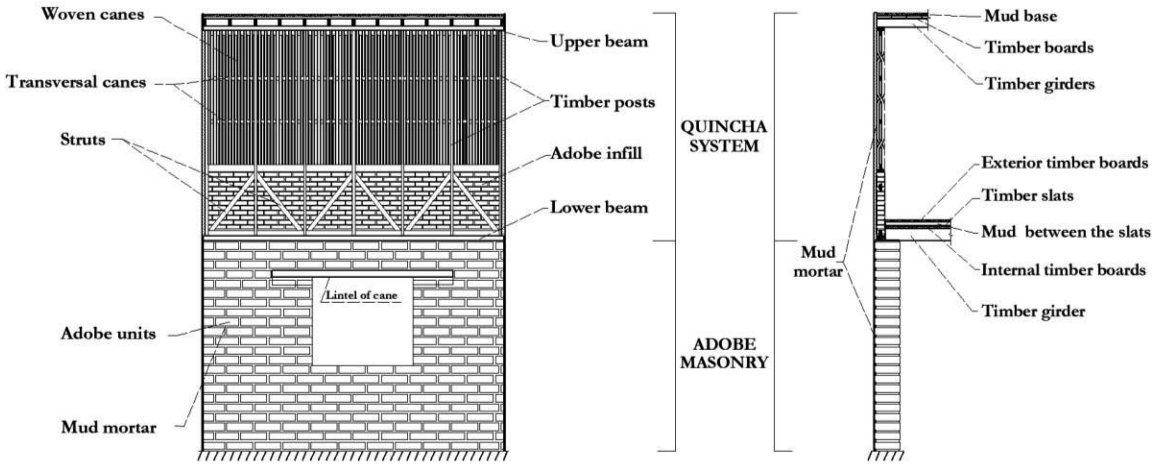

Figure 1: Typical mixed system of Adobe masonry and Quincha system

In the union of the walls of adobe of the first story and the quincha of the second story, a transition zone is generated. The bottom of the quincha panels is filled with pieces of adobe or bricks, which generate a strip of structural nexus with mixed characteristics, without being as heavy or rigid as the walls of adobe or as light and flexible as quincha. This results in a sequence that runs from the first story to the second, from highest to lowest density and stiffness and from lowest to highest lightness and elasticity [7].

3 TWO DEGREE MODEL OF TRADITIONAL SYSTEM

A simple model (Figure 2) was developed to simplify the complexity of the structure composed by adobe and quincha, since both are materials with very complex and inelastic behaviour. However, according to the data collected, the quincha can bear heavy loads, maintaining a curve with a tendency towards linearity [8, 9]; therefore, it will be considered as a homogeneous, elastic and linear element. It will be assumed that the adobe is a very fragile and rigid material that will have a linear behaviour up to a maximum resistance; if this stress is exceeded collapse will be assumed [10]. It will present a linear behaviour with a maximum limit stress.

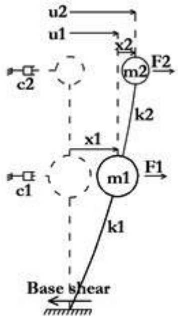

Figure 2: two degree model as inverted pendulums

where: *mi* = mass of story "i", *ci* = damper of story "i", *ki* = stiffness of story "i", *ui* = displacement of story "i", *xi* = relative displacement of story "i"

For this type of point mass structures, it is necessary to calculate the equivalent oscillator characteristics of each mode as the generalized mass "M*" and the participant mass "L*". The division L*/M* is called "participation factor" and it represents the effect of the mass distribution on the basal acceleration of the equivalent oscillator.

$$L_i^* = \{h\}^t[M]\,\{\phi_i\} \tag{1}$$
$$M_i^* = \{\phi_i\}^t[M]\,\{\phi_i\} \tag{2}$$

where: *Li** = participant mass of mode"i", *Mi** = generalized mass of mode"i", *M* = mass matrix, *h* = vector displacement transformation, ϕi = form of mode"i"

The dynamic analysis were carried out with the seismic signal of the earthquake of Lima in 1974. This signal has the direction north to the south and it is scaled to 0.4g (Figure 3). Two types of analysis were performed from this accelerogram and the results of both were compared.

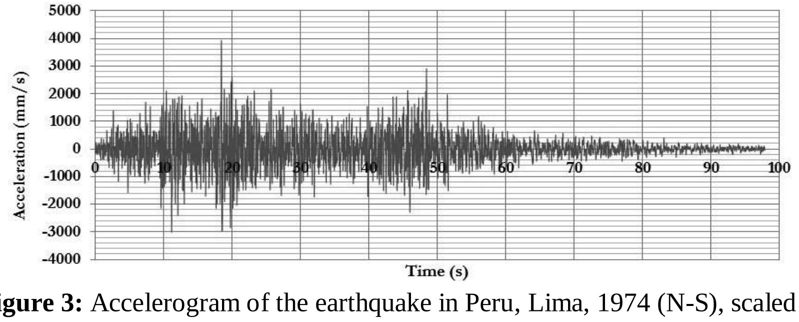

Figure 3: Accelerogram of the earthquake in Peru, Lima, 1974 (N-S), scaled to 0.4g

3.1 Modal spectral analysis

From the mathematical point of view the movement of a complex vibrator can be represented by superposition of the movements of the vibrators that represent the different natural modes of vibration. Therefore, it is necessary to evaluate the response for each mode and then overlay the influence of the different modes (Figure 4). The modal spectral method is applicable only to linear structures. This first limitation is extremely important in the practical analysis of earthquake resistant structures and although it is known it is little taken into account.

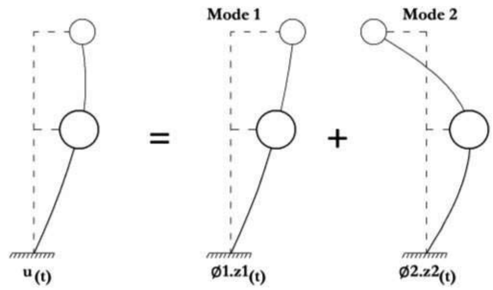

Figure 4: Displacement expressed as a linear combination in time of the modal forms

The responses of each mode are maximum values produced at different times and can't be added directly. For this reason, there are criteria to combine these modal values as the equation provided by the peruvian norm [11]. The equation (3) is used for the following responses.

$$r = 0.25\sum_{i=1}^{N}|r_i| + 0.75\sqrt{\sum_{i=1}^{N}(r_i)^2} \tag{3}$$

where: r = Maximum modal response, r_i = Any parameter of the mode "i" spectral response

For this analysis, the spectrum had to be obtained from the accelerogram of the earthquake in 1974 (Figure3). A 5% damping was used because it is used in the peruvian norm and this value does not affect much the calculations. Finally, this curve was smoothed for better results (Figure 5).

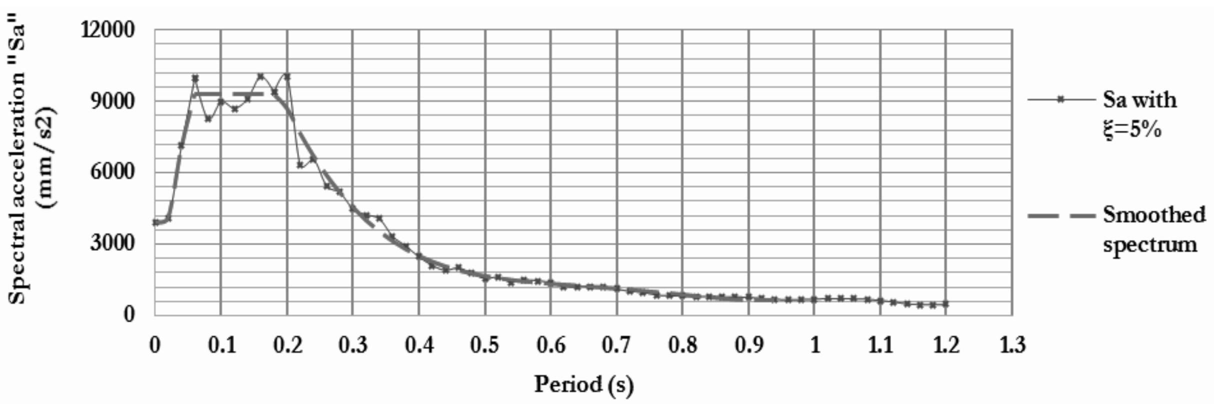

Figure 5: Spectral acceleration of the earthquake in Peru, Lima, 1974 (N-S), scaled to 0.4g

An important parameter in the modal response is the maximum base shear that will be used to compare the seismic responses.

$$Vbase = \left(\frac{L^{*2}}{M^{*}}\right).Sa \tag{4}$$

where: $Vbase$ = base shear, L^{*2}/M^{*} = effective mass, Sa = Spectral acceleration

3.2 Time history analysis

The response to each step is then calculated from the initial conditions (displacement and velocity) at the beginning of the stage and the load history during the step. Thus, the answer for each step is an independent analysis, and there is no need to combine response contributions in the step. One of these step-by-step numerical methods is the Newmark method that was performed for each mode with a linear variation of accelerations.

$$\dot{u}_{i+1} = \dot{u}_i + [(1-\gamma)\,\Delta t]\,\ddot{u}_i + (\gamma\,\Delta t)\ddot{u}_{i+1} \tag{5}$$

$$u_{i+1} = u_i + (\Delta t)\dot{u}_i + \left[(0.5-\beta)(\Delta t)^2\right]\ddot{u}_i + \left[\beta(\Delta t)^2\right]\ddot{u}_{i+1} \tag{6}$$

where: ui= displacement of story "i", $\dot{u}_1$= velocity of story "i", $\ddot{u}_1$=acceleration of story "i" Δt = time interval, $\gamma = ½$, $\beta = {}^1/_6$ (for linear variation of accelerations)

As in the spectral analysis, the contribution of both modes must be considered to obtain the answer; however, the response of each of these modes is a function of time and, in this case, it can be added directly without using a combination equation.

$$\begin{Bmatrix} u_2 \\ u_1 \end{Bmatrix} = \frac{L_1^*}{M_1^*} \,.\, z_1 \,.\, \{\phi_1\} + \frac{L_2^*}{M_2^*} \,.\, z_2 \,.\, \{\phi_2\} \tag{7}$$

where: ui =displacement of story "i", Li^*/Mi^* = participation factor of mode "i", zi = response on the time with punctual mass of mode "i", ϕi = form of mode"i"

4 SENSITIVITY ANALYSIS OF RELATIVE STIFFNESS

Base shear, inertial internal loads and relative displacements were calculated with different stiffness ratios "K1/K2". The stiffness of the first adobe story was maintained constant and the second one was modified to obtain results with different ratios K1/K2, thus it was expected to observe the effect of modifying only this ratio on the dynamic behavior.

The first effect observed was the variation of the periods of each mode. As expected, period values increase because increasing this ratio decreases the stiffness of the second story and generates an increase of the period of the system as a whole (Figure 6).

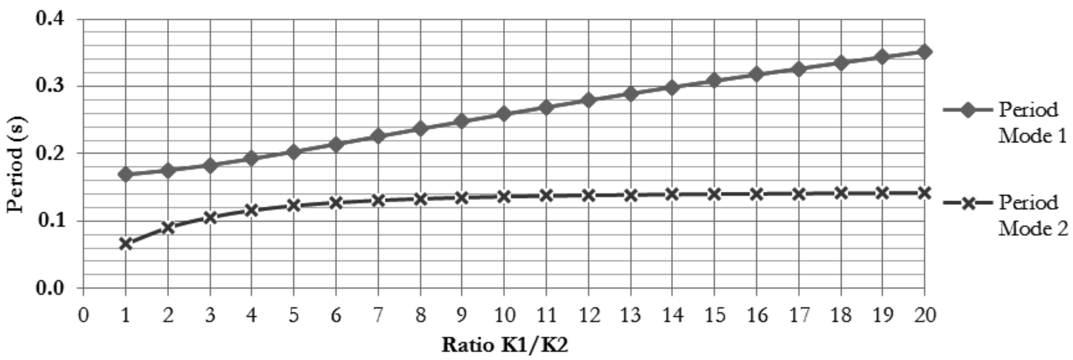

Figure 6: Effective mass percentage of Mode 1 and Mode 2 for each ratio K1/K2

However, it is appreciated that the periods of mode1 constantly increase and approximately linearly, while the mode2 periods vary asymptotically until they reach a peak of about 0.14 s.

4.1 Effective mass percentage

The effective mass percentage represents the importance of each mode in the dynamic response. Mode 1 is usually the most important, however, this assertion is only true when the stiffness K1 and K2 are similar as shown in Figure 7.

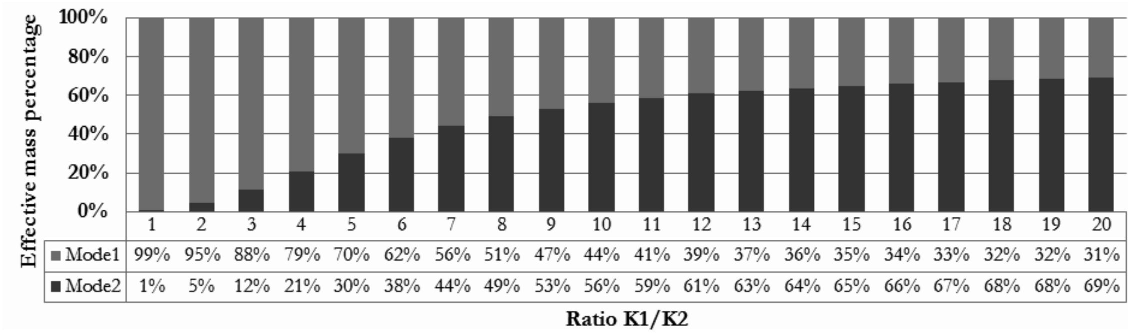

Figure 7: Effective mass percentage of Mode 1 and Mode 2 for each ratio K1/K2

As the ratio K1/K2 increases, the effective mass percentage of mode 2 increases until it reaches a value of 70%, which is notably greater than the percentages with low ratios. The mixed system of adobe masonry and quincha system presents very different stiffness and a high ratio of K1/K2, that is why the mode 2 will be very important in these systems and their behavior will be out of phase.

4.2 Base shear

The base shear was computed using two different types of analysis, the modal spectral and the time history. In Figure 8 the influence of the stiffness ratio K1/K2 in the value of shear base is shown for both analyses. It can be observed that for the modal spectral analysis there is a smooth variation curve with higher values of base shear for low ratios of K1/K2 and a reduction of the base shear as the ratio of stiffness increases. For the time history analysis there is a random variation of the shear base with respect to the stiffness ratio, this can be attributed to the idealized spectrum used in the first analysis (Figure 5). In the range of K1/K2 between 7 and 10 both curves have similar low base shear values.

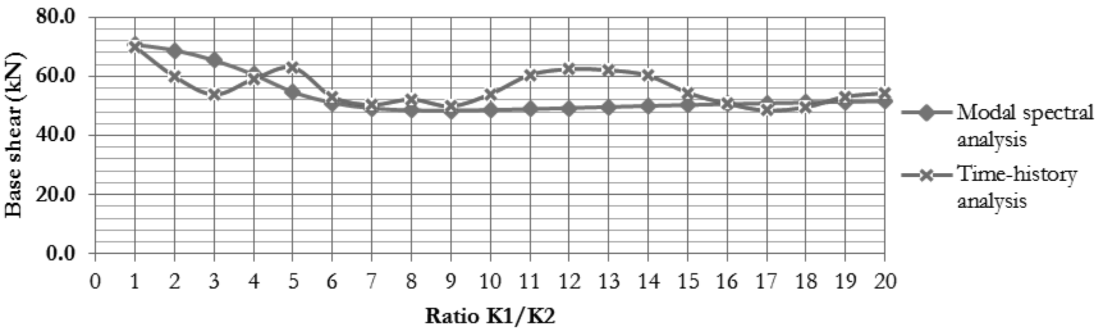

Figure 8: Base shear VS ratio K1/K2, by the modal spectral and time-history analysis

4.3 Horizontal relative displacements

The maximum horizontal relative displacement for each story was computed for the modal analysis and the time history analysis. Figure 9 shows the values of the relative displacement as a function of the stiffness ratio K1/K2. The values computed for the first story are almost the same using both types of analysis whereas for the second story there is a divergence in the computed horizontal displacement for stiffness ratios greater than 10.

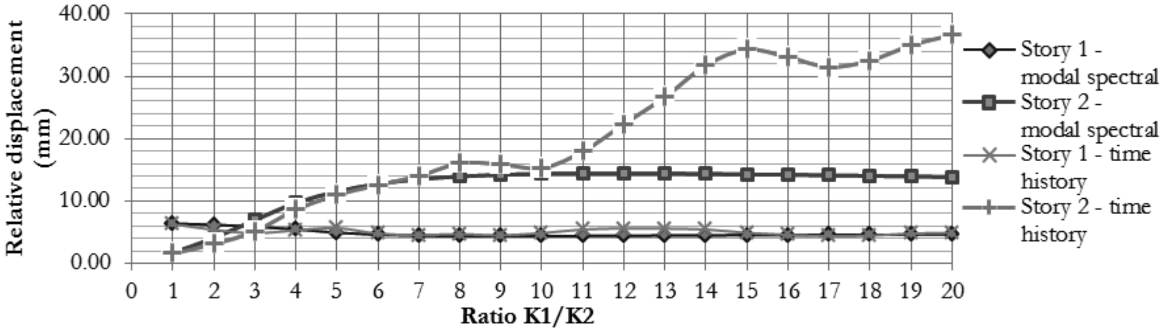

Figure 9: Stories' relative displacement VS ratio K1/K2, by the modal spectral analysis

5 SHAKING TABLE TEST DESCRIPTION

In 2006, the Catholic University of Peru (PUCP) and the National Training Service for the Construction Industry (SENCICO) carried out the "Adobe-Quincha Project" [12].

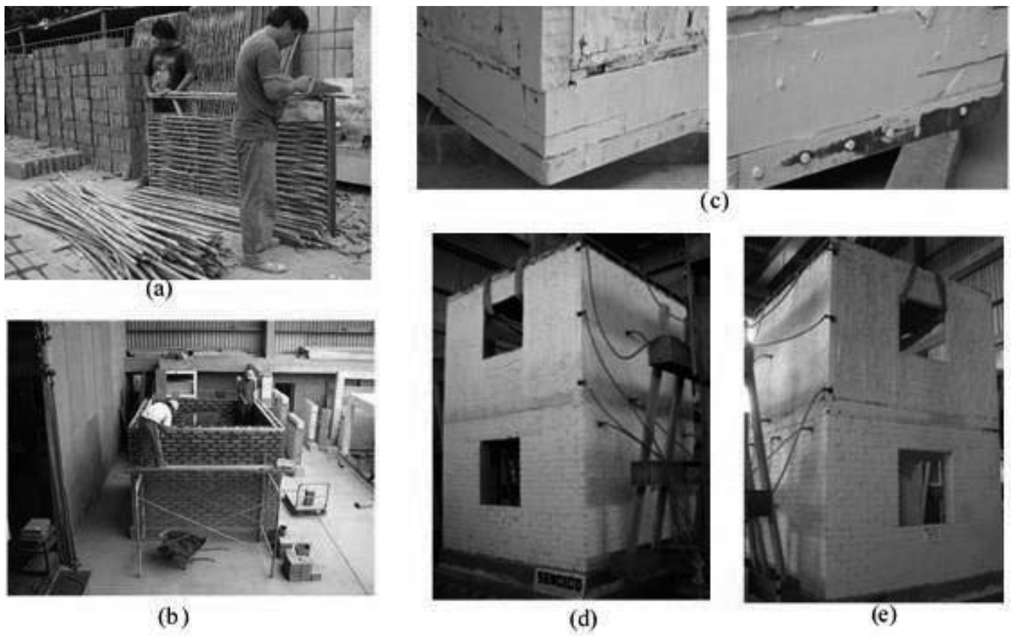

Figure 10:(a)Construction of Quincha panel; (b)Construction of Adobe masonry; (c)Joint area reinforcement; (d)Module M1 – Without reinforcement; (e)Module M2 – With reinforcement [12]

The project consisted in the construction and dynamic testing of two modules of two stories that present walls of adobe in the first story and panels of quincha in the second one (Figure 12). Both modules were constructed with the same materials and the same geometry, but they were differentiated by the addition of an external reinforcement in the joint between both stories. The first module M1-SR M1 (without reinforcement) was constructed in a traditional way with characteristics similar to those of the traditional constructions in Lima; while for the second module M2-CR (with reinforcement), small metal plates were added in the joint area of both stories.

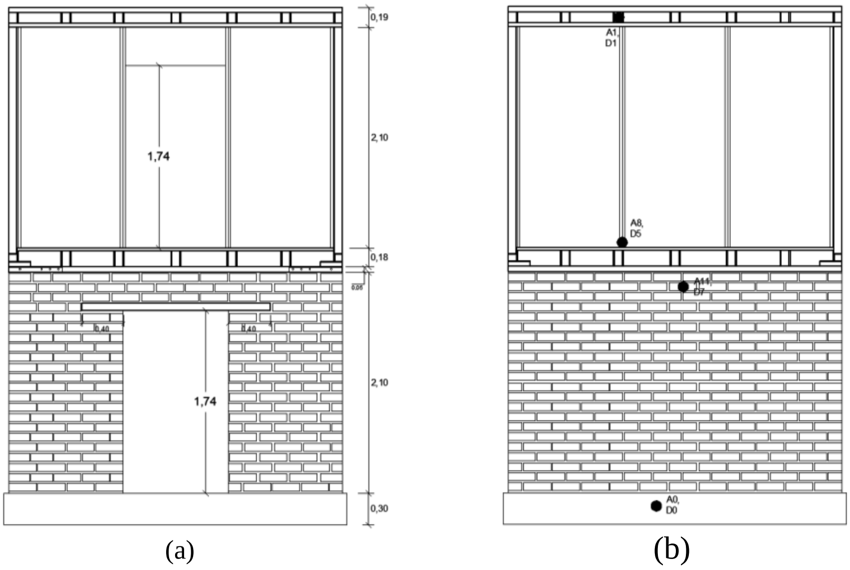

Figure 11: (a) Front view of modules M1 and M2; (b) Location of LVDT's and accelerometers

5.1 Free vibration

The free vibration tests allow determining the properties of the structure by applying four pulses of small amplitude of 1.5 mm in the vibratory table. LVDTs and accelerometers were placed at the base, at the top of the first story, at the bottom of the second story and at the top of the second story (Figure 11); thereby, it is possible to calculate the relative displacements and accelerations of each floor. The natural vibration periods of each story were calculated with the frequency domain obtained from the Fast Fourier Transform (FFT) of the acceleration register. The periods of each floor were calculated for each of the modules in six instants (Figure 12). The first one was before the test (VL0) and the following were performed after each dynamic test.

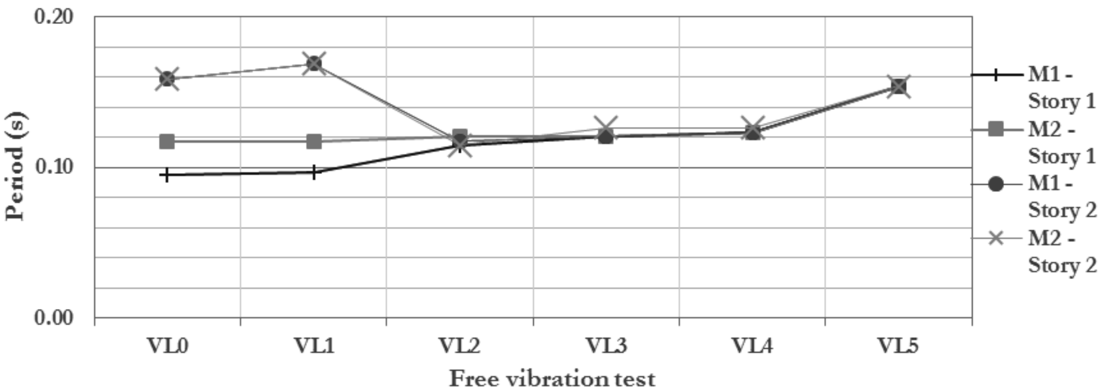

Figure 12: Periods of each story for the modules M1 and M2 by the free vibration test

The damping value of each floor in each of the free vibration tests (Figure 13) was calculated with the decay of the relative displacements. The method used was the Logarithmic Decrement between successive peak amplitudes.

$$\delta = \ln \frac{A_i}{A_{i+n}} = \frac{2n\pi\xi}{\sqrt{1-\xi^2}} \tag{8}$$

where: δ = Logarithmic decrease, Ai= Amplitude of displacement in a peak,
n = Number of cycles between peaks, ξ = Damping coefficient

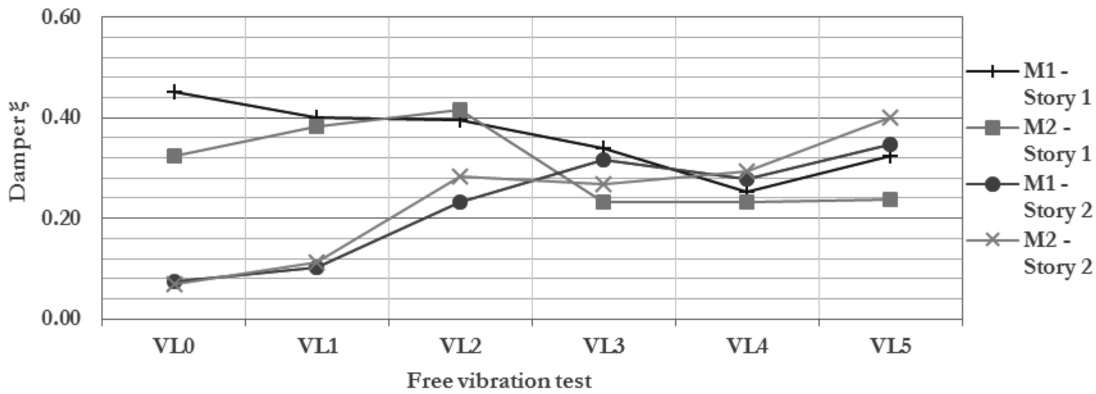

Figure 13: Damping coefficient of each story for the modules M1 and M2 by the free vibration test

The stiffness of each story K1 and K2 for both modules (Figure 14) were calculated from the periods obtained in each of the floors, since there is a direct relationship between period, mass and stiffness. In this type of structures, the mass is not very concentrated, but it possess a mass distributed throughout the structure. For this reason, the generalized mass for distributed masses will be used and the generalized stiffness of each floor will be calculated.

$$M^* = \int m_{(x)}.\left(\varphi_{(x)}\right)^2.dx + \sum M_i\,.\,\varphi^2 \tag{9}$$

$$K^* = \left(\frac{2.\pi}{T}\right)^2.M^* \tag{10}$$

where: M^* = Generalized mass, M^* = Generalized stiffness, $m(x)$= mass distributed, $\varphi(x)$ = form distributed, Mi = Mass concentred, φ = Form concentred, T = Period

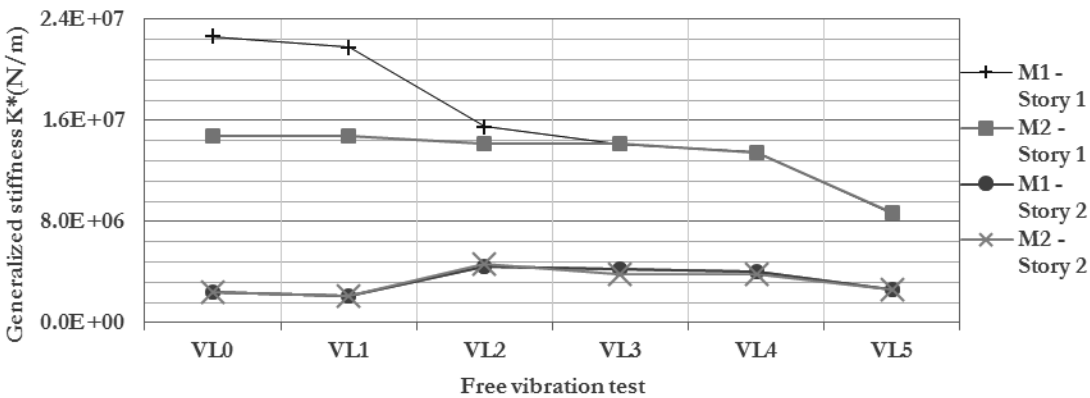

Figure 14: Generalized stiffness of each story for the modules M1 and M2 by the free vibration test

5.2 Base shear

The load sensor provides the recording of the load applied at each moment to move the platform of the vibrating table. Therefore, the shear load applied at the base of the is obtained by subtracting the inertial load of the platform and the foundation ring

$$Vb = Fa - (Mp + Ma).A_0 \tag{11}$$

where: Vb = Base shear, Fa = Load applied, Mp= mass of the platform, Ma = Mass of the foundation ring, A_0 = acceleration at the base

The maximum base shear was calculated in each of the dynamic tests with the same signal but different magnitude of scale as it is shown in the Figure 15.

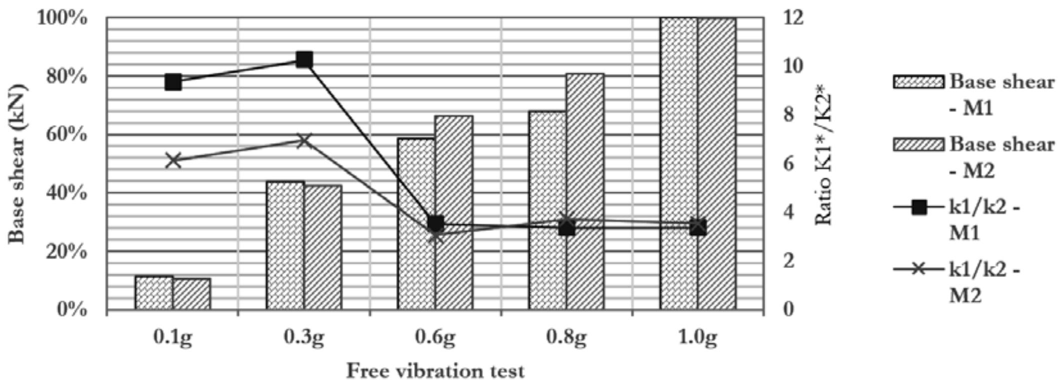

Figure 15: Maximum base shear for the modules M1 and M2 by the dynamic test

6 COMPARISON OF NUMERAL RESULTS AND EXPERIMENTAL RESULTS

The modal spectral and the time-history analysis show that the stiffness ratio plays an important role in the base shear value. Low stiffness ratios give high base shear values and these decrease as the ratio increases. The experimental results keep the same tendency in the values of base shear from the phase three and four with the scale of 0.6g and 0.8g, respectively. The reinforcement of the module M2 increases the K1 stiffness and causes a bigger base shear than the module M1. The difference of shear is not appreciated for low values of peak ground acceleration, but it becomes clear for values closer to the 0.4g.

7 REMARKS AND CONCLUSIONS

- The second mode has a great importance in the behavior of structures with different materials and stiffness between their stories. The low stiffness in the second floor causes a decrease in the displacements of the first story and less base shear.
- The results of time-history analysis and spectral analysis of the two-degree-of-freedom model show very similar tendencies. When the two stories have very similar stiffness, the base shear of the adobe walls is bigger. Figure 8 shows that the benefit of the second floor of quincha occurs mainly when the stiffness ratio K1/K2 is between 7 and 10. Also, the Figure 9 shows that in this range there are the same relative displacements with both analyses.
- For the conservation and reinforcement work, it is recommended to stiffen the adobe walls instead of the quincha panels for increase the stiffness ratio. In order to benefit the adobe masonry with quincha panels, there must be a difference of stiffness between both stories.

REFERENCES

[1] Blondet, M., Vargas, J. 1978. “Investigación sobre vivienda rural”. *Pontificia Universidad Católica del Perú*. Lima, Perú

[2] Gutiérrez, L., Manco, T., Loaiza, C., & Blondet, M. 2003. “Características sísmicas de las construcciones de tierra en el Perú: contribución a la enciclopedia mundial de construcción de vivienda”. *XIV Congreso Nacional de Ingeniería Civil*, Iquitos, Perú.

[3] Valdez, P. H. 2006. “Estructuras abovedadas de quincha en el virreinato del Perú. En construir con tierra ayer y hoy”. *V Seminario Iberoamericano de Construcción con tierra; I seminario argentino de arquitectura y construcción con tierra*, 14 al 17 de junio de 2006 (pp. 115-116), Mendoza, Argentina

[4] Ministerio de Vivienda, Construcción y Saneamiento. 2006. “Norma E.080 Adobe”. *SENCICO*. Lima, Perú.

[5] Gutiérrez, L., Manco, T. 2006. “Características sísmicas de las construcciones de tierra en el Perú: contribución a la Enciclopedia Mundial de Construcción de Vivienda”. (Tesis de título de Ingeniero Civil). *Pontificia Universidad Católica del Perú*, Lima, Perú.

[6] Cárdenas, L. 2008. “Análisis de vulnerabilidad estructural del Hotel Comercio”. (Tesis de título de Ingeniero Civil). *Universidad Ricardo Palma*, Lima, Perú.

[7] ININVI. 1989. "Antecedentes históricos de la quincha". *Instituto Nacional de Investigación y Normalización de la vivienda*. Lima, Perú.

[8] Torrealva, D., Vicente, E. s.f. “Proyecto de reforzamiento sísmico: evaluación experimental del comportamiento sísmico de muros de quincha del centro histórico de Lima – Perú”. Lima, Perú

[9] Rossi, A., Sáenz, O. 2016. “Comportamiento estructural de un muro de quincha tradicional del Centro Histórico de Lima – Muros con Diagonal”. (Tesis de título de Ingeniero Civil). *Pontificia Universidad Católica del Perú*, Lima, Perú.

[10] Montesino, M. (2016). “Caracterización mecánica de componentes estructurales en construcciones arqueológicas de tierra: El caso de Huaca de La Luna”. (Tesis de título de Magister de Ingeniero Civil). *Pontificia Universidad Católica del Perú*, Lima, Perú.

[11] Ministerio de Vivienda, Construcción y Saneamiento. 2016. “Norma E.030 Diseño sismorresistente”. *SENCICO*. Lima, Perú.

[12] Silva W., Zegarra L., Sanchez, T. 2006 “Ensayos de simulación en dos módulos de adobe y quincha de dos pisos (M1-SR: tradicional y M2-CR: Mejorado)”. *Laboratorio de Estructuras Antisísmicas. Pontificia Universidad Católica del Perú*, Lima, Perú.

SHATIS'17
4th International Conference on
Structural Health Assessment of Timber Structures
20-22 September 2017 Istanbul, Turkey

PREDICTING MECHANICAL PROPERTIES OF TIMBER ELEMENTS BY REGRESSION ANALYSIS CONSIDERING MULTICOLLINEARITY OF NON-DESTRUCTIVE TEST RESULTS

Hélder S. Sousa[1], Jorge M. Branco[1], José S. Machado[2] and Paulo B. Lourenço[1]

[1] ISISE, University of Minho, Campus de Azurém 4800-058, Guimarães. Portugal

[2] LNEC, Department of Structures, Avenida do Brasil, 101, 1700-066, Lisbon, Portugal

Keywords: Timber elements, Non-destructive tests, Regression analysis, Multicollinearity

Abstract

Information retrieved from different sources, which are necessarily uncertain to some extent, must be compiled to have a reliable assessment of a timber element. Means to obtain information are often limited to non or semi destructive tests. Therefore, the available information is an indirect measurement of the element's mechanical properties, and are incomplete predictors if not complemented with more data. In that scope, data is commonly added using different predictors in a regression analysis. If the predictors themselves are uncorrelated, the determination coefficient, R^2, is directly related to the measure being explained. However, predictors are usually correlated and thus multicollinearity exists. In extreme cases, multicollinearity results in imprecise and unstable R^2, thus the relative importance among predictors is not accurately measured.

Inclusion of all predictors in a regression model, is typically impeded by high multicollinearity. Estimation of a predicted variable, using all combinations of explanatory predictors, may be unfeasible when the number of predictors is large, thus it is important to assess which are the most influent. This paper discusses the application of multiple regression analysis for prediction of properties of timber elements, using adjusted R^2 depending on the number of predictors and the contribution of each predictor measured by Shapley value regression procedure. Data of a multi-scale experimental campaign on chestnut timber elements was used accounting correlations of non-destructive tests with mechanical properties and differentiation by visual grading.

By measuring the relative importance of a predictor, it was showed which can be used for the assessment of existing timber elements, thus allowing for a more reliable assessment within a safety analysis of a timber structure.

1 INTRODUCTION

Correlations between non-destructive tests (NDT) and mechanical properties of timber elements have been studied in several researches, including different size scales from clear wood specimens [1, 2], to elements [3] and application to full-scale structures [4].

In [5, 6], timber elements were visually graded and tested with different NDTs for density and modulus of elasticity prediction. In that case, a regression model was used and the adjusted coefficient of determination, $R^{2,\mathrm{adj}}$, was determined for application on a prediction model of onsite elements, as well as dismantled structural timber.

Nevertheless, when multiple regression is used to incorporate several predictors within the prediction model, multicollinearity may be an issue since several of these tests are based on similar principles and relations to the mechanical properties of timber. Moreover, the mechanical properties of timber are correlated between themselves [7].

Inclusion of all predictors in a regression model, is typically impeded by high multicollinearity. Estimation of a predicted variable, using all combinations of explanatory predictors, may be unfeasible when the number of predictors is large, thus it is important to assess which are the most influent. This paper discusses the application of multiple regression analysis for prediction of properties of timber elements, using adjusted R^2 depending on the number of predictors and the contribution of each predictor measured by Shapley value regression procedure. Data of a multi-scale experimental campaign on chestnut timber elements was used accounting correlations of non-destructive tests with mechanical properties and differentiation by visual grading.

2 METHODS

2.1 Multiple regression and adjusted correlation

In a multiple regression model the resultant equation represents the linear combination of the predictors that provides the smallest value of mean squared error. In this case, the linear combination is a factorization of the predictors and the factors are given as the regression weights. The coefficient of determination, R^2, measures the proportion of the variation in the variable being explained (dependent variable) by the predictors (independent variables). The adjusted coefficient of determination, $R^{2,\mathrm{adj}}$, allows to adjust the statistic taking into account the number of independent variables in a multiple regression, and to analyze either if adding a specific predictor is significantly influencing or not the correlation value.

Adding more and more independent variables to the model will increase the correlation value, regardless if the independent variables are strongly or weakly correlated to the dependent variable. This is contrary to the objectives of the goodness-of-fit statistic. However, the $R^{2,\mathrm{adj}}$ provides an adjustment such that an independent variable that has a correlation to the dependent variable increases the $R^{2,\mathrm{adj}}$, whereas any variable without a strong correlation might decrease the value of $R^{2,\mathrm{adj}}$. This is in line with the objectives of a goodness-of-fit statistic.

In this work, the value of $R^{2,\mathrm{adj}}$ is calculated according to the following equation

$$R^{2,adj} = R^2 - \left(1 - R^2\right) \cdot \frac{(k-1)}{(n-k)} \tag{1}$$

where: n = number of observations used in the regression, k = number of predictor parameters.

2.2 Multicollinearity and Shapley value

When facing large amounts of data, retrieved from different sources, a significant number of variables are often present. It is not uncommon, when dealing with big data analysis and multiple regression models, to observe several variables, each with hundreds or thousands of measurements. In that case, statistical methods are needed as to estimate reliable models that contain all possible combinations of those explanatory variables and to obtain an adequate prediction model, that follows a likelihood based criterion, to determine a specific dependent variable. Nonetheless, including different explanatory variables, for instance in a multiple regression model, may be impeded by high multicollinearity [8].

Multicollinearity occurs when, in a regression model, several predictors that share common variation are introduced. These variables, with common variation, lead to the case that one predictor may be obtained by a linear combination of the other predictors. In that case, the weights that are given to each individual predictor, in the regression model, is no longer important because it will result in similar predictions of the dependent variable. Given those premises, different predictor factorizations yielding approximately the same predictive accuracy may be found. On the other hand, when the predictors are mutually independent variables, the weight given to the R^2 may be partitioned into unique contributions of each variable, thus the impact of each independent variable may be added to obtain the total value of R^2.

A way to define the individual contribution of each independent variable is the Shapley value that is calculated across all possible regression models, assuming all possible combinations of predictors. Basically, the Shapley value estimates the net effects obtained by averaging over all possible combinations of the independent variables on a multiple regression analysis. By providing an average estimate across multiple iterations, much of the bias found in a standard regression analysis is eliminated, thereby mitigating the unfavorable impact of multicollinearity.

The Shapley value may be obtained by the following steps: *i*) consideration of all possible combinations of predictors and obtaining the correspondent R^2 for each of those combinations; *ii*) computation of the average contribution to the R^2 of the model of each predictor This averaged value is the importance measure (or weight) of each individual predictor by itself.

In this way, the calculated importance measures are inherently reliably and stable. Moreover, the results in relative importance values may be sum to obtain the R^2 from the normal multiple regression that includes all predictors. Thus, producing relative importance measures that are a decomposition of R^2, providing stable estimates in the event of multicollinearity.

3 DATABASE AND PROCEDURE

3.1 Experimental campaign

In this work, twenty old chestnut floor beams (*Castanea sativa* Mill.) were assessed in different scales and by means of different non-destructive tests (NDT) and mechanical tests. The experimental campaign was divided into three main phases, corresponding to different scales of the timber elements. From one to the next phase, the timber elements were sawn into a smaller size in order to isolate the influence and location of defects, and also to provide a better definition of the distribution of stiffness and strength along the length and height of the beam. Detailed information about the full experimental campaign may be found in [9].

In the present work, mechanical tests consisted in 4-point bending tests and compression and tension parallel to the grain tests. The bending tests were made to each 40 cm segment of boards with 7×4 cm^2 that were sawn from the original beams. The compression and tension parallel to the grain tests were made to small clear specimens taken from those boards. Before performing the mechanical tests, the specimens were assessed by means of NDTs, namely pin penetration tests, drilling resistance tests and ultrasounds. The values taken from the NDTs were penetration depth, d_{pen} (mm), resistographic measure, *RM* (Bit), and wave propagation velocity, v (m/s). Moreover, visual grading was made for the board segments. The timber boards were visually inspected and graded on each 40 cm segment, using UNI 11119:2004 [10]. This standard establishes objectives, procedures and requirements for the diagnosis of the state of conservation and estimates nominal stiffness and strength values for structural wood elements. For strength grading of a single element on site, it considers three classes (I, II and III). The wood element is included in a given class if it fulfills all the imposed requirements, otherwise, in this study, graded as non-classifiable (NC). The visual grading included as main parameters the assessment of knots diameter, slope of grain, wane and deformation.

Bending stiffness and strength were determined according to the test procedures given in [11]. For bending, this standard suggests the determination of a local modulus of elasticity, $E_{m,l}$, and of a global modulus of elasticity, $E_{m,g}$. The $E_{m,l}$ is measured in a central distance, while the $E_{m,g}$ is measured along the full span of the beam between supports. It is noted that $E_{m,l}$ is measured in a region with null shear stress and constant bending moment, whereas the $E_{m,g}$ also considers the presence of shear.

The layout and relation between different tests are presented in Figure 1. The present database corresponds to the results of 161 bending tests for determination of stiffness, $E_{m,l}$ and $E_{m,g}$, made to different segments. From those segments, 49 were selected and bending tests for determination of bending strength, f_m, were made. For compression and tension parallel to the grain tests, a total of 60 tests for each case were made to determine stiffness ($E_{c,0}$ and $E_{t,0}$, respectively compression and tension parallel to the grain moduli of elasticity) and strength ($f_{c,0}$ and $f_{t,0}$, respectively compression and tension parallel to the grain strengths).

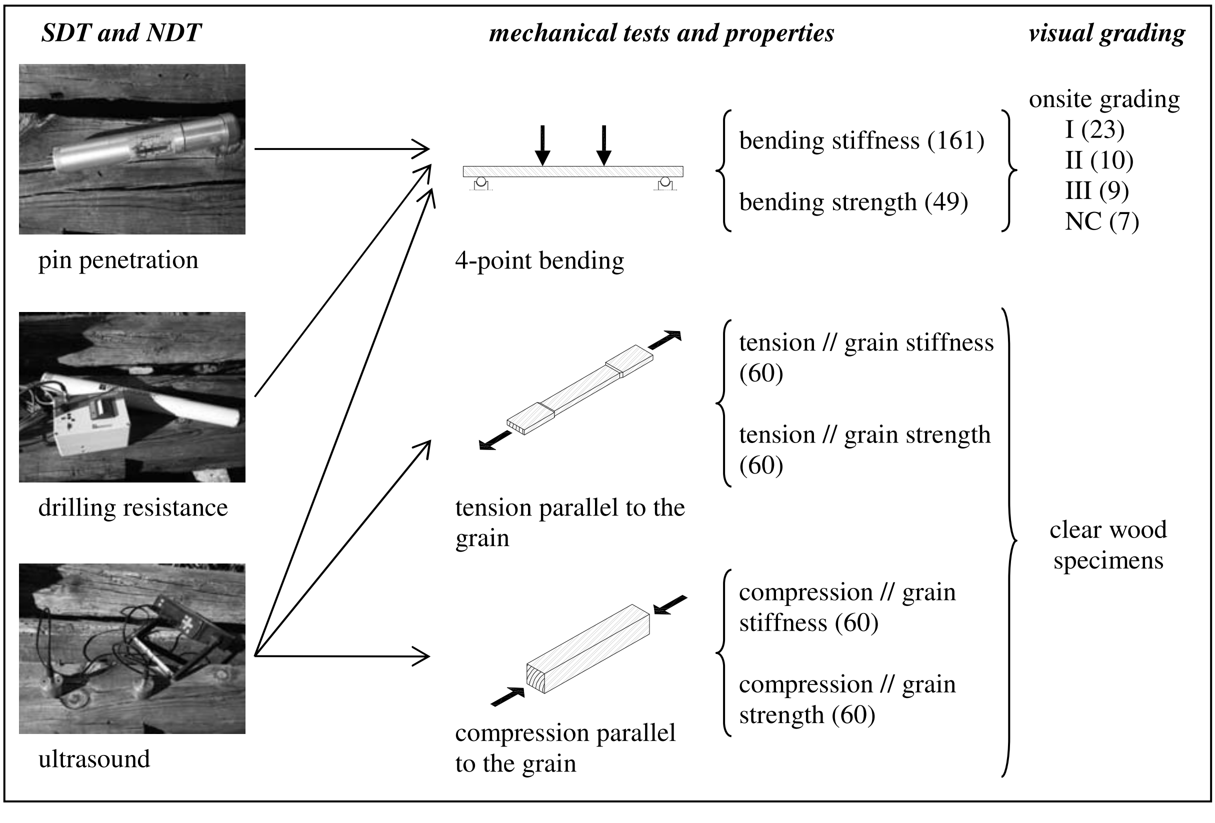

Figure 1: Experimental campaign layout and performed tests (number of tests in brackets).

3.2 Predictors and predicted variables

The complete determination of the mechanical properties of an existing timber element may only be fully determined by mechanical tests. However, these tests will inevitably lead to the destruction of the specimen itself, as to obtain its ultimate strength value. Therefore, it is common practice to perform NDTs to the elements and predict their properties by correlation with those properties, and by this procedure maintaining the element. Within this scope, the results of NDTs are the independent variables (predictors) that are determined to predict the mechanical properties of timber which are, therefore, the dependent variables. For the present work, the results of pin penetration tests, drilling resistance tests and ultrasounds are considered as the predictors, whereas bending stiffness, bending strength, compression and tension parallel to the grain strengths are the predicted, or explained, parameters.

Within a first analysis, bending stiffness and strength are predicted only by means of the NDT results, whereas in a second part, bending stiffness itself is a predictor for bending strength. For the second part, a division of results regarding visual grading is performed in order to assess the possible influence of defects in the correlation analysis and on the weight of each predictor.

Finally, results of ultrasound testing and modulus of elasticity are used for predicting compression and tension parallel to the grain strengths, within a multiple regression model.

4 REGRESSION ANALYSIS

4.1 Determination coefficients

4.1.1 Full sample

The three NDTs were used to predict the values of bending stiffness, $E_{m,l}$ and $E_{m,g}$, and strength, f_m. The results, in terms of coefficient of determination R^2 and adjusted coefficient of determination $R^{2,adj}$, are presented in Table 1. Moreover, the coefficients of each multiple regression equation are also presented for all the predictors including the intersection (value of the dependent value when the multiple regression equation intersects the dependent variable axis). Bending stiffness is predicted using only the three NDTs, whereas bending strength is predicted by both only the NDTs and also by the combination of NDTs with bending stiffness.

Table 1: Multiple regression coefficients and determination coefficients for $E_{m,l}$, $E_{m,g}$, and f_m.

Mechanical property	Predictors						Deter. coef.	
	d_{pen} [mm]	*RM* [Bit]	v [m/s]	$E_{m,l}$ [N/mm^2]	$E_{m,g}$ [N/mm^2]	*inters.*	R^2	$R^{2,adj}$
$E_{m,l}$ [N/mm^2]	-62.14	6.58	4.99	--	--	-12950	0.31	0.30
$E_{m,g}$ [N/mm^2]	-182.05	3.59	4.40	--	--	-9575	0.55	0.54
f_m [N/mm^2]	-0.080	-0.110	0.033	--	--	-85.56	0.58	0.56
f_m [N/mm^2]	0.125	-0.043	0.013	9.67×10^{-5}	0.004	-58.17	0.73	0.70

Table 2 presents the results of the multiple regression models for prediction of compression and tension parallel to the grain strengths.

Table 2: Multiple regression coefficients and determination coefficients for $f_{c,0}$ and $f_{t,0}$.

Mechanical property	Predictors				Deter. coef.	
	v [m/s]	$E_{c,0}$ [N/mm^2]	$E_{t,0}$ [N/mm^2]	*inters.*	R^2	$R^{2,adj}$
$f_{c,0}$ [N/mm^2]	-0.0009	0.0022	--	18.90	0.36	0.36
$f_{t,0}$ [N/mm^2]	-0.0031	--	0.0068	1.454	0.30	0.30

4.1.2 Division by visual grade

The segments of the timber elements that were assessed by 4-point bending tests, were also visually graded regarding its defects. The results of multiple regression models are given in Table 3 for prediction of f_m accounting partition of results by visual grade.

Table 3: Multiple regression coefficients and determination coefficients for f_m by visual grade.

f_m [N/mm^2] (by visual grade)	Predictors						Deter. coef.	
	d_{pen} [mm]	RM [Bit]	v [m/s]	$E_{m,l}$ [N/mm^2]	$E_{m,g}$ [N/mm^2]	*inters.*	R^2	$R^{2,adj}$
I	-1.698	-0.201	0.026	2.37×10^{-5}	0.003	-40.39	0.49	0.34
II	10.29	0.261	0.020	-0.002	0.005	-253.36	0.78	0.51
III	-3.106	-0.274	0.045	0.001	-0.003	-58.72	0.96	0.90
NC	-3.310	0.089	-0.008	0.005	0.004	-7.77	0.87	0.20

4.2 Predictor's importance

4.2.1 Full sample

The contributions of each predictor, in the multiple regression models for prediction of $E_{m,l}$, $E_{m,g}$, and f_m, are presented in Table 4. The results correspond to the Shapley value that measures the averaged contribution on all combinations of predictors in the multiple regression models, regarding the coefficient of determination R^2. By this way, it is possible to assess the individual contribution of each predictor considering multicollinearity influence. In the case of f_m, comparison may be done regarding the multiple regression model with and without the consideration of bending stiffness measurements as independent variables (predictors).

Table 4: Shapley values for the predictors of the multiple regression of $E_{m,l}$, $E_{m,g}$, and f_m.

Mechanical property	R^2	Shapley value				
		d_{pen}	RM	v	$E_{m,l}$	$E_{m,g}$
$E_{m,l}$	0.31	0.010	0.008	0.291	--	--
$E_{m,g}$	0.55	0.027	0.015	0.511	--	--
f_m	0.58	0.008	0.013	0.562	--	--
f_m	0.73	0.005	0.006	0.240	0.132	0.347

Table 5 presents the results of the Shapley value for the multiple regression models that were used to predict compression and tension parallel to the grain strengths.

Table 5: Shapley values for the predictors of the multiple regression of $f_{c,0}$ and $f_{t,0}$.

Mechanical property	R^2	Shapley value		
		v	$E_{c,0}$	$E_{t,0}$
$f_{c,0}$	0.36	0.092	0.267	--
$f_{t,0}$	0.30	0.035	--	0.268

4.2.2 Division by visual grade

The Shapley values for the multiple regression models used to predict each set of f_m, that correspond to the partitioned samples by visual grade, are presented in Table 6. Shapley values are given taking into account the contribution to the coefficient of determination R^2 in each visual grade.

Table 6: Shapley values for the predictors of the multiple regression of f_m by visual grade.

f_m (by visual grade)	R^2	Shapley value d_{pen}	RM	v	$E_{m,l}$	$E_{m,g}$
I	0.49	0.011	0.049	0.160	0.066	0.206
II	0.78	0.058	0.228	0.141	0.117	0.238
III	0.96	0.018	0.080	0.495	0.059	0.312
NC	0.87	0.177	0.139	0.138	0.286	0.127

5 DISCUSSION OF RESULTS

The values of the adjusted coefficient of determination obtained for the multiple regression models are similar to the simple coefficient of determination evidencing that the contribution of each predictor is sufficiently strong not to decrease the correlation to the dependent variable. However, when having a differentiation given by visual grading, significant decrease on the correlation is found, specially for grades I, II and NC. This may be due to the partitioning of the measurements to lower number samples. Nevertheless, in this case it is demonstrated that it is important to analyze the adjusted coefficient of determination before inferring on the correlation strength.

It is also noticeable that adding the stiffness parameters, $E_{m,l}$ and $E_{m,g}$, substantially increases the value of coefficient of determination in the prediction of bending strength.

In terms of contribution of each predictor to the multiple regression analysis of each parameter, it is concluded that the wave propagation velocity is the most influent NDT parameter in the analysis, having higher Shapley values than penetration depth or the resistographic measure. This is consistent with common results, since pin penetration tests and drilling resistance are often more correlated to the density of the element and density is usually a poor predictor of stiffness and strength.

Division by visual grades evidenced an increase on the importance of the other NDT on the coefficient of determination. However, as mentioned before, these results must be analyzed carefully since lower number samples were used (between 7 to 23 measurements).

Figure 2 presents the contribution of each predictor, on the prediction of bending strength, taking into account division by visual grade. The results are given in percentage of the coefficient of determination as to allow for a direct comparison between visual grades.

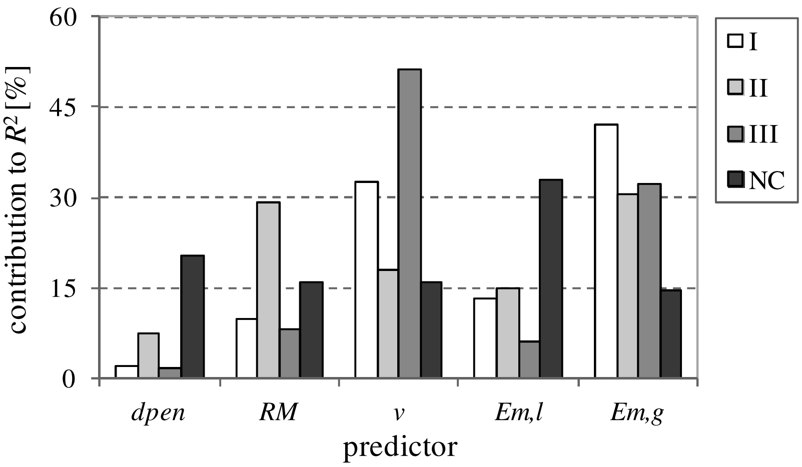

Figure 2: Contribution, accounting Shapley value, of each predictor for f_m prediction partitioned by visual grade.

In Figure 2, it is visible that the stiffness parameters, specially $E_{m,g}$, have a more significant contribution to the prediction of bending strength. This is also found in the case of compression and tension parallel to the grain measurements. This is an expectable result since the NDT results are an indirect measurement of the mechanical properties of timber, whereas a stronger correlation between stiffness and strength is found.

6 CONCLUSIONS

Multicollinearity between variables in a multiple regression model may distort the real contribution of each predictor on the result of coefficient of determination. In this work, Shapley value procedure was used in order to determine the weight of each predictor in a multiple regression analysis. The procedure was applied on the determination of mechanical properties, namely bending, compression and tension parallel to the grain strengths, of existing timber elements by using non-destructive test results and stiffness values as predictors.

In terms of adjusted coefficients of determination, values from 0.30 to 0.70 were found for bending parameters (respectively, for stiffness and strength). For compression and tension parallel to the grain, values of adjusted coefficients of determination of 0.36 and 0.30 were found, respectively.

In terms of Shapley value analysis, the ultrasound tests evidenced higher contributions than the other NDTs. However, modulus of elasticity was found to be the better predictor for strength values.

ACKNOWLEDGEMENTS

This work was partly financed by FEDER funds through the Competitivity Factors Operational Programme - COMPETE and by national funds through FCT within the scope of the project POCI-01-0145-FEDER-007633.

The financial support of FCT, through national funds, within the scope of the project Pro-timber, PTDC/ECM-EST/1072/2014, is acknowledged.

REFERENCES

[1] Lourenço, P. B., Feio, A. O. and Machado, J. S. 2007. “Chestnut wood in compression perpendicular to the grain: Non-destructive correlations for test results in new and old wood”. *Constr. Build. Mater.*, 21(8), Pp:1617-1627.

[2] Feio, A. O., Lourenço, P. B. and Machado, J. S. 2007. “Non-destructive evaluation of the mechanical behavior of chestnut wood in tension and compression parallel to grain”. *Int. J. Archit. Herit.*, 1(3),Pp: 272-292.

[3] Sousa, H. S., Branco, J. M. and Lourenço, P. B. 2012. “Assessment of strength and stiffness variation within old timber beams”. In: 8th SAHC, Wroclaw, Poland.

[4] Branco, J. M., Sousa, H. S. and Tsakanika, E. (2017). “Non-destructive assessment, full-scale load-carrying tests and local interventions on two historic timber collar roof trusses”. *Eng. Struct.*, 140, Pp:209-224.

[5] Cavalli, A. and Togni, M. 2013. “How to improve the on-site MOE assessment of old timber beams combining NDT and visual strength grading”. Nondestruct. Test. Eva., 28(3), Pp:252-262.

[6] Cavalli, A., Bevilacqua, L., Capecchi, G., Cibecchini, D., Fioravanti, M., Goli, G., Togni, M. and Uzielli, L. 2016. “MOE and MOR assessment of in service and dismantled old structural timber”. *Eng. Struct.*, 125, Pp:294-299.

[7] JCSS. 2006. “JCSS Probabilistic Model Code, Part 3: Resistance Models – 3.5 Properties of Timber. Probabilistic Model Code”. Joint Committee on Structural Safety.

[8] Hastie, T., Tibshirani, R. and Friedman, J. 2009. “The elements of statistical learning: Data mining, inference and prediction”. 2nd ed. Berlin, Germany: Springer.

[9] Sousa, H. S., Branco, J. M. and Lourenço P. B. 2016. “Use of bending tests and visual inspection for multi-scale experimental evaluation of chestnut timber beams stiffness”. *J. Civ. Eng. Manag.*, 22(6), Pp:728-738.

[10] ENIU. 2004. “UNI 11119:2004 On site inspections for the diagnosis of timber members”. UNI Milano.

[11] CEN. 2010. “EN 408:2010 Timber structures – Structural timber and glued laminated timber – Determination of some physical and mechanical properties”. European Committee for Standardization.

SHATIS'17
4th International Conference on
Structural Health Assessment of Timber Structures
20-22 September 2017 Istanbul, Turkey

NUMERICAL MODELLING OF THE CYCLIC BEHAVIOUR OF TIMBER-FRAMED STRUCTURES USING *OPENSEES*

Relja Lukic[1], Elisa Poletti[2], Graça Vasconcelos[2] and Hugo Rodrigues[3]

[1] Ojdrovic Engineering Inc., Canada

[2] ISISE, University of Minho, Portugal

[3] Polytechnic Institute of Leiria, Portugal

Keywords: simplified FEM, Timber-Frame, Hysteretic laws, Opensees

Abstract. *Timber frame structures constitute an important cultural heritage of many countries, since they represent a typical anti-seismic construction adopted worldwide and are worth preserving. While these structures have recently been studied experimentally to better understand their behaviour during seismic actions, little studies have been carried out on the numerical modelling of such structures, which could help in improving interventions and retrofitting measures in existing buildings.*

This paper presents a study on the applicability of numerical models in predicting the global response of timber-framed shear walls during earthquake events. Based on the in-plane cyclic testing of traditional timber frames with and without masonry infill performed in a previous experimental campaign, numerical models were developed that capture the cyclic response of traditional timber frame walls including flexural behaviour, pinching and strength degradation. The numerical models were constructed in the finite element software OpenSees with calibrated springs representing nailed connectors found in traditional half lap joints and based on experimental results.

A parametric study was conducted on the half-timbered frame model by varying wall configuration and studying cumulative energy dissipation and the effect of slenderness and load capacity with increasing drift.
All models developed showed a very good approximation of the experimental results, in terms of initial stiffness, maximum load and energy dissipation. Future work includes the development of a macro-model and modelling of a whole timber-framed building in order to improve modelling capacities and predictions.

1 INTRODUCTION

Ancient heritage is abundant with timber-framed structures that function as strengthening solutions with infill and as independent structural systems. In earthquake areas they have been used as seismic-resistant construction and their good behaviour during seismic events has been documented and observed in a number of countries (e.g. Portugal, Italy, Greece, Turkey, Peru and Haiti). However, building typologies like Pombalino buildings in Lisbon have not experienced seismic activity and therefore their behaviour is unknown. Pombalino buildings and others are under risk of failure during seismic events if their mechanical behaviour is not properly quantified and understood. Traditional timber framed walls exhibit nonlinear hysteretic response under in-plane cyclic loading. It is important to define numerical modelling strategies for this type of constructive element in order to understand their mechanical behaviour.

Timber frame walls create an internal timber skeleton that can reduce the out-of-plane vulnerability of solely masonry constructed walls. Due to their low cost these types of walls exist in several countries especially in the local vernacular architecture. They can be composed of various infill materials ranging from brick and stone masonry to mud and cane. The timber not only better resists horizontal loads, but also provides a confining effect on the masonry structure improving its mechanical properties [1].

Timber shear wall systems are typically composed of internal braces forming an X-shape called the Cross of St. Andrew and are typically found in seismic countries such as in Italy and Portugal. Portuguese Pombalino buildings, introduced after the 1755 earthquake and subsequent tsunami and fire by the prime minister of the time, the Marquis of Pombal, consist of external load bearing masonry walls and internal timber-framed shear walls (Figure 1), called frontal walls [2]. In Italy, the so called “casa baraccata”, introduced after the 1823 earthquake by the Borbone house, has a timber frame also embedded in the exterior masonry walls [3]. In Greece and Turkey a variety of timber-framed structures can be found (Tsakanika and Mousakis 2010; Guney 2006) and they have proved to resist well to seismic actions when appropriately maintained. Of course these constructions also represent typical vernacular architecture for non-seismic regions, such as Germany, France, the UK, and in general all northern European countries.

Figure 1: Frontal walls in Pombalino building

The different connection types and geometry greatly affects the dissipative capacity of the walls. It is specifically because of these differences that researchers have started studying in detail the behaviour of traditional timber frame constructions.

Few works are available in literature on the numerical modelling of traditional timber-framed structures, while more literature is available on modern timber frames. Portuguese Pombalino walls were modelled using non-linear properties in a 2-D model and adding a hysteretic model for the joints [4] [5]. Quinn and D'Ayala [6] modelled Peruvian timber frames adopting semi-rigid spring elements calibrated on experimental results.

Opensees is an open source software which allows to use and alter existing hysteretic models. It has great potential for timber modelling and various works can be found on such field

This paper presents a procedure for the development of a working timber frame model subject to in-plane cyclic loading.

2 SUMMARY OF EXPERIMENTAL RESULTS

To study the seismic response of traditional Portuguese timber frame walls, quasi-static in-plane cyclic tests were performed on real scale specimens [1]. Half lap joints were used for the connections between the elements of the main frame, while the diagonals were simply nailed to the frame. In general the walls showed a good capacity and ductility. Results greatly varied depending on the level of vertical pre-compression and on the presence of infill, which could alter the response of the wall from a shear one to a flexural one [1].

From the previous experimental campaigns [1] [7], the following observations can be deduced:

1. Nonlinear behaviour of the bottom connections influences the overall response of the walls leading to a predominant rocking (flexural) mechanism. The observed strength degradation and pinching in the wall response is related to the observed pinching behaviour of the tested connections due to immediate loss of strength;
2. Infill walls tested at lower vertical load levels resulted in generally smaller opening of connections because walls rotated as a whole limiting local deformations in connections, however, at higher load levels deformations were larger;
3. Timber frame walls experienced larger deformations and damages at the joints under both vertical load levels since absence of infill material created a prevalent shear resisting mechanism allowing for unrestricted deformations;
4. Deformation of frame members while applying load was generally caused by uplifting of the posts from the bottom beam leading to elongations of the diagonals inducing high shear concentration within the central connection and resulting in failure. Movement of diagonals is larger in unfilled timber frame walls;
5. Unloading of the walls is influenced by the difficulty of the post to recover its original position due to the plastic deformation of the nail;
6. The quality of interlocking in the connections increases the loading capacity of the nail connector. Out-of-plane opening occurs due to asymmetry in thickness of half-lap connections;
7. Bottom beam did not uplift from steel profile for all tests conducted on walls and frames.

For a full description of the experimental results, see Poletti and Vasconcelos [1].

The identified locations of nonlinearities within the frame, namely the joints, were used in the development of a working numerical model. Nonlinear response of the tested traditional connection helped in the calibration of uniaxial material models available in OpenSees.

3 NUMERICAL MODELLING OF EXPERIMENTAL RESULTS

The geometry of the model is representative of the timber frame tested at the Laboratory of Structures at the University of Minho. A simplification to the member length was made to create a square frame consisting of four equal cells having the dimensions 0.95 x 0.95 m2 for a total height and length of 1.90 m. All members have the same cross sectional areas except for the top and bottom beams. The modulus of elasticity for the timber elements is 1.1 x 107 kN/m2 according to experimental testing on the wood species *Pinus pinaster*.

Horizontal and vertical timber members of the timber frame wall (Figure 2 right) are modelled as nonlinear beam-column elements to allow for nonlinear analysis. The diagonal bracing members are modelled as truss elements transferring only tensile and compressive forces. The member sections are modelled as elastic without shear deformations. Appropriate linear co-ordinate transformations were applied to transfer local coordinates of the members to global coordinates of the frame model. The base nodes remained fixed while the global response is controlled by the calibrated springs.

All end nodes of members in the frame were duplicated at joints for the insertion of two-node link elements as springs in order to assign uniaxial material models applied in corresponding direction of influence. The central connection was separated into 8 pairs of two-node links. For the 2-D model, three degrees-of-freedom are considered for the links, namely translations along x (direction 1), translations along y (direction 2), and rotations about local z-axis (direction 3). This element has zero length and couples the rotations and translations of connected nodes sharing the same global coordinates (Figure 2 right).

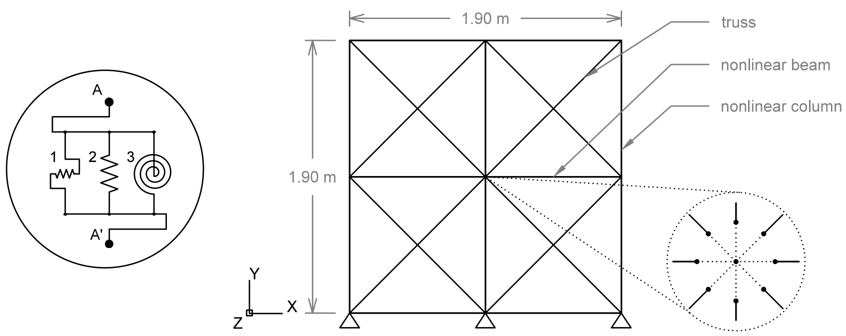

Figure 2: Schematic of the numerical model: two-node link element (left) and frame geometry (centre).

The response of the tested half-lap connection was first analysed (Table 1 and Figure 3) in order to calibrate two-node link elements acting as springs with the appropriate uniaxial material model to represent the global hysteretic behaviour in three directions: axial, shear, and rotations. Two-node link elements are applied at the base supports and in all internal elements while the outer frame was assumed to remain elastic. Calibrated uniaxial material models were used in the definition of the base supports and in appropriate connections within the timber frame.

Table 1: SAWS parameters for calibration of rotational spring.

Parameter	25 kN	50 kN
Intercept strength of shear wall spring element, F0	5.5	7
Intercept strength for spring element pinching branch, FI	0.65	1
Spring element displacement at ult. strength, DU	0.015	0.015
Initial stiffness of shear wall spring element, S0	473	500
Stiffness ratio of the asymptotic line, R1	0.12	0.12

Stiffness ratio of the descending branch, R2	-0.065	-0.09
Stiffness ratio of the unloading branch, R3	2	6
Stiffness ratio of the pinching branch, R4	0.055	0.055
Stiffness degradation parameter for the shear wall spring element, alpha	1.35	1.7
Stiffness degradation parameter for the spring element, beta	1.2	1.2

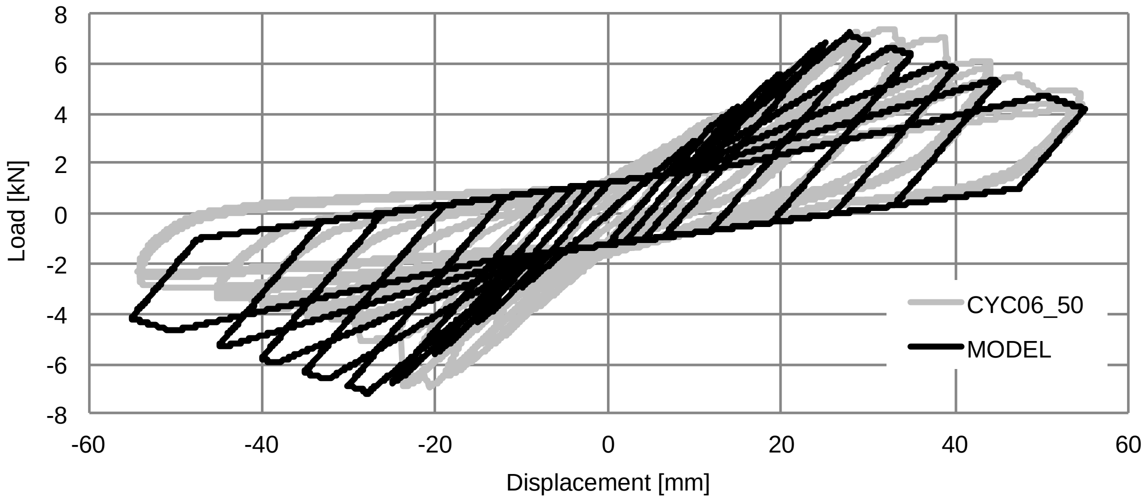

Figure 3: Calibration of rotational spring with SAWS for single joint

Three timber frame models (Figure 4) were studied with different configurations of springs in an attempt to achieve the experimental results, mainly the nonlinear (hysteresis) loops in the global load-deformation curve and the uplift of the base connections.

All diagonal members have Pinching4 in the axial direction with either elastic no-tension (ENT) and elastic-perfectly plastic gap (PP gap), element in parallel in order to make sure they work only in compression and are not depicted in the schematics for simplicity. In order to replicate the shear damage observed in the central connection, SAWS was added in the axial direction within the definition of the horizontal beam two-node link for Models 1 and 2.

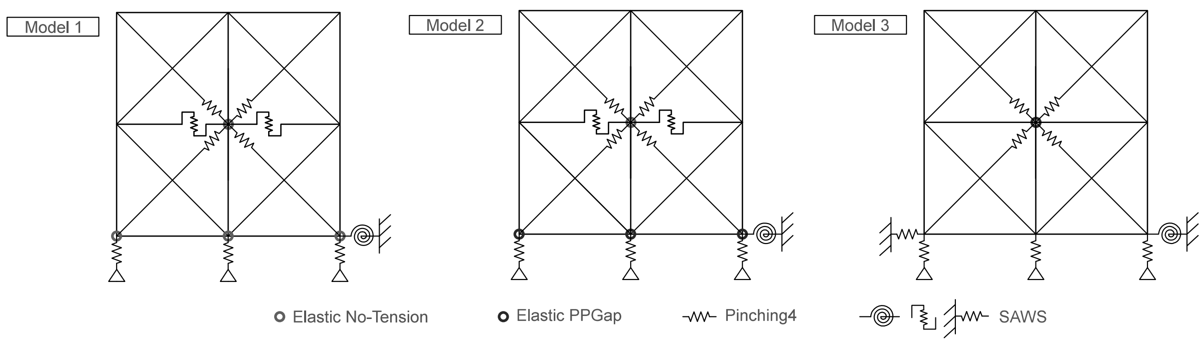

Figure 4: Studied models for timber frame wall with varying locations of nonlinearity

Timber frame model 1 was constructed with Pinching4 in the axial direction and SAWS in the rotational direction at the base while the shear response remained elastic to induce flexural (rocking) behaviour. Due to issues with convergence and to better represent the nail pull-out an ENT material with large stiffness was used in parallel with Pinching4. This configuration is also used in the axial direction for all diagonal members.

Timber frame model 2 is similar to model 1 except that the base connections have a compression-only PP gap element with a large strength in parallel with Pinching4. A gap of 2 mm was defined as measured in the pull-out of the nail connectors. This element was used to induce the flexural rocking mechanism (one post uplifts while the opposite crushes).

Timber frame model 3 was constructed with Pinching4 in the axial direction and SAWS in the rotational direction at the base. Nonlinearity in shear was added using the calibrated SAWS model with a larger intercept strength and initial stiffness of the spring. Pinching4 was also used in the axial direction for diagonals joining at the central connection. No gap element was used in parallel with Pinching4 in the base connections, instead a larger compression backbone was defined to avoid crushing of the bottom beam.

The pushover analysis was conducted using increments of 0.1 mm for a maximum displacement of 90 mm. The cyclic analysis used the same increment spacing with the following displacement cycle-peaks: 15 mm, 30 mm, 40 mm, 50 mm, 60 mm, and 70 mm. The cyclic analysis was performed only up to 70 mm due to early failure of UTW50 at 70.85 mm [1].

4 ANALYSIS AND DISCUSSION OF RESULTS

After initial analysis attempts of timber frame model 1, it was clear that the proposed configuration does not result in a comparable load-deformation response (Figure 5a). The initial stiffness and overall load capacity of this model is not representative of the experimental results. However, the model, in general, is able to reproduce damage (shearing) of the middle beam at the central connection and sliding of diagonal members which is in accordance with damages achieved in the experimental testing.

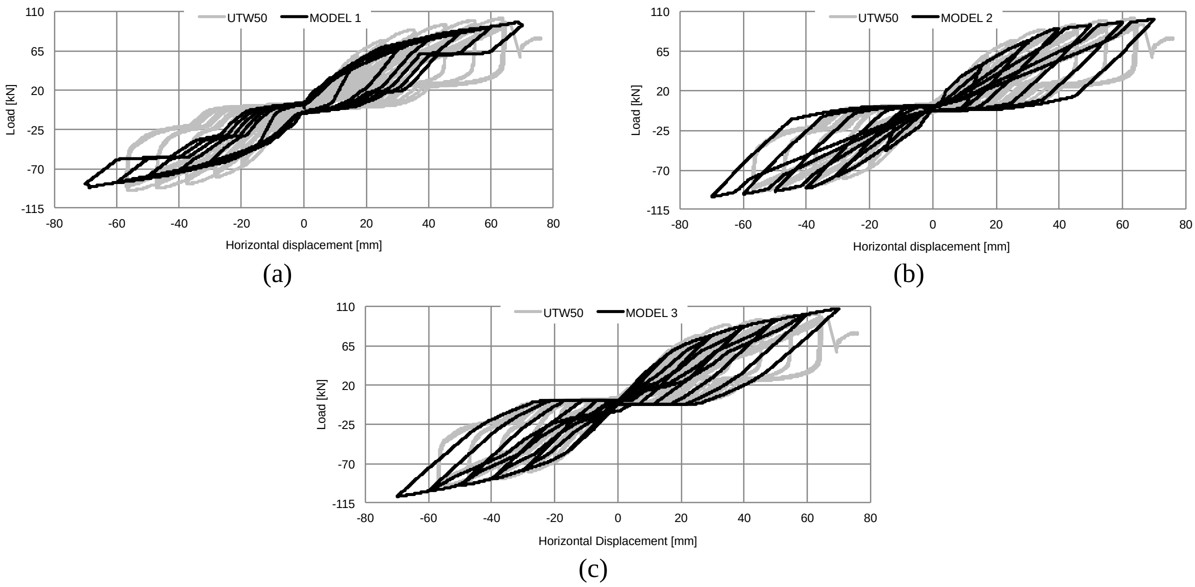

Figure 5: Comparison between experimental results and model output: (a) model 1; (b) model 2; (c) model 3.

The initial stiffness and overall load capacity of timber frame model 2 and timber frame model 3 is representative of the experimental results. However, in timber frame model 3 the hysteresis loops are poorly defined and reloading is minimal (Figure 5c). Timber frame model 3 does not replicate sliding of the diagonals or damage in the central connection. The resisting mechanism is shear at the base as evident by the global lateral movement of the frame. It is considered that this deformed shape is not acceptable when compared to experimental results given that no sliding at the base was recorded during the experiment.

Timber frame model 2 best represents the global response of the experimental results. Concentrating the nonlinearities at the base and in the central connection proved to be reasonably accurate. Elastic PP gap elements in the axial direction in parallel with Pinching4 at the base induce the nonlinear (hysteresis) response while SAWS controls the rocking behaviour. Pinching4 in parallel with elastic no-tension results in the diagonals acting in compression only. Visible damage of the central connection and sliding of the diagonals is not noticeable, possibly due to the gap material at the base that restricts movement of the diagonals and prevents shearing of the middle beam.

Timber frame model 2 was selected and updated to include the confining and stiffening effect of masonry in a simplified way by deleting nonlinearities in the central connection and only controlling behaviour at the base, based on the experimental results observed, since infill would induce a rocking response in the wall. Stiffness of the diagonal members and the connections was increased to 1.65 x 107 kN/m2. The backbone of the tension side of Pinching4 was also increased to better capture the total load capacity and initial stiffness. SAWS in the base connections was adjusted to include the large intercept strength of the spring for the pinching branch. The model is comparable to the results of UIW50 experimental testing up to the first failure of the specimen occurring at 70 mm horizontal displacement [1].

4.2 Influence of aspect ratio

A study was conducted on the developed half-timbered frame model considering different geometric configurations. The influence of the height to length ratio on the lateral response of the wall is compared with initial stiffness and load capacity. Also compared is the lateral load-drift response and cumulative energy dissipation between wall configurations.

The geometric configurations for both wall types are analysed and compared using a total drift of 10% with displacement cycle-peaks at 1% increments of total height (Table 2).

Table 2 Initial stiffness and load capacity for different configurations of half-timbered walls

Wall	Aspect ratio [H/L]	Maximum Load [kN]	Initial Stiffness, K_{in} [kN/mm]
1x2	0.5	340.25	53.13
2x2	1	170.12	18.54
3x2	1.5	113.41	8.41
1x1	1	105.56	16.00
2x1	2	52.78	4.19
3x1	3	35.18	1.70

Results from the parametric analysis show that the response of the timber-framed walls with infill (half-timbered walls) is similar to the response of timber frame walls except with an increase of initial stiffness (Figure 6a). The loading capacity remained the same since the influence of masonry was defined in the model by only changing modulus of elasticity in the diagonal members and connections. A similar exponential trend for load capacity and initial stiffness with increasing height to length ratio was observed (Figure 6b).

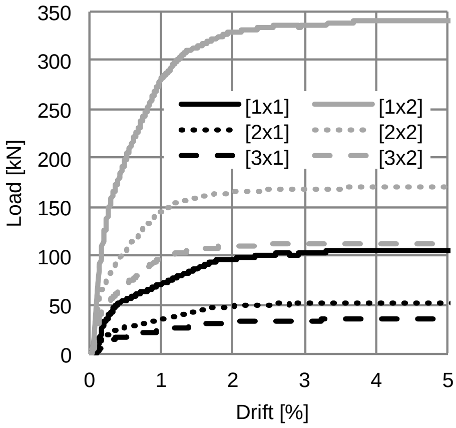

(a)

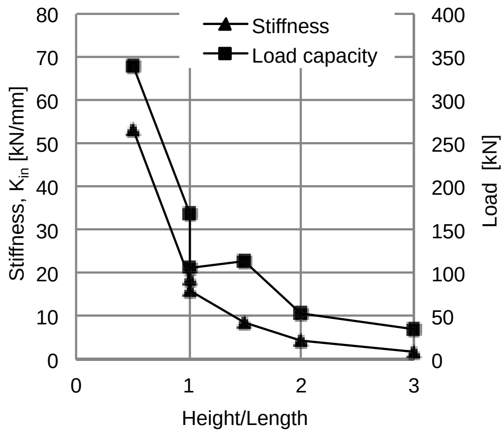

(b)

Figure 6: (a) Influence of the height to length ratio on the lateral response of half-timbered walls; (b) initial stiffness and load capacity

5 CONCLUSIONS

- Timber-framed infill walls have a complex behaviour resulting from material properties, interfaces, connection detailing, and quality of workmanship.
- Simple models are necessary to reduce the computational effort and obtain user-friendly models.
- Opensees was usefull in providing existing hysteretic models that could be calibrated on existing experimental results, with the disadvantage of a large number of parameters to be calibrated.
- Height-to-length ratio greatly influences strength, stiffness and energy dissipation.
- A macro-model will be developed based on these results in order to further simplify the model and develop of a set of rules for analysing timber-framed structures under horizontal loadings where hysteretic behaviour, pinching, stiffness and strength degradation as well as locations of energy dissipation and damage are characterised.

REFERENCES

[1] Poletti E., Vasconcelos G. (2014). Seismic behaviour of traditional timber frame walls: experimental results on unreinforced walls. *Bulletin of Earthquake Engineering*, 13(3), Pp. 885-916.

[2] Mascarenhas, J. (2004). *Constructive Systems – V*. Livros Horizonte, Lisbon, Portugal.

[3] Ruggieri, N., Tampone, G. & Zinno, R. (2015). In-plane vs Out-of-plane “Behaviour” of an Italian Timber Framed Sys-tem: the Borbone Constructive System. Historical Analysis and Experimental Evaluation. *International Journal of Architectural Heritage*, DOI: 10.1080/15583058.2015.1041189

[4] Kouris L., Kappos A.J. (2012). Detailed and simplified non-linear models for timber-framed masonry structures, *Journal of Cultural Heritage*, 13(1): 47–58

[5] Kouris L. A. S., Meireles H., Bento R., Kappos A.J. (2014). Simple and complex modelling of timber-framed masonry walls in Pombalino buildings, *Bulletin of Earthquake Engineering*, 12: 1777–1803

[6] Quinn N., D'Ayala D., 2013. Assessment of the realistic stiffness and capacity of the connections in quincha frames to develop numerical models, *Advanced Materials Research*, 778: 526-533

[7] Poletti E., Vasconcelos G., Branco J.M., Koukouviki A.M. (2016). Performance evaluation of traditional timber joints under cyclic loading and their influence on the seismic response of timber frame structures, *Construction and Building Materials* 127, Pp. 321-334.

SHATIS'17
4th International Conference on
Structural Health Assessment of Timber Structures
20-22 September 2017 Istanbul, Turkey

LOAD-BEARING CAPACITY OF HISTORIC TIMBER WITH FOCUS ON THE WOOD CORROSION

Wolfgang Rug[1], Gunter Linke[2]

[1] University for Sustainable Development Eberswalde, Germany, wolfgang.rug@hnee.de

[2] Ingenieurbüro Rug GmbH, Wittenberge, Germany, linke@holzbau-statik.de

Keywords: Wood corrosion, Destructive testing, Non-destructive testing, Ultrasound

Abstract. *The accurate assessment of exiting timber structures is substantial for a substance-friendly redevelopment. The first measurement is the exact determination of the timber members' properties. Visual methods are providing only insufficient reliable results. Therefore, the combination of visual and non-destructive/semi destructive methods is required. The use of ndt/sdt methods allows determining the material properties and their variation. The present study deals with preliminary investigations of the ultrasonic method concerning their applicability for the determination of the load-bearing capacity of timber with special focus on the influence of chemically-aggressive media. Subject of the study were timber members (spruce, glulam & solid wood) which served 98 years in a salt warehouse. The timber was visibly affected by wood corrosion. To evaluate the applicability of the ultrasonic method comparative tests have been carried out (ultrasonic measurements, determination of the density and flexural test according EN 408). The test results revealed a relatively weak correlation between the ultrasonic speed and the other properties. However, it must be considered that the ultrasonic speed has been measured in the unaffected core of the specimen. The strength and stiffness was clearly reduced due to the wood corrosion in the peripheral cross section. The strength and stiffness of the undamaged core can be determined sufficiently accurate with the ultrasonic method. Based on these results a recommendation for the application of the ultrasonic method in timber structures with wood corrosion can be provided. The ultrasonic method is used to determine the strength and stiffness of the unaffected core. Additionally, the density can be determined by core-drilling. The thickness of the corrosion layer should be determined with the dynstat method which has been verified in previous studies. With a sufficient sample and the evaluation of the material properties variation the stability of the construction can be accurately evaluated.*

1 INTRODUCTION

The invention of the glued laminated timber by Otto Hetzer in 1906 allowed the building wide-spanning constructions [1-4]. Amongst others this innovative construction method was used to erect halls in the fertilizer and potassium salt industry, which is proven until today by several preserved buildings (see also www.otto-hetzer.de).

However, this field of application subjects the timber to particular environmental conditions [5]. The production processes as well as stored substances are releasing chemically-aggressive media, which can cause irreversible structural modifications of the wooden members. The modification of the wood due to chemically-aggressive media is not taken into consideration in the static calculations according the currently valid version of the Eurocode 5 [6]. Some suggestions concerning this problem are listed in [5].

Though, the knowledge of the degree of the modification is a significant requirement for static calculations concerning the load bearing capacity especially in the course of redevelopment or reconstruction.

2 WOOD CORROSION

Timber has a natural chemical balance. This makes timber highly resistant against chemically-aggressive media. If the correct environmental conditions are present, the wooden members will be subjected to corrosion [5].

The wood corrosion is a structural damage beginning on the surface, which is caused by chemical and physical reactions. These reactions are caused in particular by strong acidic and strong alkaline media (pH $\leq$ 2 respectively pH $\geq$11). If the corrosion is caused by salts, the cell structure is destroyed by crystallization processes. The lignin and the hemicelluloses are degradated due to hydrolytic splitting.

Several studies on timber constructions under influence of chemically-aggressive media have shown that the destructive mechanism is dependent on the type of the impacting media [5].

The level of the destruction depends on the several aspects. These aspects could also be called a corrosion system, which is depicted in Figure 1.

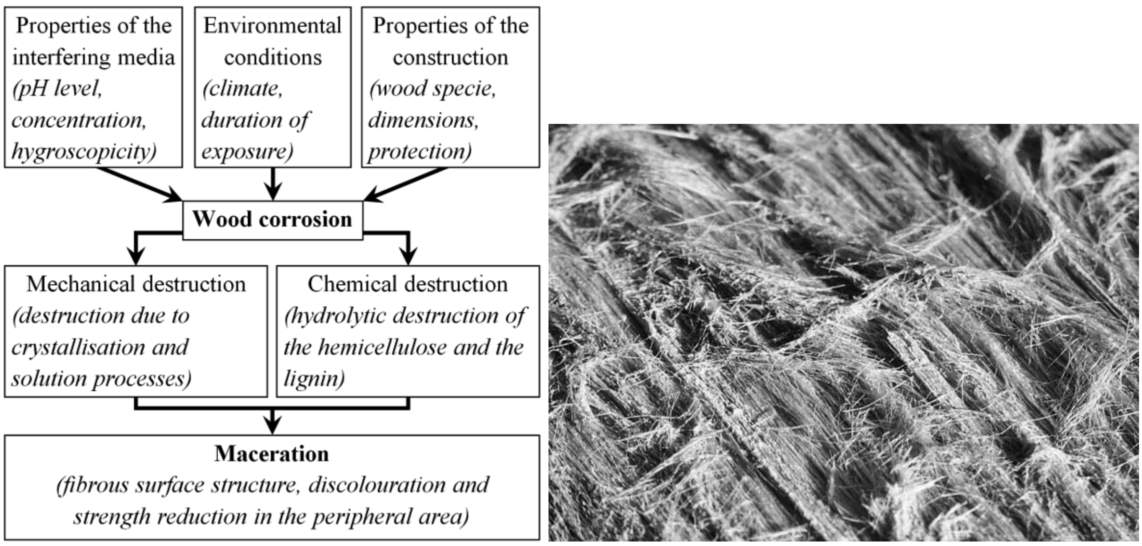

Figure 1: wood corrosion; left: schematic depiction; right: maceration on the surface

The studies carried out so far have shown that the alteration respectively destruction of the wood structure is limited to the cross-section near the surface. This destruction is visible by a greyish-brown discolouration and a fibrous surface structure. In some cases, the separation of whole strips of wood along the annual ring limits was observed. Furthermore, the peripherical cross-section shows a reduction of the strength. In the inner cross-section, there is no such strength reduction.

Glued laminated timber has a higher resistance concerning the wood corrosion if large, compact members are used and no large shrinkage cracks are appearing. Furthermore, the type of glue significantly influences the resistance against chemically-aggressive media.

3 SUBJECT AND AIM OF THE STUDY

The effect of the salts on the load bearing capacity of the historic timber and glued laminated timber has been examined in a number of studies [7-10]. The focus laid on the extent of the corrosion layer [7], the remaining strength of the historic casein glued joints [8] as well as the load-bearing capacity of solid timber and glulam members [9, 10]. The latter is outlined in the following.

The studies were divided in the determination of the material properties, which are required for strength grading – density, bending strength and modulus of elasticity – according EN 408 [13] as well as non-destructive ultrasonic measurements. The results should be used as a basis for future investigations concerning the structural stability of existing glued laminated timber constructions which are additionally stressed by chemically-aggressive media.

The study's subject was a warehouse erected in 1912 by the use of the HETZER-construction method. The load-bearing structure of the warehouse consisted of eleven parabolic trusses made from glued laminated timber according to the patent DRP. 197773 [4]. The trusses (wood species: spruce) had a double-T cross-section (see Figure 2). After the demolition of the ware house in April 2010 several parts of the construction have been transferred to the University of Applied Sciences, Eberswalde/ Germany (HNE Eberswalde) to carry out technical studies on the wooden members.

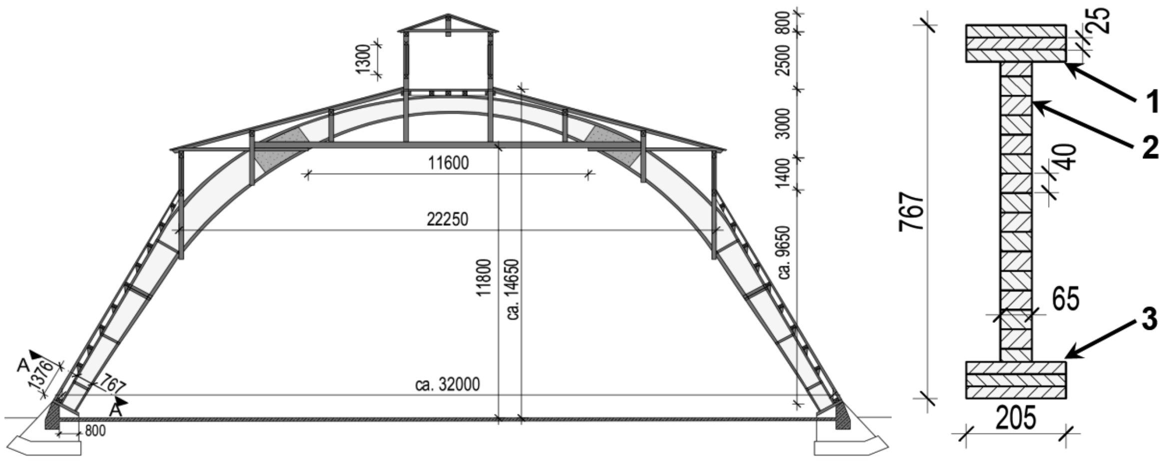

Figure 2: left: view on the truss construction; right: sectional view A-A – 1: top chord; 2: web; 3: bottom chord (all dimensions in mm)

The material had clearly visible marks of corrosion. The surface was greyish-brown discoloured and fibrous. The discolouration reached a depth of 20-25mm from the surface. Furthermore, the already mentioned separation of wooden strips could also be found. The Figure 3 shows the macroscopic appearance of the sample material exemplarily.

Figure 3: left: fibrous surface structure and greyish discolouration as well as salt deposits on the surface; right: sectional view on a chord and the web (the borders of the discolouration are marked in red, the glued joints are marked blue)

4 RESEARCH METHODOLOGY

4.1 Sampling

The material tests have been conducted on large scale specimen. Therefore, forty specimens were cut from the solid timber and glulam members who were salvaged after the demolition of the construction. Table 1 gives an overview on the amount and the dimensions of the examined specimen.

Table 1: dimensions of the examined specimen

Sample series	Sample size	dimensions b/h/ℓ [mm]	remarks
Solid timber	10	104/134/2376	
	30	86/176/2910	
glulam	10	65/141/2300	min. 3 lamellas per specimen
	30	63/100/1605	min. 3 lamellas per specimen

4.2 Determination of material properties according to EN 408

The main part of the comparative study was the determination of the material properties which are required for the classification according to EN 338 [11] (strength classes for solid timber) respectively EN 14080 [12] (strength classes for glued laminated timber). For this purpose the properties listed below are required to assign the samples to one of the strength classes in accordance with EN 338:2010 [11], article 6.2.2 as well as EN 14080:2013 [12], article 5.1.6.3:

1. characteristic value of the density ρ_k
2. characteristic value of the bending strength $f_{m,k}$
3. mean value of the modulus of elasticity parallel to the fibre direction $E_{0,mean}$

The bending strength as well as the modulus of elasticity was determined with the test method described in EN 408:2012 [13], articles 10 and 19. This test method is also known as 4-point bending test. This means that the specimen is placed on two supports while the test load is applied on two points on the top surface of the specimen (see Figure 4).

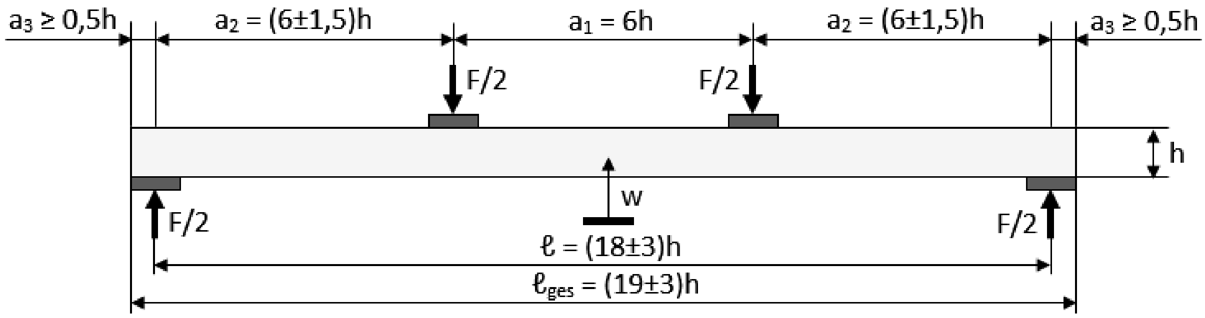

Figure 4: Test setup for the 4-point bending test according to EN 408:2012 [13], articles 10 and 19

The test load is applied with a constant velocity which is adjusted in a manner that the rupture of the specimen occurs after t = (300±120)s. During the tests the test load was measured with a digital load cell. The deflection in the middle of the specimen's span width was measured with two incremental position sensors.

The bending tests have been accompanied by the determination of the density according to EN 408:2012 [13], article 7 and the moisture content according to EN 13183-1:2002 [14].

4.3 Ultrasonic time-of-flight measurements

In advance of the bending tests ultrasonic time-of-flight measurements have been carried out on the specimen. The ultrasonic time-of-flight measurement is a non-destructive test method for the reliable determination of the physical and mechanical properties of timber members. The advantage of this test method is that it can be applied on timber members in existing constructions with relatively small. The knowledge of the limiting parameters is a necessary requirement for the reliable application.

Several studies concerning the application of the ultrasonic time-of-flight measurement for the strength grading of timber have been published in the last decades. The majority of these studies were carried out on new timber. There are only few studies regarding the application of this test method for the determination of material properties of old timber in existing constructions. Furthermore, these studies had a limited sample size and were object-related. Extensive systematically studies are still lacking until today (see [15]). This is particularly valid for timber members which were exposed to chemically-aggressive media.

The ultrasonic velocity of the sample material has been determined using the Sylvatest Trio (CBT CBS, Lausanne/CH, see Figure 5).

Figure 5: ultrasound measuring instrument Sylvatest Trio (CBT CBS, Lausanne/CH); left: measuring apparatus; right: measuring cables with transmitting and receiving probe

The time-of-flight of the ultrasonic impulse was measured directly (the probes were placed on both ends parallel to the grain) and indirectly (the probes were placed on one surface in an angle of 30° to the grain) in the longitudinal direction of the specimen (see Figure 6).

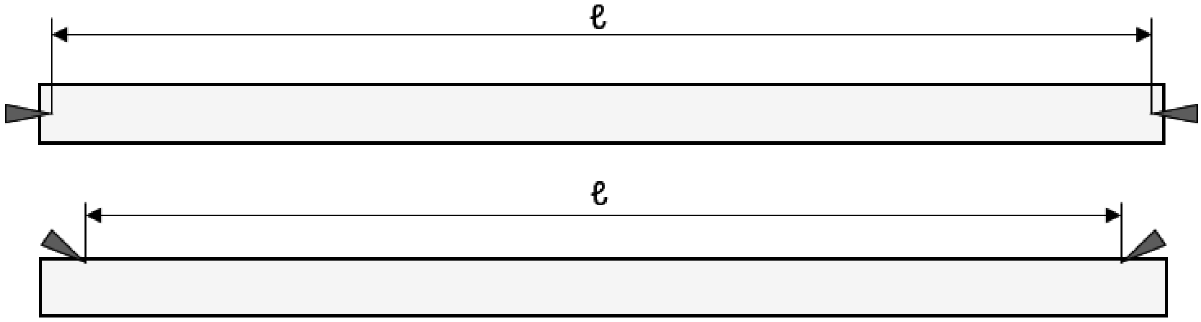

Figure 6: measuring setup; top: direct longitudinal measurement; bottom indirect longitudinal measurement

The environmental climate as well as the moisture content was determined in addition to the time-of-flight measurements and to interpret respectively to adjust the measured ultrasonic velocity. The environmental climate was determined with a digital thermo hygrometer (GANN Hydromette BlueLine Compact). The moisture content estimated by measuring the electrical resistance according to EN 13183-2:2002 [16] using the GANN Hydromette HT 85 with insulated electrodes (t = 45mm). The measured ultrasonic velocity has then been adjusted to reference conditions of ω = 12% (see equation (1)) and υ = 20°C (see equation (2)) with the empiric equations given in [17].

$$v_{12} = v_{\varpi} + 29 \cdot \left(\varpi - 12\right) \quad (\text{für } \varpi \leq 32\%) \tag{1}$$

where: v_{12} … ultrasonic velocity for ω = 12%; v_{ω} … ultrasonic velocity for $\omega \neq 12\%$; ω … moisture content

$$v_{20} = v_{\upsilon} \Big/ \left[1 - 0{,}0008 \cdot \left(\upsilon - 20\right)\right] \quad (\text{für } \varpi = 12\%) \tag{2}$$

where: v_{20} … ultrasonic velocity for υ = 20°C; v_{υ} … ultrasonic velocity for $\upsilon \neq 20$°C; υ … temperature

5 RESULTS & DISKUSSION

5.1 Failure behaviour

Usually only bending failures have to be expected in a 4-point bending test since the central part where the test load is applied is free of shear stress due to the test setup. The maximum of the shear stress is located at the supports. There, a shear failure can appear when the specimen has relatively low shear strength.

The tested sample material has shown inconsistent failure behaviour. The solid timber specimen failed mainly due to bending stress. Only five out of forty specimens have shown combined failure behaviour (see Figure 7).

Figure 7: exemplary illustration of a combined failure – sample series „solid timber“; left: bending failure between the support and the load application; right: shear failure along the growth rings on the support of the same specimen

Twenty of the forty tested glulam specimen failed due to bending stress. The other twenty specimens failed due to shear stress or showed a combined shear and bending failure behaviour (see Figure 8).

Figure 9: exemplary illustration of a combined failure – sample series „glulam“; left: bending failure in the centre of the specimen; right: combined failure with a bending failure beneath the load application and a shear failure along the glued joint

Generally, the sample material has shown typical fracture behaviour for macerated timber. The fractures were short-fibred and brittle. In some cases, wooden strips broke loose along the growth rings.

5.2 Density, bending strength and modulus of elasticity

The test result had to be adjusted due to a moisture content of ω ≠ 12%. The adjustment was carried out according to EN 384:2010 [18], article 5.3.4.2 as listed below:

- Density: reduction by 0,5% per %-point moisture content above ω = 12%; increase by 0,5% per %-point moisture content below ω = 12%
- Bending strength: no adjustment needed
- Modulus of elasticity: reduction by 1,0% per %-point moisture content below ω = 12%; increase by 1,0 % per %-point moisture content above ω = 12%

After the adjustment to a reference moisture content of ω = 12% the test results have been examined concerning statistical outliers according to the GRUBBS test. In the result no statistical outliers have been found.

The results of the statistical analysis of the adjusted physical and mechanical properties are listed in the tables 2 & 3.

Table 2: results of the statistical analysis of the density, bending strength and modulus of elasticity – sample series „solid timber“

	Density ρ [kg/m³]	Bending strength f_m [N/mm²]	Modulus of Elasticity E_m [N/mm²]
Quantity	40	40	40
Minimum	348,8	18,7	6009,1
Mean value	421,9	38,7	11225,4
Maximum	508,8	67,8	20614,8
Standard deviation	33,1	12,1	2836,6
Variation coefficient	7,8%	31,3%	25,3%
Characteristic value	379,6	19,2	11903,0

Table 3: results of the statistical analysis of the density, bending strength and modulus of elasticity – sample series „glulam“

	Density ρ [kg/m³]	Bending strength f_m [N/mm²]	Modulus of Elasticity E_m [N/mm²]
Quantity	40	40	40
Minimum	376,5	9,8	6143,4
Mean value	458,7	42,1	8919,4
Maximum	567,4	66,4	12104,6
Standard deviation	48,0	12,4	1426,1
Variation coefficient	10,5%	29,4%	16,0%
Characteristic value	377,6	19,1	6519,6

The statistical distribution of the material properties bending strength and modulus of elasticity are exemplary shown in figure 10.

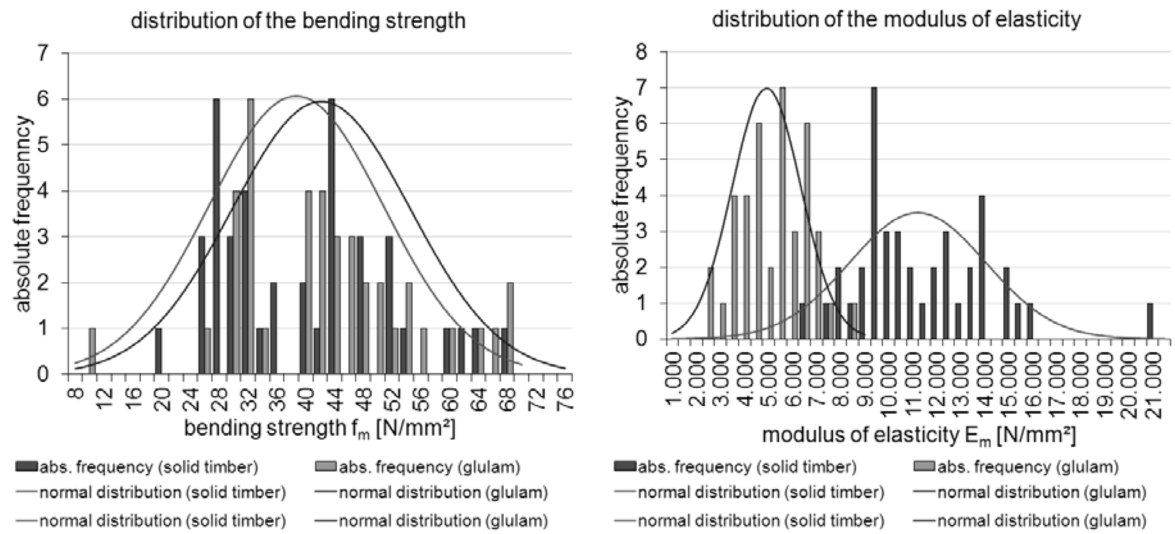

Figure 10: distribution of the bending strength and the modulus of elasticity

The evaluation of the test results is carried out as a comparison with the material properties of solid timber and glulam timber according to EN 338:2010 [11] and EN 14080:2013 [12]. The characteristic values of the tested sample material's properties were determined according to EN 384:2010 [18] (solid timber) as well as EN 14358:2007 [19] (glulam). The characteristic values are listed in table 2 & 3.

To assign the sample material to a certain strength class according to EN 338:2010 [11], article 6.2.2 respectively EN 14080:2013 [12], article 5.1.6.3.2 the characteristic values of the density ρ_k and the bending strength $f_{m,k}$ as well as the mean value of the modulus of elasticity $E_{0,mean}$ at least have to equal the characteristic and mean values of the corresponding strength class. In the case of solid timber the mean value of the modulus of elasticity has to equal at least 95% of the modulus of elasticity of a certain strength class.

The tested solid timber specimen can be assigned to the strength class C18 according to EN 338:2010 [11]. The characteristic bending strength is decisive for this assignment. Considering the characteristic density and the mean value of the modulus of elasticity an assignment to the strength class C30 are possible (see table 4).

Table 4: comparison between the characteristic values of the tested sample material (sample series „solid timber") and the characteristic values of solid timber of the strength classes C18, C24, C27 and C30 according to EN 338:2010 [11]

	solid timber	C18	C24	C27	C30
Density ρ_k [kg/m³]	379,6	320	350	370	**380**
Bending strength $f_{m,k}$ [N/mm²]	19,2	**18**	24	27	30
Modulus of elasticity $E_{0,mean}$ [N/mm²] (95% of the modulus of elasticity)	11903	9000 (8550)	11000 (10450)	11500 (10925)	**12000** **(11400)**

The tested glulam specimen cannot be assigned to a strength class according to EN 14080:2013 [12]. The characteristic bending strength as well as the mean value of the modulus of elasticity is decisive for this assignment. Considering the characteristic density an assignment to the strength class GL22h is possible (see table 5).

Table 5: comparison between the characteristic values of the tested sample material (sample series „glulam") and the characteristic values of homogeneous glulam of the strength classes GL20h, GL22h and GL24h according to EN 14080:2013 [12]

	glulam	GL 20h	GL 22h	GL 24h
Density ρ_k [kg/m³]	377,6	340	**370**	370
Bending strength $f_{m,k}$ [N/mm²]	19,1	20	22	27
Modulus of elasticity $E_{0,mean}$ [N/mm²]	6519,6	8400	11000	11500

The fact that the tested glulam specimen could not be assigned to a strength class of modern days homogeneous glued laminated timber according EN 14080:2013 [12] illustrates the necessity of a closer inspection of historic glulam constructions to exactly asses the material properties in the course of redevelopment or reconstruction projects.

5.3 Ultrasonic time-of-flight measurements

The comparative ultrasonic time-of-flight measurements have been evaluated with a linear regression analysis between the results of the time-of-flight measurements and the physical-mechanical material properties density, bending strength and modulus of elasticity. The correlation coefficients as well as the regression equations are listed below in table 6.

The correlation and regression analysis revealed that the relation between the measured ultrasonic velocity and the physical-mechanical properties of the sample material are partially very weak. Especially the relation between the ultrasonic velocity and the density of the solid timber specimen (directly & indirectly measured) and the glulam specimen (indirectly measured). The remaining correlation coefficients have a value between r = 0,147-0,470 which is a medial value at best.

Table 6: results of the correlation and regression analysis

Sample series “solid timber”	Directly measured ultrasonic velocity v_{dir}	Indirectly measured ultrasonic velocity v_{ind}
Density ρ	$r = 0{,}010$	$r = 0{,}097$
	$\rho = 0{,}002v_{dir} + 412{,}1$	$\rho = 0{,}013v_{ind} + 352{,}3$
Bending strength f_m	$r = 0{,}287$	$r = 0{,}441$
	$f_m = 0{,}017v_{dir} - 59{,}8$	$f_m = 0{,}021v_{ind} - 77{,}7$
Modulus of elasticity E_m	$r = 0{,}147$	$r = 0{,}323$
	$E_m = 2{,}041v_{dir} - 600{,}2$	$E_m = 3{,}583v_{ind} - 8737{,}7$
Sample series “glulam”	**Directly measured ultrasonic velocity v_{dir}**	**Indirectly measured ultrasonic velocity v_{ind}**
Density ρ	$r = 0{,}379$	$r = 0{,}037$
	$\rho = 0{,}119v_{dir} - 239{,}1$	$\rho = 0{,}007v_{ind} + 415{,}4$
Bending strength f_m	$r = 0{,}374$	$r = 0{,}340$
	$f_m = 0{,}030v_{dir} - 135{,}3$	$f_m = 0{,}017v_{ind} - 60{,}2$
Modulus of elasticity E_m	$r = 0{,}470$	$r = 0{,}323$
	$E_m = 4{,}409v_{dir} - 16843{,}3$	$E_m = 2{,}360v_{ind} - 5025{,}6$

The reason for such weak relations can be found in the effect of the chemically-aggressive media. The alteration respectively damage of the sample material due to the chemically-aggressive media in the peripheral cross section could not be exactly measured with the ultrasonic time-of-flight measurements. In fact, the measured ultrasonic velocity represents the unaffected core of the cross section whereas the determined material properties density, bending strength and modulus of elasticity are significantly affected by the chemically-aggressive media.

Previous studies on the extent of the alteration have revealed a thickness of the so-called corrosion layer of t = 5-10mm. Such a significant reduction of the load-bearing cross section has a clear effect on the mechanical properties. The same applies for the increased density under consideration of the determined salt content of up to 13% in the peripheral cross section (see [7]).

The regression equations for the bending strength and the modulus of elasticity of the tested sample material in comparison of the regression equations for new, unaffected spruce according to [20] are exemplary shown in figure 11. It is therefore obvious that the equations which were determined for bending strength of the tested sample material are quite congruent compared to the equations in [20]. Concerning the modulus of elasticity at least a similar progression can be recognised. Therefore it can be concluded that despite the weak correlation relation the ultrasonic time-of-flight measurement is an appropriate non-destructive test method to determine the strength respectively stiffness of the unaffected core section of solid timber and glulam members which have been exposed to chemically-aggressive media.

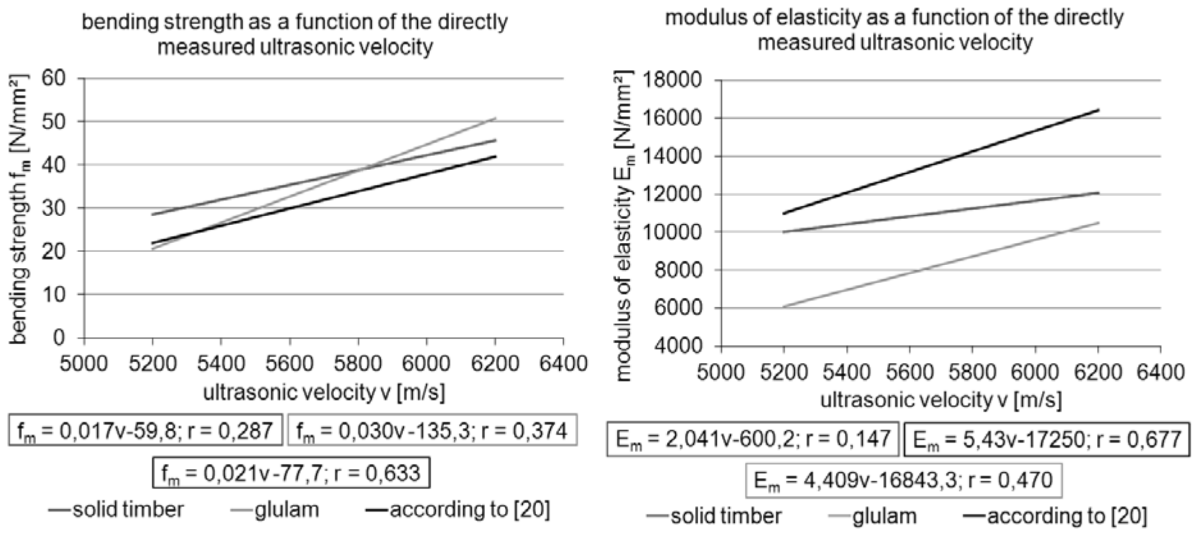

Figure 11: regression equations for the bending strength and the modulus of elasticity of the tested sample material and according to the literature [20]

6 CONCLUSIONS

The results of this study have proven the effected of chemically-aggressive media on the load-bearing capacity of solid timber and glulam which is apparent in the macroscopic alteration and destruction of the peripheral cross section as well as in the reduction of the strength and stiffness of the sample material.

A comparison with the normatively regulated characteristic material properties of new, unaffected solid timber and glulam clarifies this result.

The significant alteration respectively degradation of the material makes a detailed inspection of comparable existing structures in the course of redevelopment and reconstruction absolutely necessary. The particular focus has to be laid on the exact determination of the existent material properties.

The comparatively carried out ultrasonic time-of-flight measurements have shown that the damage of the material due to the effect of the chemically-aggressive media is could not be determined with this particular test method. The measured ultrasonic velocity represents the strength and stiffness of the unaffected core section.

Therefore, studies on comparable constructions should be carried out in the following manner:

- The extent of the damage – i.e. the thickness of the corrosion layer – can be precisely determined on drill cores with the help of the dynstat method
- The strength and stiffness of the unaffected core section can be measured with the ultrasonic time-of-flight measurement
- The density should be determined on drill cores as well

With a sufficient sample size the stability and load-bearing capacity of the construction can be exactly assessed and evaluated.

ACKNOWLEDGMENT

This study was financed by private donations. The authors would like to thank the donors for the generous support.

LITERATUR

[1] Rug, W. 1994. „Innovation im Holzbau – Die Hetzerbauweise (Teil 1)“. *Bautechnik* 71(4), PP: 213–219.

[2] Rug, W. 1995. „Innovation im Holzbau – Die Hetzerbauweise (Teil 2)“. *Bautechnik* 72 (4), PP: 231–241.

[3] Rug, W. 2006. „100 Jahre Hetzer-Patent“. *Bautechnik* 83(8), PP: 533–540.

[4] DRP. 197773. 1906. Gebogener Holz-Bauteil für vereinigte Dach-Pfosten und -Sparren

[5] Rug, W. and Lißner, A. 2011. “Untersuchungen zur Festigkeit und Tragfähigkeit von Holz unter dem Einfluss durch aggressive Medien“. *Bautechnik* 88(3),PP: 177–188.

[6] DIN EN 1995-1-1:2010 – Eurocode 5: Bemessung und Konstruktion von Holzbauten – Teil 1-1: Allgemeines – Allgemeine Regeln und Regeln für den Hochbau.

[7] Rug, W., Linke, G. and Lißner, A. 2016. “Studies on the wood corrosion on a historic glu-lam-construction”. World Congress on Timber Engineering 2016, Vienna (Austria), PP: 3048-3057

[8] Linke, G. 2016. “Study on the glued joints of historical glued laminated timber”. Young Engineers Colloquium 2016, Hamburg (Germany)

[9] Haupt, M. 2013. “Festigkeitsuntersuchungen an historischem Brettschichtholz”. Diploma thesis. University of sustainable Development, Eberswalde (Germany)

[10] Piotter, L. 2014. “Festigkeitsuntersuchungen an mazeriertem Vollholz”. Diploma thesis. University of sustainable Development, Eberswalde (Germany)

[11] DIN EN 338:2010 – Bauholz für tragende Zwecke – Festigkeitsklassen

[12] DIN EN 14080:2013 – Holzbauwerke – Brettschichtholz und Balkenschichtholz – Anforderungen

[13] DIN EN 408:2012 – Holzbauwerke – Bauholz für tragende Zwecke und Brettschichtholz – Bestimmung einiger physikalischer und mechanischer Eigenschaften

[14] DIN EN 13183-1:2002 – Feuchtegehalt eines Stückes Schnittholz – Teil 1: Bestimmung durch Darrverfahren

[15] Linke, G., Rug, W. and Pasternak, H. 2017. “Festigkeitssortierung von Bauholz in historischen Gebäuden – Bericht zum Stand der Technik”. *Bauingenieur 92* (05-2017), in preparation

[16] DIN EN 13183-2:2002 – Feuchtegehalt eines Stückes Schnittholz – Teil 2: Schätzung durch elektrisches Widerstands-Messverfahren

[17] Sandoz, J.-L. 1993. „Moisture content and temperature effect on ultrasound timber grading“. Wood Science and Technology 27 (5), PP: 373-380

[18] DIN EN 384:2010 – Bauholz für tragende Zwecke – Bestimmung charakteristischer Werte für mechanische Eigenschaften und Rohdichte

[19] DIN EN 14358:2007 – Holzbauwerke – Berechnung der 5%-Quantile für charakteristische Werte und Annahmekriterien für Proben

[20] STEIGER, R.1991. „Festigkeitssortierung von Kantholz mittels Ultraschall“. *Holz-Zentralblatt Nr. 59* (1991), PP: 985-989

SHATIS'17
4th International Conference on
Structural Health Assessment of Timber Structures
20-22 September 2017 Istanbul, Turkey

DETERMINATION OF BEARING STRENGTH OF WOOD PEG CONNECTIONS

Gi Young Jeong[1], **and Jin Hyuk Kong**[1]

[1] Chonnam National University

Keywords: Connection, Wood Peg, Glulam

Abstract

Wood peg connections have been used in timber frame building. However, there is a lack of study on bearing strength of wood peg connections.

The objective of the study is to determine the bearing strength of different orientation of wood peg connections. The bearing strength of wood peg connection was evaluated using methods from ASTM D 5764, Church and Tew (1997), Schmidt and Daniels (1999), and test method from the current study. Specimens including two differently oriented wood pegs parallel to the grain (PA), perpendicular to the grain (PE) and two differently oriented main members associated with wood peg positions (RL-PA, TL-PA, RL-PE, TL-PE) were prepared.

The results showed that bearing strength values of wood peg connection were significantly influenced by the orientation of main member and wood peg. When the bearing test for wood peg connection was conducted based on the current test method, the load-displacement curves were highly different by peg orientation. The load-displacement curve from ASTM D 5764 (2013) did not show yield load. The load-displacement from Church and Tew (1997) showed the highest difference was observed compared to the load-displacement evaluated from the other methods. The load-displacement curve from Schmidt and Daniels (1999) did not show a distinctive difference by main member and peg orientation.

1 INTRODUCTION

Wood peg connections have been used to connect beam to beam, column to beam, column to column in timber frame building. Due to the grain orientation of wood, different loading conditions could be applied to the main member and wood peg. The current design guideline for dowel-type connection may apply for wood peg connection, however, it is doubt that the current design guidelines in building code could be used for the prediction of the bearing properties of wood peg and wood peg connection associated with differently oriented main member.

To predict the bearing properties of wood peg connection, experimental test data associated with failure behavior is crucial to develop equations. Thus, the current study, different test methods were compared to obtain bearing properties of wood peg connections. Church and Tew (1997), Schmidt and Daniels (1999) and ASTM D 5764 (2013) showed different test methods for bearing properties of wood peg connection. The three previous methods and the new method were compared for the determination of bearing properties of differently oriented wood peg connections. Digital image correlation was used to capture strain distribution of wood peg connection.

2 MATERIALS AND METHODS

2.1 Materials

Figure 1 shows differently oriented main members and wood peg made of ash. Main member was 5-ply glulam made of Japanese cedar. The first letter indicated the plane perpendicular to the loading direction. The second letter indicated the loading direction. Different diameters of wood peg was fabricated from ash tree. Two different wood peg grain directions including PA (parallel to the load direction) and PE (perpendicular to the load direction) were tested associated with the different orientation of the main member. To evaluate a reliable test method for wood peg connection, two different orientations of the main member defined as the radial-longitudinal (RL) and tangential-longitudinal (TL) and wood peg of 20mm diameter were prepared.

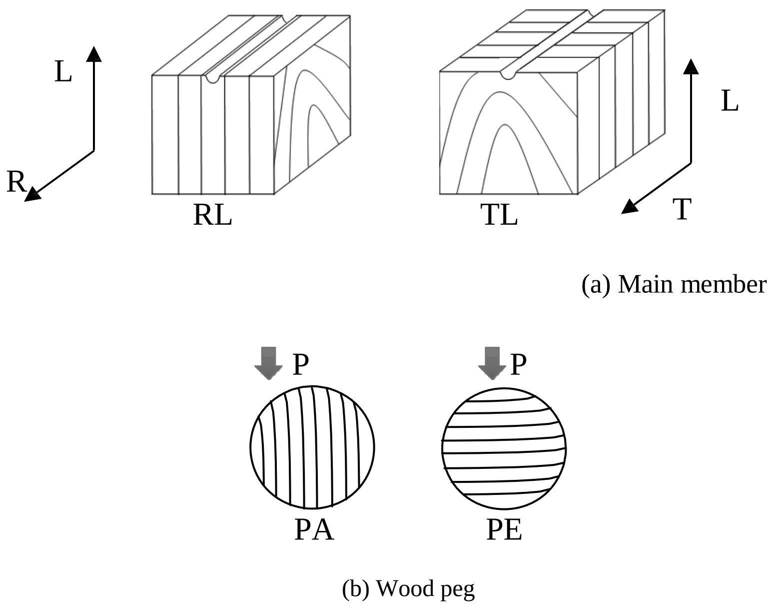

Figure 1: Six differently oriented glulam associated with pin position

2.2 Methods

To evaluate the bearing properties of wood peg connection, methods from ASTM D 5764, Church and Tew (1997), Schmidt and Daniels (1999), and the current study were conducted. Universal testing machine (UTM) equipped with a 150kN load cell was used to apply compression load. The load was applied until the load was dropped 60% from the peak load. Digital image correlation (DIC) was used to analyse the strain distributions for the different test methods.

Figure 2 shows the different test methods to evaluate the bearing properties of wood peg connection. Figure 2a shows ASTM D 5764, which applies the load directly to the wood peg. Figure 2b shows the method used in Church and Tew (1997), which applies the load to the main member to avoid crushing of wood peg. Figure 2c shows the methods suggested from Schmidt and Daniels (1999). This method needs to conduct two separate bearing tests for main member and wood peg. Load-displacement curves from main member and wood peg were analytically combined to calculate bearing properties of wood peg connection. Figure 2d shows the method used in the current study, which used the metal plate with a semi cylindrical slot to prevent the crushing of the wood peg. The load was applied to the main member.

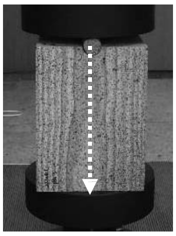
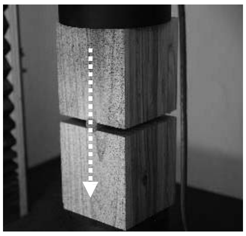

(a) ASTM D 5764 (b) Church and Tew (1997)

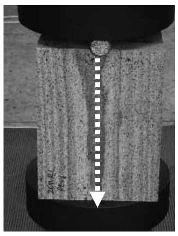


(c) Schmidt and Daniels (1999)

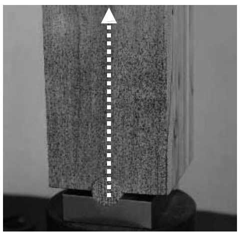

(d) The current study

Figure 2: Path to capture strain distributions of wood peg connections from different test methods

Figure 3 shows experimental test setup to determine bearing properties of differently oriented wood peg connection using the method in the current study. Universal test machine equipped with a 150kN load cell was used. To analyse strain distribution of wood peg connection, a digital image correlation technique was applied. Two CCD camera was mounted on a stereo plate with the distance of 35 cm between two cameras. The angle of camera was adjusted to see the same point of view in the specimen. The distance between camera and object was 50cm to provide enough field of view to analyse the strain distribution of the specimen and clear image. To obtain proper contrast, a LED lamp was used to light specimen evenly.

The image was taken at a rate of 10 frame until the specimen was failed or after yield. The resolution of the image was 640×480 pixel. The pixel dimension was $7.4\,\mu m \times 7.4\,\mu m$. Digital image correlation was conducted using Aramis software (GOM).

Figure 3: Bearing test associated with DIC set-up for bearing properties of wood peg connection

3. RESULTS AND DISCUSSION

Bearing properties of differently oriented wood peg connections were determined from different test methods (Figure 4). The two solid lines indicated that bearing strength of wood pegs in PA (loading direction is to parallel to the grain) and PE (loading direction is to perpendicular to the grain). While the highest difference of bearing strength by peg orientation was found from the current method, bearing properties from the other methods were not significantly different by wood peg orientation. When bearing properties of wood peg connection from Church and Tew (1997) were compared, the bearing strength of RL with PE was higher than the bearing properties of TL with PA.

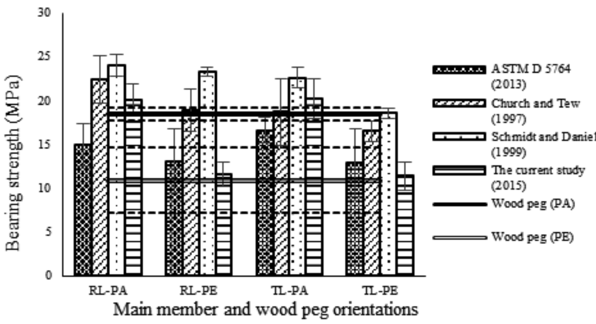

Figure 4: Bearing strength of differently oriented specimen evaluated from different test methods.

Figure 5 shows load-displacement curves of wood peg connection from different test methods. The load-displacement curve from ASTM D 5764 (2013) did not show yield load. This is due to the fact that the load applied directly to wood peg and wood peg was crushed and densified simultaneously, which resulted in load increase continually. The loaddisplacement from Church and Tew (1997) showed yield load. The load-displacement curve from RL-PA and TL-PA, and from RL-PE and TL-PE using the method from Church and Tew (1997), the highest difference was observed compared to the load-displacement evaluated from the other methods. The load-displacement curve from Schmidt and Daniels (1999) did not show a distinctive difference by main member and peg orientation. The results were due to the fact that the method from Schmidt and Daniels (1999) used the load-displacement curves from main member and the load-displacement curve from wood peg and combined the load-displacement based on the same displacement point. When the load-displacement curves were combined, the load-displacement curve from main member controlled the entire curve. Therefore, the results of the load-displacement curves from Schmidt and Daniels (1999) would be similar as shown in Figure 5. The load-displacement curve from the current study showed the highest difference by wood peg orientation. The load-displacement curve from RL-PA and TL-PA showed a similar trend and the load-displacement curve from RL-PE and TL-PE showed a similar trend.

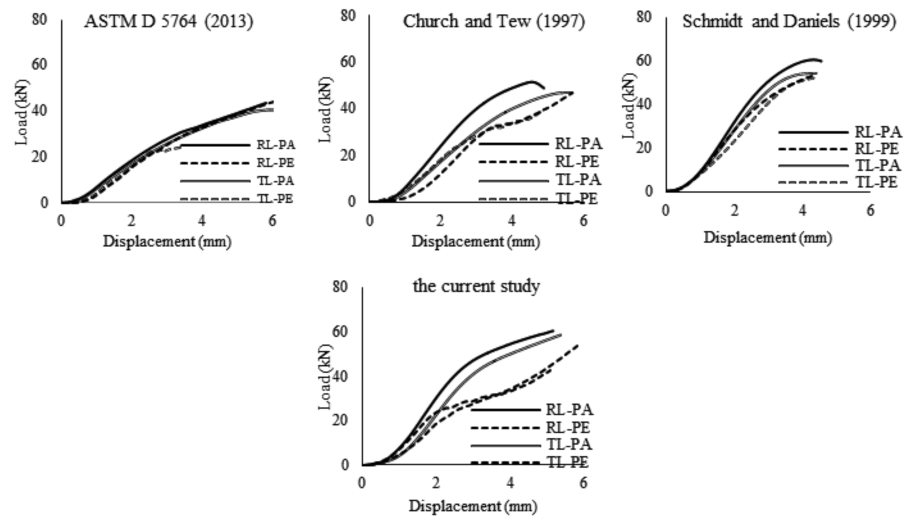

Figure 5: Load-displacement curves from different test methods

Figure 6 shows the strain values along the path from the different test methods. From ASTM D5764 (2013), two peaks observed in the upper tip of wood peg near a loading head and bearing area. From Church and Tew (1997), the highest strain occurred at bearing area. From Schmidt and Daniels (1999), the highest strain occurred at the bearing area but showing the lowest strain values compared to the other test methods. From the current test method, the highest strain values occurred at the bearing area around the bearing area. Comparing the four different test methods, the current test method showed the highest strain values around the bearing area between the main member and wood peg.

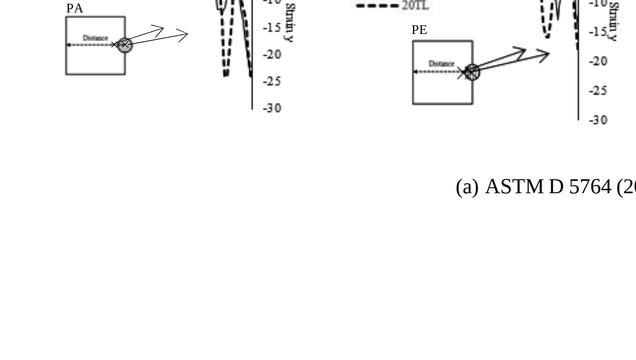

(a) ASTM D 5764 (2013)

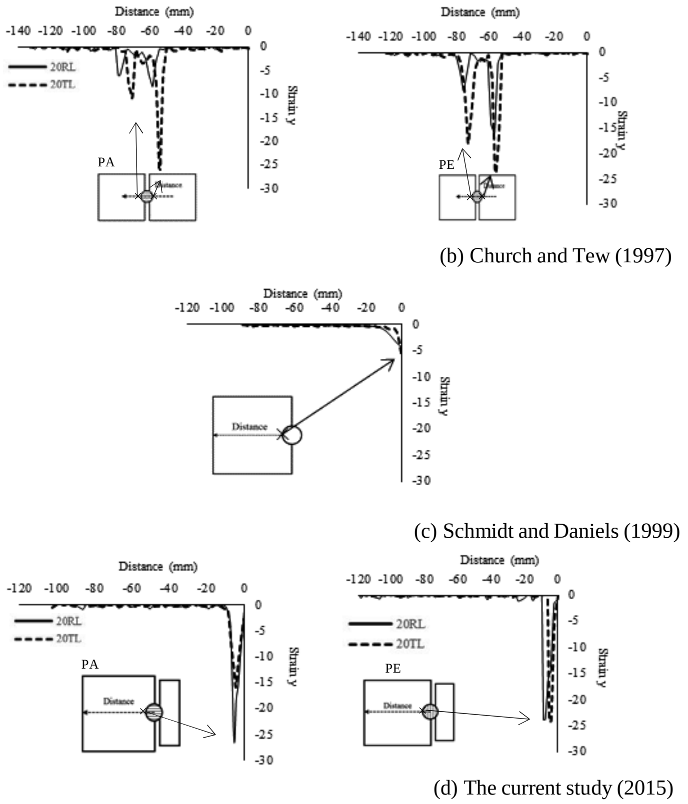

(b) Church and Tew (1997)

(c) Schmidt and Daniels (1999)

(d) The current study (2015)

Figure 6: Strain values along the path from different test methods

4. CONCLUSIONS

To determine bearing strength of wood peg connection, different test methods were evaluated. When the bearing test for wood peg connection was conducted based on the current test method, the load-displacement curves were highly different by peg orientation. The strain distribution from the method suggested in this study showed the high strain distribution occurred around bearing area between wood peg and main member. The smallest difference of the bearing strength between RL-PE and TL-PE was found since wood peg failure occurred from RL-PE and TL-PE. From the bearing strength of differently oriented wood peg connections and strain distributions, the current test method could be applied for the determination of bearing strength of wood peg connection.

REFERENCES

[1] ASTM. 2013. “.Standard test method for evaluating dowel-bearing strength of wood and wood based products (D5764-97a). Annual book of standards, vol.04.10. Philadelphia(PA), USA. America Society of Civil Engineer.

[2] Church, J. R., and Tew, B. W. 1997. Characterization of bearing factors in pegged timber connections. J. Struct. Eng. 123(3):326-332.

[3] Schmidt, R. J., and Daniels, C. E. 1999. Design considerations for mortise and tenon connections. Research report, Department of Civil and Architectural Engineering, University of Wyoming, Laramie, WY 82071.

CHAPTER VI

INTERVENTION, RESTORATION AND PREVENTION

SHATIS'17
4th International Conference on
Structural Health Assessment of Timber Structures
20-22 September 2017 Istanbul, Turkey

IN PROGRESS RESTORATION OF THE GOLDEN PALACE MONASTERY IN MANDALAY, MYANMAR

Stephen J. Kelley, FAIA, SE, FAPT, FUSICOMOS[1]

[1] Consultant, World Monuments Fund

Keywords: teak, traditional construction, termites, water management, diagnosis, treatment

Abstract

The World Monuments Fund with an Ambassadors Grant for Cultural Preservation has been involved with the restoration of the Golden Palace Monastery in Mandalay, Myanmar. The monastery, built in the traditional Burmese architectural style, is known for its teak carvings of Buddhist myths, which adorn its walls and roofs.

The wooden structure was originally located at the royal palace when Mandalay was founded by Mindon Min in 1858. Upon Mindon Min's death, his heir, ordered the building dismantled and removed from the palace. It was relocated in the eastern part of Mandalay and reconstructed in 1883 as a monastery. The Monastery fell into disrepair during World War II. Allied bombings at the end of WWII caused severe damage in Mandalay; and the rest of the wooden structures within the Mandalay Royal Palace burned as a result of Allied bombing; but the Golden Palace Monastery due to its move from the Palace site escaped the direct impact of the bombing.

A low tech methodology was followed during the WMF assessment and diagnosis. It was determined that the entire wooden structure was in good to fair condition except for the veranda posts. Therefore, a structural intervention was recommended that will address the peripheral columns that support the veranda. The intervention entails carefully dismantling the veranda and veranda balus-trade, removal of all posts and assess whether they can be reused, repair of replacement of the posts and careful reassembly of the veranda using the same materials if at all possible. All new posts would be composed of teak. A new culvert system beneath the veranda of the monastery to carry away groundwater has been proposed. The work is being carried out in stages so that the Golden Palace Monastery can remain open during the intervention.

1 INTRODUCTION

The World Monuments Fund (WMF) with an US Ambassadors Grant for Cultural Preservation has been involved with the restoration of the Golden Palace Monastery (Shwe-nandaw Kyaung) in Mandalay, Myanmar.

The Golden Palace Monastery is an authentic example of 19th Century Konbaung teak architecture and also a significant work of decorative wood-carving. It is a large multi-tiered building with four separate roof levels. Carved wooden flame-like decorations define the roof lines, which also contain abundant embellishment and ridge and corner roof ornaments as well as numerous avian creatures. There are rich carvings on the bargeboards of the roof eaves. Surrounding the building at the main entry level is an imposing teak veranda with elaborately carved balustrades and marble finials atop the support posts.

The building interior consists of a main hall to the east and a reception hall to the west, with a Buddhist image on the altar in the main hall facing east. Both the main and reception halls reveal the layered roofs above, and the topmost ceiling is supported by the central 10 longest pillars. The interior surfaces are finished in lacquer and gold leaf.

1.1 Significance

The monastery, built in the traditional Burmese architectural style, is known for its teak carvings of Buddhist myths, which adorn its walls and roofs. Unique to the monastery are the wood figures affixed to the outside walls of the structure and the inner partition.

The Golden Palace Monastery remains as one of Myanmar's most significant buildings because of its relation to Mindon Min. It is the only remaining wood palatial structure built by King Mindon Min. The Golden Palace Monastery is the only surviving structure of the former royal palace of Mandalay and therefore represents an invaluable testimony of one of the most important cultural practices in pre-modern Myanmar, that of building wooden structures encapsulating deep symbolism.

The Golden Palace Monastery was one of seven monasteries protected by the Archaeological Survey of Burma from 1919 on the grounds of their historical and architectural significance. Out of those seven monasteries listed, only the Golden Palace Monastery remains.

1.2 Acknowledgements

The author would like to acknowledge His Excellency U Aye Myint Kyu and the Ministry of Culture, and the Department of Archaeology and National Museum, especially its Mandalay Division. International consultants involved with the restoration include Rudy Christian of the USA, Alexey Kirichenko of Russia, Chris Marrion of the USA, Brian Ridout of the UK, Francois Tainturier of France, and the author. All consultants were led by Jeff Allen of the World Monuments Fund.

2 BUILDING HISTORY AND CHRONOLOGICAL DEVELOPMENT [1]

2.1 Mindon Min

Mindon Min (1808 – 1878) was the penultimate king of Burma and served from 1853 till his death in 1878. He founded the last royal capital of Burma in Mandalay in 1857. He was one of the most popular and revered kings and spent most of his reign modernizing the kingdom and defending the northern portion from British encroachments. His reign was notable as a period of cultural flowering before the imposition of total British colonial rule. His new capital, with palaces and monasteries, were masterpieces of traditional Burmese architecture.

The wooden structure now known as the Golden Palace Monastery was originally located at the royal palace when Mandalay was founded by King Mindon in 1858. It was situated to the north of the *Hman-nan*, 'Glass Palace' off the main East-West axis, symbolically the most important of the complex. Known as the Mya Nan San Kyaw, it was a part of Mindon Min's royal apartments and was the pavilion in which King Mindon died in 1878.

2.2 Relocation of the Structure

Upon Mindon Min's death, his son and heir, Thibaw became convinced that his father's spirit still haunted the grounds, so he ordered the building dismantled and removed from the palace. It was relocated in the eastern part of Mandalay east of the Atumashi Kyaung where most of the religious structures built by King Mindon were located. The building was reconstructed over the course of five years at its present site as a monastery dedicated in 1883 as a work of merit to the memory of Mindon Min (Figure 1). It was also renamed "Goolden Palace Monastery" as the monastery both outside and inside was lacquered and gilt.

Figure 1: The Golden Palace Monastery from the south as it appeared in 1905.

Eight years after his death the northern portion of Burma fell to Britain as a result of the Third Anglo-Burmese War. Because of its relocation outside the royal palace in 1883, the Golden Palace Monastery did not experience any looting. It miraculously escaped major fires in 1890 and 1894 which destroyed the nearby Atumashi Kyaung.

2.3 Damage and Maintenance in the 20th Century

The SNDK was declared "protected monument" in 1908 along with seven other Mandalay teak monasteries under the provisions of the Ancient Monuments Preservation Act, VII, of 1904. Upkeep of the monastery principally consisted of patching the roof and floor; applying earth oil to the timber elements as a treatment for termite attack; and clearing of jungle around the building.

The monastery fell into disrepair during World War II, and the structure was occupied by Japanese soldiers who were reported to have used the decorative wood panels as fire wood. Allied bombings at the end of WWII caused severe damage in Mandalay; and the rest of the wooden structures within the Mandalay Royal Palace burned as a result of Allied bombing; but the Golden Palace Monastery due to its move from the Palace site escaped the direct impact of the bombing.

After WWII, maintenance was left entirely to the monks. The monastery was re-listed as a protected monument in 1956-7, and various minor repair works followed this listing. A documentation process was intermittently followed in the post WWII, Independence, and post-1962 periods by the Department of Archaeology. In 1962 the existing roof was replaced by a new painted corrugated roof.

Most of the decorative wood carvings on the roof did not survive into the post War period. However, from the late-1960s to the mid-1970s restoration work concentrated on having the four roof tiers and roof ridges of the north elevation completely decorated with carved panels.

Figure 2: Concrete buttresses added in 1991 to counteract a westward lean of the structure.

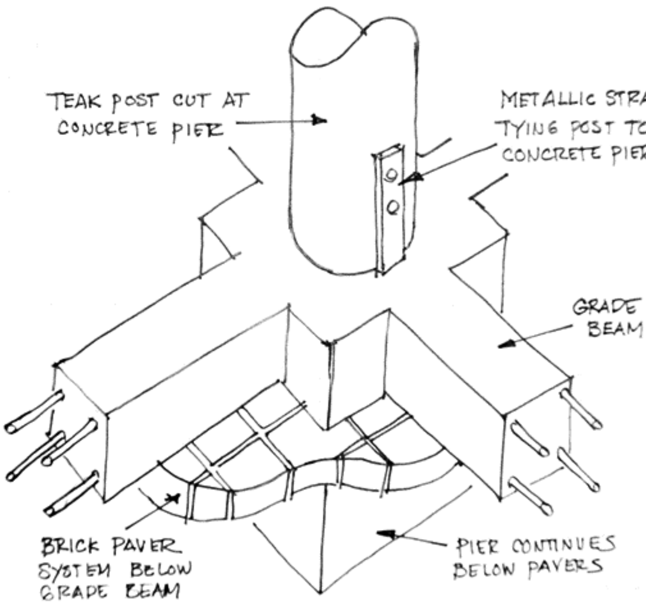

Figure 3: Concrete collar beams added at interior posts at grade to stabilize post leans.

2.4 The 1995-1996 Restoration Campaign

In 1990-91, a major intervention was undertaken with the construction of three reinforced concrete buttresses on the western part at the ground level of the building designed to stop the structure from leaning further towards the west (Figure 2). The 1995-96 restoration campaign, work focused on placing the leaning posts back into their vertical position. The procedures to accomplish this included: digging around the base of the leaning posts where the leaning occurs; righting the posts and filling the hole with concrete to prevent the structure from further leaning; forming a reinforced concrete grid that collared all the interior posts at grade (Figure 3); and the installation of steel brackets that further engaged the post to the concrete grid. Carved roof panels were installed at the roof eaves of the three remaining sides of the building: east, south, and west.

3 CONSTRUCTION TECHNOLOGY

3.1 Teak as a Building Material [2]

Myanmar is amply endowed with teak in the dry forests and on the southern and western slopes of the lower hills of Myanmar. Teak (*Tectona Grandis*) is a deciduous hardwood tropical tree that grows to maturity in 60 to 80 years. It is a moderately hard wood that is relatively impervious to changes in temperature and moisture. Teak has a natural resistance to termites because it contains chemicals (quinones) that repel the insects. The mature heartwood of teak, which makes up the bulk of the large posts in teak monastery construction contains most of the quinines and is therefore largely immune from attack. If, however, the heartwood is colonized by a fungus then these chemicals are broken down and the wood becomes available to the termites.

3.2 Wooden Framework and Siding [2]

The Golden Palace Monastery is composed of wooden posts that were originally set in the ground and that are connected at the first floor level with heavy timbers. Nails were not widely used as connectors. Rather the beams and joists were connected to the posts by mortise and tenon with the beams being threaded through mortise holes in the poles and then shimmed to fit tightly (Figure 4). This method provided moment frame stability, allowed for dismantling and reassembly, and repairs could be performed with relative ease.

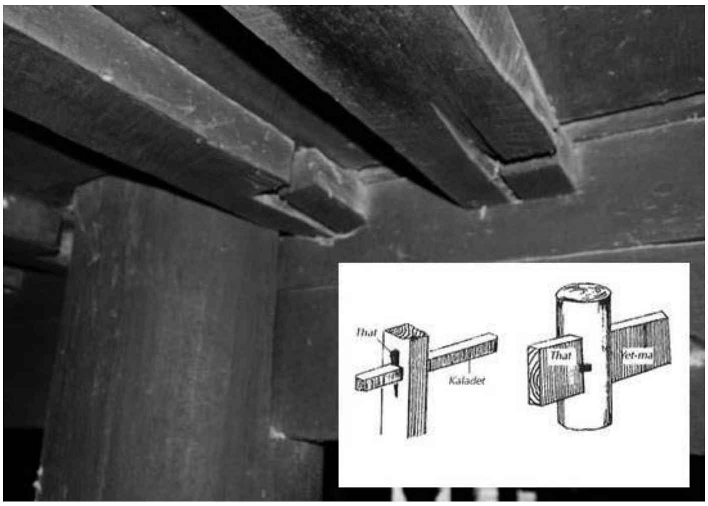

Figure 4: Mortise and tenon post and beam construction.

The roof framing is in four tiers with each tier expressed on the interior ceilings, the top layer with a false level ceiling. There are 104 pillars inside the building, and 46 pillars in the periphery of the veranda with caps in marble. The exterior of the veranda features balustrades of carved decorative panels.

The building exterior is clad in barge board with applied carved wooden features. The exterior of the building was once gilded, though only vestiges of the gilding remain. The exterior exposed framework and the decorative carvings at the first level and below have been treated in the past with an application of earth oil which gives them a dark color.

3.3 Interior Finishes

The building interior consists of two spaces: a main hall in the west and a reception hall in the east, with a Buddhist image on the altar in the main hall facing east. In the periphery of these adjacent halls is the surrounding veranda. Almost all of the inside of the monastery except for the floorboards are gilded (Figure 5).

Figure 5: Interior view looking westward at the Buddha altar.

3.4 Roofing

Above the enclosed space are a series of four cascading gable and shed roofs with dormer roofs to the east and west. The eaves, fascia and ridge boards are festooned with highly ornamental teak carvings the fascia decorative carvings stand above the drip line of each level of the roof.

The roof slopes are clad in corrugated sheet metal roofing that is painted red. Built in gutters are at all drip lines and are obscured by the carved fascia panels. The original roofing system, wooden batten boards that are oriented along the slope, are still present beneath the corrugated roof.

3.5 Foundations [2]

In the erection of wood monasteries the pillars were placed about 1.5 meters into the soil and set on brick or stone bases. The tallest posts were set first, which would typically be in the middle of the structure.

4 DIAGNOSIS

4.1 Methodology

The Golden Palace Monastery, though quite precious, is a rather simple structural system. It was determined that the investigative work leading up to the diagnosis could be a physical condition survey utilizing simple diagnostic techniques. The following methodology was followed during the assessments:

4.1.1 Visual inspection of the structure from the ground, platform level, interior and roof.

4.1.2 Inclination measurements, sounding and moisture content readings of posts at the ground and platform levels.

4.1.3 Selective drilling coring of posts at the ground level.

4.1.4 Performing soils analysis.

4.2 Visual Inspection [3]

From the visual inspection two types of termites were found attacking the teak. The first is a subterranean species *Hypotermes xenotermitis*. These are termites that nest underground and feed on rotting wood and organic debris (Figure 6). They will forage up from the nest in rot pockets or juvenile wood within the timber, in tubes constructed from mud and feces or behind patches of mud plaster. The second was a species of dry wood termite, which was located by small heaps of termite 'frass'. This is probably a species of *Cryptotermes*. Dry wood termites do not need to be in contact with the ground but they still prefer damp conditions and will only attack teak decayed by fungi. Most of the decay and termite damage is associated with the veranda posts.

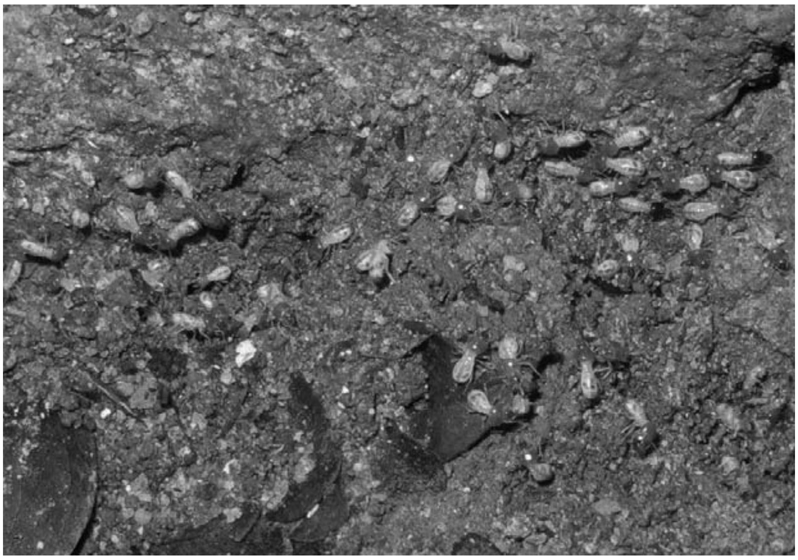

Figure 6: Subterranean species *Hypotermes xenotermitis* (photo by B. Ridout).

4.3 Inclination measurements, sounding and moisture content of the posts [4,5]

The leans in each of the posts were measured at 4 cardinal directions at the ground and platform levels. Because the posts taper four measurements were made at each cardinal face to account for the taper in the lean calculations. At the ground level the greatest leans are in the magnitude of 4 degrees but leans of such magnitude are rare. The orientation of the post lean has no strong pattern but otherwise might be characterized as outward. Interior posts with unique leans must have been either erected or repaired with these leans in place. At the platform level the largest leans are in the magnitude of 1 degree which is not significant. There is no apparent lean of the overall structure (Figure 7).

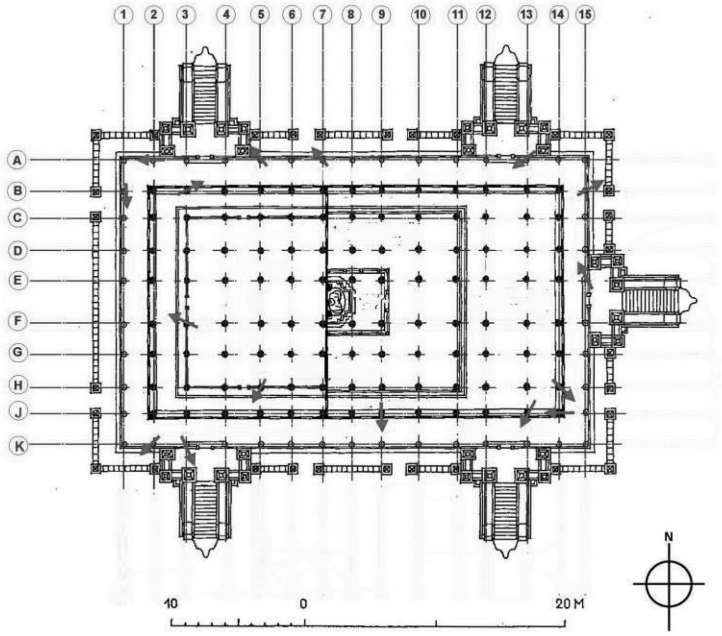

Figure 7: Red arrows indicate significant leans at the ground level.

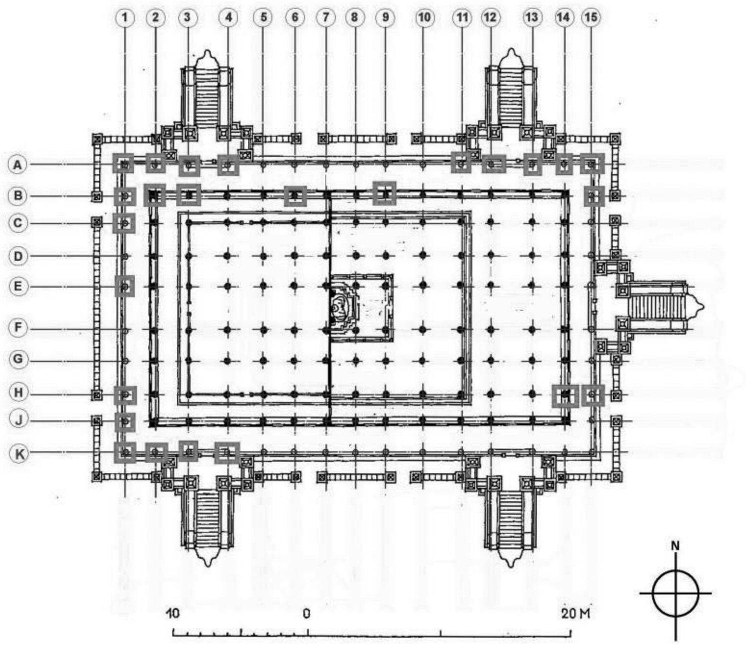

Figure 8: Green squares designate posts that were found to be in poor condition due to sounding.

Each of the posts were sounded at ground and platform levels with a hammer. During the sounding each post was rated as good, fair or poor. The posts rated poor were beneath the veranda in all cases, and it is concluded that this is due to their exposure to rainwater (Figure 8).

A measurement of the moisture content (MC) in each of the posts and selected beams was obtained using electrical resistance with the aid of a ***Delmhorst Moisture Meter***. The results of these measurements reveled that only some of the veranda columns had elevated moisture contents.

4.4 Selective coring of posts at the ground level [4,5]

Nine wood plugs, each of 1 cm diameter, were removed from eight posts at the ground level. At eight locations, the wood, though varying in density based on the resistivity in drilling, was found to be sound throughout the depth of the sample. There was no sign of either termite or fungal decay (Figure 9).

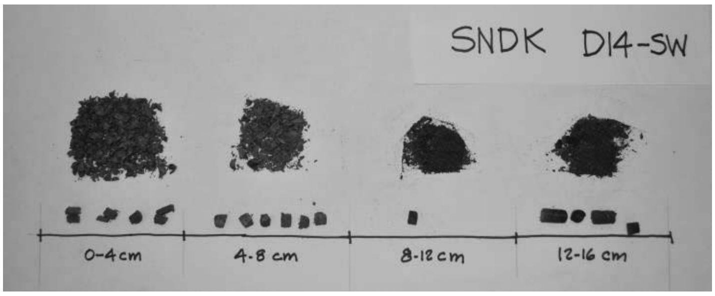

Figure 9: Representative sample of one of the nine 1 cm diameter cores removed from the posts.

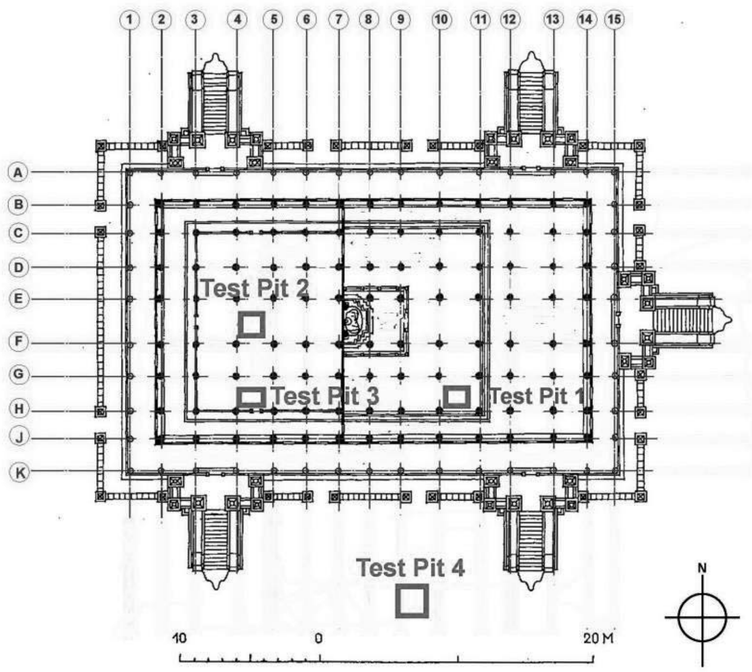

Figure 10: Location of the three test pits beneath the monastery (plus one to the south of the monastery).

4.5 Soils Analysis [4,5]

Three test pits were hand-dug beneath the monastery (Figure 10). It was discovered that there were concrete and brick piers below each interior post indicating that the posts had been encapsulated below grade by an added concrete foundation (Figure 3). It was also discovered that baked clay pavers were in place directly below the added grade beams and the basement level had been raised. Further probing of the veranda posts indicted that 42 of the posts have been cast into a concrete foundation and penetrate that foundation by 4 to 8 inches. The posts are in an extreme state of decay where they go below the concrete slab.

The Golden Palace Monastery is located on the flat, expansive, alluvial flood plain of the Irrawaddy River. The three test pits beneath the monastery and a fourth located to the south of the monastery reveal that the clay is damp and compacted. The soil was found to be a clay with high plasticity in the upper 1.5 meters and low plasticity below. Fat clay extends down to about 3 meters with lean clay below. These are poor soils for infiltration. The soils will become saturated quickly, and it would not take very intense rain to exceed the soil infiltration capacity, producing runoff. As the soils are not favorable for infiltration, the drainage solution would likely lend itself toward the conveyance-based approach.

5 TREATMENT

Repair treatments of the monastery follow principles of conservation, defined as maintaining and managing change to a heritage asset in a way that sustains and where appropriate enhances its significance. Treatment recommendations follow principles laid out the *Venice Charter*, *Nara Document, Principles for the Conservation of Historic Timber Structures*, and *ISCARSAH Principles*.

5.1 Structural intervention on the veranda posts

It was determined that the entire wooden structure was in good to fair condition except for the veranda posts. This finding is due to the long-term exposure of these posts to water infiltration. Therefore, a structural intervention is recommended that will address the 46 peripheral columns that support the veranda on all four sides. The intervention entails carefully dismantling the veranda and veranda balustrade, removal of all posts and assess whether they can be reused, repair of replacement of the posts and careful reassembly of the veranda using the same materials if at all possible (Figures 11 and 12). All new posts would be composed of teak.

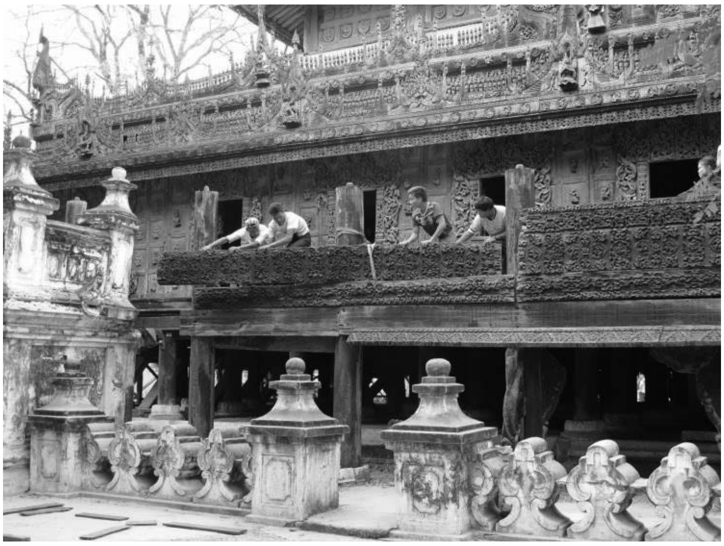

Figure 11: Removal of the decorative balustrade boards on the north elevation of the monastery (photo by R. Christian).

5.2 Improvement of Groundwater Management

One of the concerns was the inadequate management of groundwater in and around the monastery. It is proposed to introduce a culvert system beneath the veranda of the monastery that will carry groundwater to a nearby reservoir (Figure 13).

Figure 12: Removal of a veranda post on the west veranda of the monastery (photo by R. Christian).

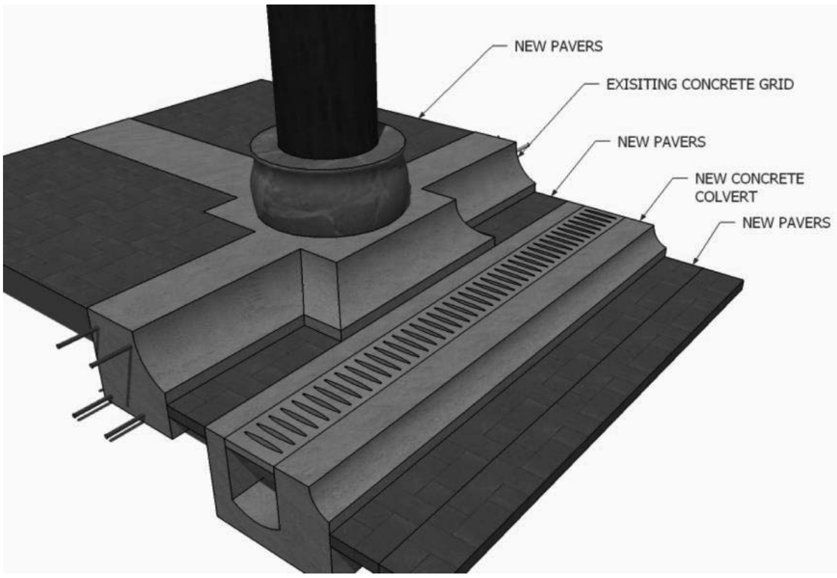

Figure 13: New concrete culvert system proposed beneath the veranda.

5.3 Foundations below the veranda posts

The subject of foundation systems below the veranda posts was debated at length. It was determined that the new posts would be set in the traditional manner: buried approximately 1.5 m below grade. The only contemporary intervention was the use of a slab of reinforced concrete at the base of each post in lieu of stone.

5.4 Scheduling

This work is being carried out in stages one elevation at a time starting with the west elevation so that the Golden Palace Monastery can remain open during the intervention.

6 REFERENCES

[1] Tainturier, Francois. Sept. 2014. Chronological Narrative of the Shwe-nandaw Kyaung Structure.

[2] Fraser-Lu, Sylvia, *Splendour in Wood, The Buddhist Monasteries of Burma*, Orchid Press, Bangkok (2001).

[3] Ridout, Brian. September 2014. Termite Damage at Shwe-nandaw Kyaung.

[4] Kelley, Stephen. May 2014. Structural Assessment of the Shwe-nandaw Kyaung.

[5] Kelley, Stephen. August 2015. Shwe nandaw Kyaung Roofing and Below Building Water Management.

SHATIS'17
4th International Conference on
Structural Health Assessment of Timber Structures
20-22 September 2017 Istanbul, Turkey

RESTORATION PRINCIPLES, DESIGN AND PRACTICE / A CASE STUDY FROM SAFRANBOLU, THE UNESCO WORLD HERITAGE [1]

İbrahim Canbulat

Master of Architecture

Keywords: Ottoman Mansions, Wooden Skeleton System, Historic Timber Structures, Restoration, Revitalization

Abstract.

Introduction:
I will discuss the structural problems of late Ottoman mansions and their probable reasons referring to our experiences from the restoration of four mansions which have been carried on by my team in the last two decades and my design approach as well as our practicing. Their structural problems gave us the traces of changes due to the socioeconomic characteristics of the new Ottoman bourgeois flourished in 18. Century.

Developments:
Macun Ağası İzzet Efendi Mansion has been restored as a residence; Hacı Memişler Mansion, Betenler Mansion and Gökçüler Mansion have been restored and revitalized as components of GüleviSafranbolu, a cultural-tourism complex. Çeşme Quarter where the four mansions are located was a typical settlement of the new Ottoman rich but the district. We can precisely specify the ages of mansions in detail by dendrochronological surveys carried on. Not only the traces of repair but also previous layers from the late 18. Century have been identified. We used to experience similar structural problems which might be called "generic" in all mansions and solutions applied in the later periods.

Remarks and Conclusion:
Those were mainly due to the enlargements of Ottoman mansions by additions horizontally and vertically in and after 18. Century. The wooden skeleton system was almost perfected, in other words evolved in the past 8.000 years by trial and error modification but failed in the last 200 years due to heavy impacts of socioeconomic changes. Four of the mansions had been altered due to socioeconomic changes over the past 220 years and more importantly the human damages they were exposed in the last fifty years.

1 INTRODUCTION

The title of the Turkish version of this paper is "*Safranbolu 4 Konak*" which is more comprehensible. *Konak* means in English "sumptuous mansion", but more correctly a residence assigned for some high-level officers like kadı, subashi, pasha, etc. who will also provide the administrative services under the same roof which also covers the residential sections. The houses of ordinary subjects used to be called *ev*. By the way, *konak* has another meaning. For the nomads or travelers, the stopovers on their destination used to be called *konak*. I use *konak* in two meanings. We moved to Safranbolu, a UNESCO World Heritage City which keeps not only her physical but also socioeconomic structure inherited from 18. Century. We started restoring our very first *konak* which used to belong to the Head Pharmacist of the Ottoman Sultan, Abdulmejid I (23/25 April 1823 – 25 June 1861). The name of the *konak* is "Macun Ağası İzzet Efendi Konağı". We were there in 1990s, just before the date of inscription of Safranbolu in "UNESCO World Heritage". There were very cultivated peoples who were sensitive and caring for the historic city. The restoration was developed in an interactive manner with the neighbours. They learned from us, we learned from them. By the time, there were very few architects in restoration and almost no specialized masons, carpenters, builders; forget the restorers. Restoration practise became another platform for sharing expertise and experience. Of course, this was the first stage (*konak*) in our life. Safranbolu inscribed in UNESCO World Heritage list in 1994 and almost synchronously entered tourism. With Gül my wife, we decided to initiate a model cultural-tourism complex comprising Ottoman *konaks* which were abandoned by their very last residents after long and exhausting life. By chance one of the *konaks* (*Hacı Memişler Konağı*) had been revitalized and operated almost for 10 years as one of the earliest *konak* hotels in Safranbolu. It was full of design and realization mistakes not only related to restoration but also lodging. Those provided us very valuable sample cases for either avoiding or improving the solutions for revitalizing a family house for busier and demanding functions. This was the second stage. Our third mansion used to belong to a family who were grandchildren of a *Kadı* (*Beten Efendi)* who was judge and high ranking officer migrated from Jerusalem to Safranbolu, got married and created a family. The mansion is small comparatively but has separated *harem* and *selamlık*. In 1960's the mansion had been divided into apartments and shared by the family members and later abandoned. Lastly, *Gökçüler Konağı*, one of the largest in Safranbolu which used to belong to a very rich family, after changing hands (to be) repaired for modern house and partly demolished by a *Gast Arbeiter* turning back home town. Of course, authorities interfered and stopped but left the building dilapidated. This was our last (?) *konak* on our way which delighted and appreciated our life.

In this paper, I like to share our experiences and way to solve those restoration, revitalization and architectural problems in short "design". I believe in necessity of sharing experiences which is valuable for all professions who are in "making". Unfortunately, restoration is a practical job which is made by plumb, axe, saw and hammer. Therefore, sharing experiences is very essential in our profession. I hope SHATIS is aiming to provide this interactive atmosphere since most of the others which I –also- participate are for speaking and writing staff. I don't want to be misunderstood; I very much enjoy the theoretical and guiding literature as well.

All those took more than 20 years. In this time restoration became more institutionalized and interdisciplinary but not perfected; became more popular, of course political and commercial domain. On the other hand, tangible heritage is limited and very fragile. I hope we will not be blamed by our grandchildren for our wrong doings and not transferring the heritage in proper conditions.

2 SAFRANBOLU 4 *KONAK*

Safranbolu mansions consist of a rough stone masonry ground floor and one or two upper floors with wooden frame structures, adobe brick infilled. Inside and outside are mud plastered and top layer white glazed (*perdah*: mixture of lime, marble dust and organic fibers). Safranbolu mansions have rural as well as urban characteristics. Ground floors are called "*taşlık*" and used mainly for service areas like stables for cows, horses and storages for wood for heating, grain, etc. as well as a transitory space between public and private domain, of course vineyards and gardens. Upper floors consist several rooms (*ev*) all suitable for 24-hour life cycle of a core family with build in cupboards and storages, a fireplace suitable for cooking as well, a shower cubicle but without any furniture which is substituted by divans running along the windows. All rooms are connected to common spaces like sofa, in some cases with an *eyvan*. The second floors might be added on top of the first floor in later periods. Then the lower floor became more women's court with service rooms like kitchen room (*aşevi*) in some cases connected dish washing cubicle, cold storage (*karanlık oda*) and a sofa mostly open to outside (*çardak*) like an inner balcony. [2]

I will firstly, explain the restoration works on the mansions in detail and later share my findings and state hypothesis for generalizing the characteristics of Ottoman mansions, comprising their common structural problems which we experience during restoration works.

2.1 Macun Ağası İzzet Efendi Mansion (1849-50) [3]

Figure 1: Street View (South) after Restoration

long exceeding the dimensions of the spans. We ordered the substitute wooden elements (yellow pine) to be cut from the forest, shaped to original dimensions and chemically treated. The structure was raised and damaged wooden elements were exchanged.

The very fragile, peeled off and cracked frescoes on the mud plaster was making the restoration highly risky and difficult. The consolidation and restoration of frescoes were either made insitu or disassembled and placed of temporary bases and placed on original positions after restoration. As mentioned above the interior frescoes were under many layers of paints which were in different chemical composition. As the consequence, chemical processes were not effective and all the paint had to be manually removed.

By the restoration of Macun Ağası İzzet Efendi Konağı, we got two awards one of the City of Safranbolu and the other of The Chamber of Architects of Turkey for "Best Conservation and Revitalization" in 2006.

2.2 Hacı Memişler Mansion (1849+6) [4]

Figure 3: Hacı Memişler Mansion, Street View

Hacı Memişler Mansion (Figure 3) was commissioned by a wealthy merchant family who were in yarn and textile business. They had 3 adjacent mansions but all were sold to different persons in later times. We made a dendrochronology survey with Istanbul University, Faculty of Forestry's academic staff and found out the sample wood was cut from the forest in 1855. Dating was scientifically correct but not in accordance with the local history which states that Çeşme Quarter was developed in 18. Century. We were lucky to find out the debris of one third of the mansion in the back yard, down the earth. After referring to local history we have seen that there happened a fire in mid of 19th Century and all district was damaged and remade afterwards.

2.3 Betenler Mansion (1856+2) [5]

Figure 5: Betenler Mansion, Garden View

Betenler mansion (Figure 5) is in chalet type with a surrounding garden and have visual connection to exterior. Originally, it was commissioned by Beten Efendi, a *kadı*. Rather good separation of *selamlık* and harem indicates that the mansion was used also for administrative functions. *Selamlık* section composed of a waiting hall and connected home office and Harem which was separated by the doors occupy half of the first floor with a large kitchen and sofa and as the upper floor with 4 bedrooms one of which is *Başoda* (Main Room).

As stated above, when we bought the mansion it was converted into two apartments; ground floor was shared horizontally and upper floors vertically by two siblings. New rooms and a kitchen were made on sofa which was waiting hall before. There was a custom in 1960's to change the original windows with larger and modern ones which used to be called "Bride's Windows". Another problem was the erosion of the vegetable soil which was carried by the early settles to their gardens where the district on the hills of a canyon since the original soil was not suitable for plantation. Almost the half of the ground floor was under the earth which caused excessive damage on wooden elements as well as stone walls. We have experienced the similar structural problem related to the unsupported wall at upper

Figure 6: Restoration of Window Frames

Macun Ağası İzzet Efendi Mansion (Figure 1) is comparatively small but well designed, commissioned with utmost care and highly decorated with frescoes and special carpentry works like ceiling with mirror (*aynalı tavan*). It is a chalet type mansion with a front garden contrary to typical Ottoman mansions which are on streets but having deaf façade, seeking privacy. I guess the owner was either in Istanbul, the capital of Ottoman or returned to Safranbolu with his money and cultural accumulation after long service at the Ottoman Palace, since we see the finesse taste of styling of a person from the capital city. We were told by our neighbors that he had sponsored the wall paintings of Grand Vezir Köprülü Mehmet Paşa Mosque (opening 1662) from and same painter had painted his own mansion, too. From the date rosettes on the outer frescoes and on interior wall of *Selamlık*, it was made in 1266 hijri: 1849-50 (Figure 2). During the restoration, we found many recycled wooden elements with the marks of fire damage and cracked rubble after being exposed to excessive heat. Therefore, we know that the date of the repair or the date of frescoes but we cannot estimate the date when the mansion constructed, initially.

Figure 2: Restoration of Wall Paintings

By the way I like to note that material recycling was a common practice in Safranbolu seeking building economy. For example, one can easily see a stair beam is used as door lintel. Unfortunately, the mansion was changed many hands one was the imam of the district masjid who painted the walls to holly green and the last owners divided the mansion into three apartments each on one floor.

From the Frescoes on façades, we used to know the existence but could not imagine that there were many frescoes, too inside hidden under several layers of paints. The outer and inner plasters were made from mud with some small cut straw, after white lime and marble dust glazed. By laboratory analysis we got the exact formula of the glaze and learned that the wall paintings were made by fresco technique since the wall paintings were applied while the glaze was wet. This made removing paints easier by manual work.

The important problem was to understand how the mansion was before the last modifications. The findings were surprising since some of the stone walls had been demolished just to earn larger and interrupted spaces and a new section was added in two floors high *taşlık*). We had to remove all new construction works to find how original building was. One of our surprising experience was to see some walls of the upper floor were not supported whereby there was a critical sag on the ceiling under. Anyhow, under any occurrence, the original mansion had very well-tuned architectonics.

To put the structure in original conditions we had to construct the missing rough stone (mud mortar) walls and repair wooden structure since some of the original elements were either reshaped or totally scrapped while adding new spaces. The original dimensions of structural wooden elements were unusual and not in accordance with our experiences: they were very

Gökçüler Mansion (Figure 7) is the biggest of 4 mansions. It commissioned by *Gökçüler* Family who were very wealthy and should be in agriculture and forestry, this can be seen from the heritage of *Gökçüoğlu Hacı Mehmet Ağa* who should be personally renovated the mansion in 1850s [6] after the district fire. When the family members lost their strong position, the mansion turned to a rental house and at the end sold to a retired person back from Germany. When we started commissioning the restoration we have seen that the mansion, including the roof structure terribly destroyed to make it a more modern building. Some parts of the mansion were dilapidated and untouched for many years. Worse than these, the neighbor on south of the parcel made a very deep cut to make a new mansion and that caused displacement at the south-east corner of the mansion vertically about 45 cm. We needed to strengthen the foundation, as well. All the plan of the interior had been changed, all original carpentry works were removed. The last owner tried to change the geometry of roof and had made many walleyes. This caused the rain water to penetrate the mansion and cause excessive damage. The adjacent barn was destroyed and most probably was used as quarry. The ground floor was filled with debris about 80 cm.

We started from the foundation and made a very strong retaining-wall, after strengthening the base restored the rough stone shoes with the technology which can be seen at Hattusa, the Capital of Hittites and lifted the mansion as a limit where the wooden skeleton keeps the integrity. It took about 3 years to put the mansion in original architectonics and was the most difficult among four mansions for the structural restoration. *Gökçüler* Mansion was the only exception without any structural problem which we have experiences at previous 3 mansions. Now, we know that both the upper floors were planned and made two together after the fire but not the upper floor at a later period, so the load bearing members were correctly placed and supported. I assume that the lower floor's western part of the mansion had not faced a very heavy damage and kept but its southern part and upper floor were destroyed and had to be remade. This time we gathered about 16 samples from different places of the mansion for dendrochronology. The results of the survey proofed that the original mansion was made in 1790s but the building was renovated after 1850. The details of the findings will be discussed in the following section.

We were lucky that the removed carpentry works which were disassembled but kept in the barn. Although not many pieces were lasted we could understand the original design and finishing. One by one we checked and their original places were found. It was a tidy job to complete the missing parts, combine with the originals and to assemble like "Anastylosis"

Figure 8: Restoration of Frame

The last owners of Hacı Memişler Mansion converted it into hotel after substantial modifications and operated about 10 years. When we bought, at first glance the building was seen almost in good condition but after extensive surveying, we understood that there were many alteration, addition of extra bedrooms with bathrooms in common spaces of the original mansion. Also, they demolish some stone walls of the ground floor just to get larger and brighter reception and breakfast hall. Safranbolu is very close (40 km) to the North Anatolian Fault Line and the intervention to the structural system made the building vulnerable to earth quakes. Last but not less important: after 10 years' heavy usage, the wooden elements of the wet cores were fully rotten and damaged by fungus and carpenter ants. Worse than these the effected parts had been replaced with reinforced concrete which accelerated the speed of damages and made very high dead load on wooden skeleton. The previous owners had built also an annex building for extra storages and boiler room necessary for the hotel.

Our restoration started with the remaking the demolished stone walls and close the extra openings. We disassembled the extra bedrooms, bathrooms and repaired the damaged structural elements. We decreased number of bedrooms from 7 to 5 and bed capacity from 20 to 10. Increasing the capacity of mansions for higher hotel bed capacity is typical everywhere, due to commercial objectives of the hotel owners. We achieved the original structure and space hierarchy. Presently, in Safranbolu there are about 100 mansion hotels. Personally, I watch very closely [5] but I am very much scared of ongoing wrongdoings. During survey, we recognized that there was the same structural problem at this mansion, too but in later periods it was discovered, the missing structural wall was recognized and the problem had been solved by an extra girder underneath the upper wall.

We broke and removed all concrete floors under the wet cores and developed a special plywood sinks covered with glass-fiber reinforced polyester. By these the usage of cement based solutions were excluded. Our solution for the wet cores is unique and after 10 year's utilization still don't have even minor problems. Also, my design for the beds is unique. There is no furniture in Ottoman houses until 19th Century, as mentioned above. I used the divans with extra removable stands in front and placed matrasses on top which is an exclusive solution, respectful to the authenticity but providing more modern solutions without interfering to the original building. We are happy to see that some hoteliers and architects started using our designs for similar *konak* hotels, recently.

Figure 4: Restoration of Wet Cores

3 CHARACTERISTICS AND STRUCTURAL PROBLEMS OF SAFRANBOLU MANSIONS

Although the appearances are similar, Safranbolu houses can be classified in three categories. Moslem houses in *Çarşı*, the center; Kıranköy, the Greek Orthodox district and *Bağlar* (vineyards), the summer district which is one of the earliest examples, worldwide. [7] The Moslem houses either in *Çarşı* or *Bağlar* do not have any integrated shops or workshops but Kıranköy houses majority have one on their ground floor. At Moslem houses, there is not any connection room except *sandık odası* (dressing room) opening to master bedrooms, but at Greek Orthodox houses the rooms are mostly connected to each other. Almost, all Greek Orthodox houses have small chapels and an oven for baking and cooking. *Bağlar* houses have higher ceilings and specious t*aşlık*, *çardak* and sofa like semi-open spaces. Of course, the main reason why is the warm summer climate and more frequent relations with outside e.g. gardens, vineyards, etc. as well as spaces for preparation of preserves for winter time and recreation. Moslems have open fire places called *kazan ocağı,* cooking in their garden like flat breads and molasses, etc.

Safranbolu houses are placed on the slopes of a *castron* which is called *Kale*, a Byzantine citadel. The parcels are shaped by retaining walls and as stated above leveled with the vegetable soil carried by ox or mulls. This is typical Ottoman city scape since settling on hills which were surrendered by Seljuks and later Ottomans provide easy to defend points due to their geomorphology, from the late Roma – early Byzantine period. Therefore, we can repeat the same generalization: Ottoman houses do not obstruct the view of each other (and provide privacy), due to placing on slope. As stated above main entrances are placed on the street only with a gate large enough for the entrance of one mull with full load and surrounded by gardens on the back side of course smaller in *Çarşı* but very large in *Bağlar*. In the beginning the parcel sizes were rather large but afterwards divided to smaller ones due to the increase of number of new houses because of more population.

The houses were not higher than two floors until 18. Century. In Safranbolu all the ground floors are made of rough stone walls with mud mortar and *sar* (joiner) which are very tin wooden planks at the width of the wall, horizontally placed every after 100 – 130 cm heights as reinforcement against lateral forces. External walls are connected high garden walls like buttresses. Stone masonry also good for insulating the wooden structures from the moisture and makes the leveling of the upper floor on inclined parcels easier. The original slope of the canyon mostly is not touched and easily can be used as stable or storage spaces. Safranbolu houses solved the sanitation with attached toilet cubicles on north façade, generally. Position may change due to the direction of the slopes and relative positions of the neighbors. Upper floors were of wooden skeleton with mud brick infill with wooden plank covered hip roofs. The ground floors were mainly for animals, storage and in rich families' houses, there is a *hazine* (treasury) with very thick walls up to 150cm, under a cross vault. These are mainly to secure valuables from fire hazard. Upstairs had mostly an outer sofa which connected to 2-3 rooms and a wet core. This was typical until 18. Century. This type is classified as *Hayat House* by Doğan Kuban and "First Period Houses" by Sedat Hakkı Eldem. [8] Until 18. Century, it was prohibited to build houses with more than 2 floors high. This was liberated and regulated by 1725 Land Codes, as Moslems' houses are allowed highest 12 *zira* (lower arm length) (9.1 m) and none Moslems' 9 *zira* (6.8 m); later in 1827 Moslems' 14 *zira* (10.6 m) and none Moslems 12 *zira* (9.1 m). [8] On the other hand, in 1857, by Land Codes, private proprietorship is accepted and subjects were no more afraid of showing their wealth. This caused more liberal socioeconomic environment as well as private, spacious and larger residences on all Ottoman territory. Also, the social characteristics of the Ottoman district basing on mainly kinship and time to time artisanal collectives are left and social segregation started. [9] *Çeşme Mahallesi*

(Quarter) where all the 4 mansions were built is a typical Ottoman elites' settlement with sumptuous mansions.

It is obvious that most of the upper floors were made on top of the previous floors later. From 16. Century the typical plan scheme was with open sofa [10] but in 18. Century upper floors were with inner sofa (*iç sofalı*) mostly, under the influence of Baroque style reaching from Europa. These two different styles were used two together although their structural plans were different. This can be seen from the staircases. The stair running to first floor was at the sides and parallel to an exterior wall but the stair running upper floor should reach upper sofa and directed to the center, time to time without well-defined structure and cannot be solved in the same stair core. In cases, like *Macun Ağası İzzet Efendi, Hacı Memişler* and *Betenler* mansions the builders just placed the upper floors on to the previous lower floors as they were. We recognized that the builders of *Betenler* Mansion were more qualified and tried to decrease the dead weight of the upper wall by using *bağdadi* (lathe and plaster) which was comparatively lighter than mud brick infill. In *Hacı Memişler* Mansion the problem was solved by placing a wooden girder later. Only the builders of *Gökçüler* Mansion were qualified and modified the plan of lower floor to fit the upper floor properly. It is interesting to witness that the *hayat evi* (open sofa) plan type lower floor has been changed to *iç sofalı* (inner sofa) type by adding two bedrooms and one *eyvan* to original *çardak*, at the same time. Anyhow, we recognize that there were 2 different periods which can be seen from the finishing of the mansion and dendrochronological analyses. This can be also witnessed on many Ottoman mansions even in Balkans and were recognized by two architectural historians Ayda Arel and Nur Akın but they did not question and discuss the probable reason why.

Safranbolu family is small comparatively, mostly in three generation, 5-6 members. They used to use neighboring villagers on crop sharing base. They used to control all caravan operation in between Anatolia and Black Sea Ports (Amasris, Inepolis and Sinope) as well as transit trade. They were also culturally rich people. Due to this characteristic, they never need many children and it is rumored that they had very effective birth control drugs. After adding a new floor, they had the difficulty to fully utilize it. In the beginning, there were only *selamlık*, a service kitchen, toilet and the negative space was left as *köşk*, *gurfe* (veranda) around. This was typical for the new riches. In later periods the *gurfe* was first closed to outside and afterwards new rooms added under the roof. This happened in lower floors as well, open spaces are closed to outside and new rooms added. Visualizing the *Çarşı* houses in winter, it is very difficult to imagine a busy life at upper floors with poor heating and insulation. Senior Safranbolu people [12] suggest that they used to be utilized upper floors mainly for guests; they were show places. In 18. Century, Safranbolu elite created some real supreme spaces used to be called *havuzlu köşk, divanhane* around the pools, either under the same roof or as separate pavilions. This is very excusive without any similar anywhere in Ottoman territory.

Under the roof only the rooms are insulated but negative spaces were left open for the air circulation. They used cold roofs, there was no ceiling on the sofas, either. The rooms used to be insulated with *bulgurlama* (presses earth under the floors and over the ceilings), in an extend this helps as sound insulation, too. Heating was with braziers with burned wood from fireplaces. Fireplaces were not effective for heating since chimneys were not efficiently solved and used for cooking mainly. As stated above *ev* (room) were self-sufficient for 24 hours' life cycle of a core family. The floor mattresses used to be rolled and stored in cupboards. The rooms turn from bedroom to a living room with surrounding divans. Kitchen room was suitable for sleeping as well for the elderly members of the family like grandmothers who used to be responsible of cooking. You should imagine windows until 19th Century without glass. The rooms were mostly dark in cold seasons when the *kara kapak* (wooden shutters) were closed. Only, very few riches could afford the expensive *revzen* a kind of small top windows with gypsum framed Murano floors on this mansion as well. This time it was just the staircase whose walls were sunken about 15 cm.

First, we disassembled the additional divisions and kitchen cupboards and sink. We removed the displaced earth and restored the stone walls of the ground floor. We placed a heavy wooden girder under the staircase. One of the time consuming and tiring work was to remove the paints on original wooden ceilings and cupboards. This was another modernization touch. We could remove the thick layer of oil based paint with chemical hot air blower, agents and scrapers.

During the cleaning process, we could find 2 sets of window frames which were disassembled but not scrapped just hid under the roof. Our happiness was not only for the original window frames but also related to the restitution project since we did not know what type of windows were used, originally. A set of three were neo-gothic windows disassembled from the *şahnişin* (bay window) of the upper floor and the set of five was from the sofa of the lower floor. It was interesting to find out that the window frames of the sofa were without glass but only fencing. Until the 19th Century sheet glass was not available in Ottoman territory. Normally, they used to use wood shutters in cold seasons. The other windows of the mansion were with sheet glass but the sofa left without as a semi open / semi closed inner balcony which was common in the past. By the careful examination of nail holes, we could place the window frames to their original positions.

2.4 Gökçüler Mansion (late 18th Century and 1850) [5]

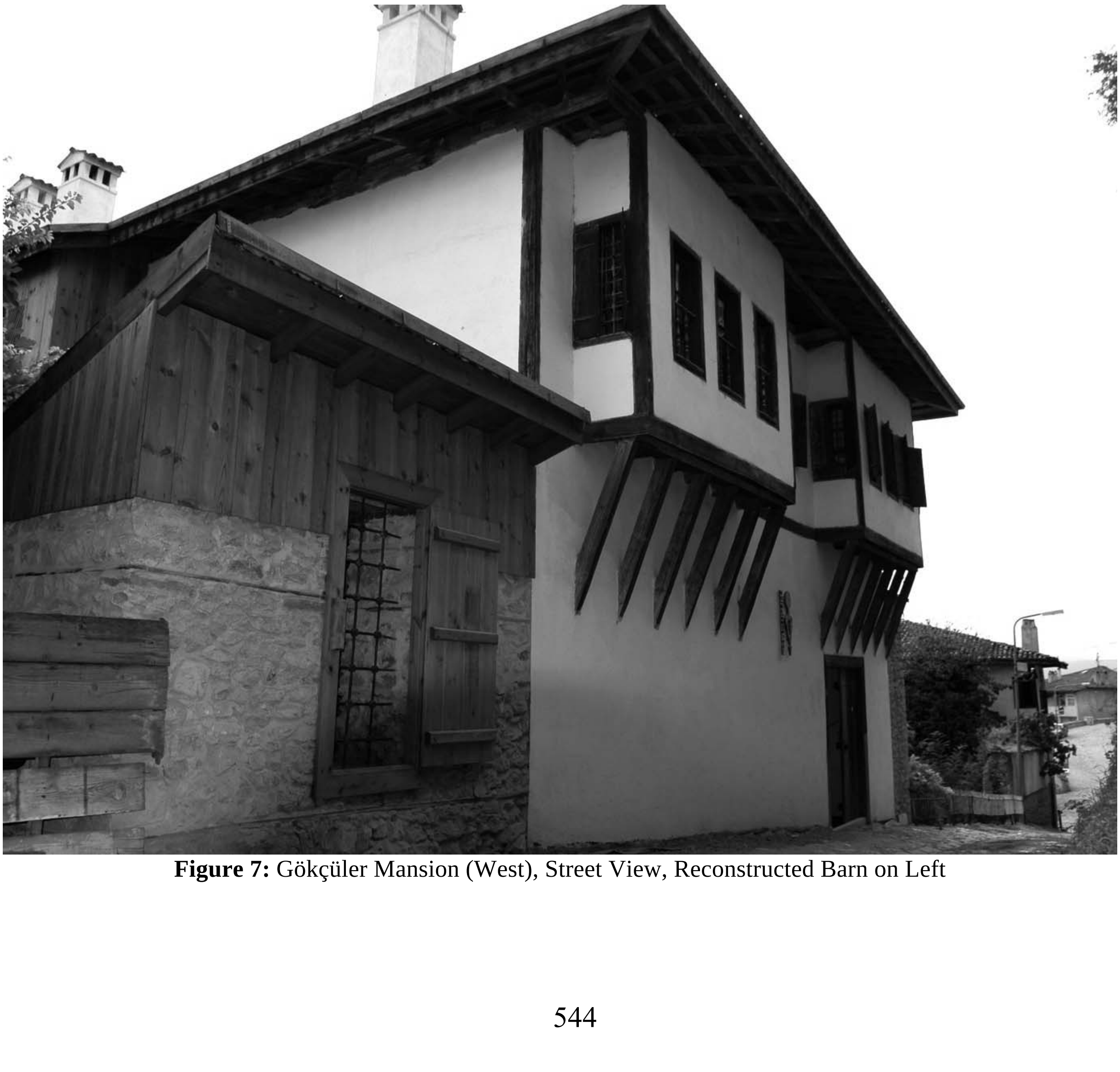

Figure 7: Gökçüler Mansion (West), Street View, Reconstructed Barn on Left

glasses. As an extension of the rooms the sofas were used to be used for food preparation and to host the friends in big groups. Sofas and *çardaks* were social spaces for religious ceremonies and other activities social like feasts, wedding, etc.

Another problem of Safranbolu houses (like all Ottoman houses) is related to the roof constructions. Ottomans never used *asma çatı* (roof trusses) but *oturtma çatı* (piles, beams and rafters) with bedavra (wooden roof planks). Most probably this was same at Byzantine period since, Romans, Byzantine and Ottomans solved the long spanning upper structures with arches, vaults and domes. *Oturtma çat*ı has the tendency to sag and expand. As discussed above Ottoman mansions were enlarged vertically and horizontally without solving the above discussed structural problems. Wooden frame is very efficient and flexible for modifications, additions and expansions. Especially in later periods when the mansions are getting more articulated, roofs became more complicated with valleys where rain water insulation was serious problem. All these are discussed in another paper: "**The Ottoman Mansions: Evolution of Structure and Form**".

REFERENCES

[1] Turkish edition of this paper was published at Canbulat, İbrahim (2014) Safranbolu 4 Konak. *Geleneksel Mimarinin Yaşayan İnsan Hazineleri*, Edited by Özlem Karakul, Grafiker Yayınları, Ankara, pp. 139-154.

[2] For further information refer to Günay, Reha, 1998, *Tradition of the Turkish House and Safranbolu Houses*, Translated by C. Birkan, YEM Yayınları, İstanbul.

[3] From the rosette on the wall of of *Selamlık:* 1266 hijri.

[4] After dendrochronology analysis. I like to thank Dr. Nesibe Köse and her team for valuable collaboration and their expertise.

[5] Canbulat, İbrahim (2016) "Safranbolu", *UNESCO World Heritage in Turkey 2016*, Turkish National Commission for UNESCO, Ankara. pp. 224-250.

[6] Karacakaya, Recep etc. (2013) *Safranbolu Şer'iye Sicili / 2133 Numaralı Defter*, Safranbolu Belediyesi, Safranbolu, pp. 579-580. He used to possess 84 different property.

[7] Cerasi, M. M. (1999) *Osmanlı Kenti / Osmanlı İmparatorluğu'nda 18. ve 19. Yüzyıllarda Kent Uygarlığı ve Mimarisi*, Çeviren: Aslı Ataöv, YKY, İstanbul. The trans-human lifestyle of Turkoman eventually developed to such a result.

[8] Kuban, Doğan (1995) *the Turkish Hayat House*. Eren, İstanbul and Elden, Sedat Hakkı (1984, 1986, 1987) *Türk Evi / Osmanlı Dönemi*, 3 Volumes, T.A.Ç. İstanbul.

[9] Denel, Serim, 1982. *Batılılaşma Sürecinde İstanbul'da Tasarım ve Dış Mekanda Değişim ve Nedenleri*, ODTÜ, Ankara.

[10] Eldem, Sedat Hakkı (1984, 1986, 1987) *Türk Evi / Osmanlı Dönemi*, 3 Cilt, T.A.Ç. İstanbul.

[11] Taş, K. Z., 1966. "16. Yüzyılda Safranbolu İdari Yapısı ve Vakıfları" *Ankara Üniversitesi, Dil Tarih – Coğrafya Fakültesi, Tarih Bölümü, Tarih Araştırmaları Dergisi*, 18: 29.

[12] Arel, Ayda. (1982) *Osmanlı Konut Geleneğinde Tarihsel Sorunlar*. EÜ, Güzel Sanatlar Fakültesi, İzmir and Akın, Nur (2001) *Balkanlarda Osmanlı Dönemi Konutları*, Literatür, İstanbul.

[13] Ahmet Sarıaltın and others.

SHATIS'17
4th International Conference on
Structural Health Assessment of Timber Structures
20-22 September 2017 Istanbul, Turkey

RECENT DEVELOPMENTS IN REMEDIAL AND NON-PRESSURE WOOD PROTECTION SYSTEMS: BORON-BASED COMPOUNDS

S. Nami Kartal, Evren Terzi

Faculty of Forestry, Istanbul University, Istanbul, Turkey

Keywords: Boron, Remedial treatments, Wood protection, Preservation

Abstract

Extending the life of timber structures is an important issue in the protection industry. There are various approaches available to diminish the susceptibility of wood and wooden structures to biodegradation such as design, construction practices, maintenance, and protection/preservation. Wood under proper conditions (sufficient moisture [>19%], oxygen, temperature, food source [wood cell material]) is degraded by several wood-degrading fungi and insects; however, wood protection techniques help wood and timber structures increase service life against moisture and biodegradation.

Depending on the application methods, wood-protecting preservatives are generally categorized into two groups: (i) preservatives for remedial treatments and (ii) preservatives for pressure treatments. Preservatives to be used for remedial purposes are available in various forms such as liquids, rods, pastes, or gels. In remedial treatments, the chemical compounds in the system distribute into wood that is rich in moisture. In addition, such treatments are proper for wood materials not treated previously. Due to their good diffusion properties, remedial-type wood preservatives can be even applied into large wooden members. Boron compounds have been receiving a lot of attention for preserving both historic structures and newly constructed timber structures since they are capable of acting as both insecticides and fungicides, have low toxicity, are cost-effective and have good mobility in wood. Boron based wood preservatives can be grouped into various categories such as timber treatments, exterior (surface) treatments, remedial treatments, treatments for composite/panel products etc.

In recent wood preservative systems, boron based chemicals are most multipurpose compounds available for use today. There has been a considerable increase in the number of boron formulations on the wood protection market globally. This paper evaluates recently developed boron-based formulations in remedial treatments in timber structures.

1 INTRODUCTION

Wood preservatives for remedial treatments are generally categorized by a variety of physical states:

(i) Thixotropic pastes and preservative greases,
(ii) Oil borne and waterborne solutions and emulsions,
(iii) Preservative rods and pads,
(iv) Liquid and solid fumigants [1].

Remedial wood preservatives may have various modes of movement and efficacy. Internal or external application methods are available for such wood preservatives to control decay fungi and wood destroying insects in wood structures. Their range, speed, and duration of efficacy might be also different. They are used in some cases as a supplemental component to common wood preservatives and to extend service life of previously untreated wood and wood products [1]. The main objective of remedial treatments is to distribute preservative into areas of a structure that are exposed to moisture/wetting or not previously protected by preservatives. Remedial wood preservatives do not easily penetrate into the wood under pressure; but by means of treatment holes made in large wood members, applications are available [2].

Boron-based remedial wood preservatives are effective for in-place treatments of wood structures. Various techniques like spraying, immersing, brushing, injection etc. are available for boron compounds since they are readily soluble as in water and some other solvents. On the other hand, boron compounds are easily absorbed and penetrate by diffusion mechanism into the wood structure. Boron in the form of its oxides and salts is an extremely effective natural wood preservative with a wide range of activity against fungi, insects and termites. Boron wood preservatives are cost-effective, colorless, non-volatile, they don't evaporate, degrade, or yield an odor during service; and are non-corrosive, requiring no special fasteners [3, 4].

2 GENERAL CONSIDERATIONS - BORON BASED WOOD PRESERVATIVES

Borates have played an increasing role in wood preservation worldwide since environmental concerns regarding the use of heavy metal containing conventional wood preservatives and wide-spectrum/high toxic chemicals have risen in recent years. Boron-based biocides are suitable wood preservatives for the protection of wood from decay fungi and almost all species of insects and termites and they show very low mammalian toxicity. Boron compounds provide complete protection against biodegradation in dry conditions and in indoors even though it is leachable from wood when treated wood is used outdoor [4].

Boron compounds can be categorized as (i) Inorganic boron compounds and (ii) Organic boron compounds.

Boric acid ($B(OH)_3$) is one of the most important inorganic boron compounds. It can be translucent, flaky crystals or white powder. It is very soluble hot water. It is very toxic to fungi, bacteria, insects and termites [5, 6].

Borax (Sodium tetraborate decahydrate – $Na_2B_4O_7 \cdot 10H_2O$) is also an inorganic boron compound which is colorless crystal and soluble in hot water. Its toxicology and biological effects is the same as boric acid [6, 7].

DOT (Timbor – disodium octaborate tetrahydrate – $Na_2B_8O_{13} \cdot 4H_2O$) is the most water-soluble of the commercially available inorganic borates. Its toxicology and biological effects is the same as boric acid and borax [5]. Its high solubility has led to the worldwide usage of DOT in the dip or pressure treatment of solid wood and panel products [6]. Toxicology and biological effects of DOT (disodium octaborate tetrahydrate) is the same as boric acid and borax. Its high solubility has led to the worldwide usage of DOT in the dip or pressure treatment of solid wood and panel products. Today in the North American market, there are various commercial DOT products for termite attack in wood under various brands such as TIM-BOR, BORA-CARE, SOLUBAR, NIBOR-D, HI-BOR, SILLBOR WOOD, POLYBOR, BOARD DEFENSE, BORASOL, TIMBERSAVER40, ARMOR-GUARD, BOR-RAM, BORATHOR, SHELL-GUARD, etc. [2, 4, 8].

Zinc borate ($2ZnO_3B_2O_3{\bullet}3.5H_2O$) and calcium borate ($Ca_2B_6O_{11}{\bullet}5H_2O$) are also inorganic compounds that have very low solubility in water and it is not used for solid wood in pressure treatments. Zinc and calcium borates are used as a fire retardant for composite products by incorporating in powdered form during blending process with glue and wood particles [9]. Zinc and calcium borates are also effective against wood degrading fungi, insects and termite attack [6].

Inorganic boron compounds are also listed as wood preservative in the various international standards, which include formulations prepared from sodium octaborate, sodium tetraborate, sodium pentaborate, and boric acid.

A number of organic boron wood preservatives are available commercially mostly developed from inorganic borates or boric acid [6]. These preservatives might be in different forms such as vapor phase, liquid phase, and solid phase. Trimethyl borate (TMB), triethyl borate (vapor phase treatment), Borester 7 (vapor phase treatment), Boracol (pastes, bandages, and solids), triethylene glycol (pastes, bandages, and solids) are essential organic boron compounds [6, 10].

3 WOOD PRESERVATIVES FOR REMEDIAL TREATMENTS IN WOOD STRUCTURES

Characteristics of wood preservatives for in-place treatments can be evaluated under three categories [2]:

(i) Diffusible Wood Preservatives,
(ii) Non-diffusible Wood Preservatives, and
(iii) Fumigants.

Diffusible wood preservatives move slowly through water within the wood structure and do not bond to the wood structure. This characteristic of diffusible preservatives makes them diffuse easily within wood as long as adequate water is available. Thus, wood moisture content, grain direction (longitudinal, tangential or radial), and strength of solution are important factors to obtain complete diffusion in wood [2].

Boron compounds are the most commonly available diffusible preservatives. Boron-based treatments have several advantages. Besides all advantages stated above, borate formulations do not impede finishes and other surface treatments. These wood preservatives are present in a range of forms including powders, gels, thickened glycol solutions, solid rods, and pastes [2]:

- Powdered borates: These compounds are usually 98% DOT in powder form. DOT is mixed with water for spraying or brushing. Solution strength is generally in the range of 15% DOT. Powdered borates can also be poured or packed into holes for internal treatments of wood structures.

- Thickened glycol–borate: These formulations are normally offered with a 40% or 50% DOT content. The thick liquid is then diluted 1:1 or 1:2 with water, yielding a solution containing approximately 22% or 15% DOT.

- Glycol–borate solutions: These can be applied by spraying or brushing or used to apply on cut-ends or in holes. By adding foaming agents, these formulations can be also used as foams.

- Borate gels: These are currently less widely used than other diffusible boron compounds. The gel includes 40% DOT and is provided in tubes for application with standard caulking guns. They can be applied to voids, cracks, and treatment holes, which are oriented horizontally or downward placed in wood structures.

- Rods contain active diffusible preservatives compressed or fused into a solid for ready application into treatment holes. Application of such rods is quite easy and free of risk of spillage; however, wood moisture is necessary to assist the initial diffusion process in wood.

- Paste formulations: Pastes have more complex mixture of actives than other types of diffusible compounds. The paste treatments can be used for internal treatment of holes by application with a caulking gun.

Gel (JECTA GEL, BORACOL etc.), paste (Cu-BOR, Cu-RAP20, MP400-EXT etc.) or rod (IMPELROD, FLUROD, COBRAROD etc.) formulations are commercially available for remedial treatments in buildings and wooden members in timber structures [2]. These are easily applied in pre-drilled holes that are an important practice for remedial treatments.

Kartal (2009) reviewed that another diffusible preservative system for remedial treatments is a water-soluble copper naphthenate / boron paste [11]. The boron in these systems moves well from the point of application, while the copper naphthenate moves to only a limited extent [12]. As a result, this treatment might be useful for treating the inner surface of large voids, where the copper naphthenate would coat the surface of the void, while the boron would diffuse further into the wood [11].

Non-diffusible liquids do not penetrate more than 1 or 2 mm across the grain of the wood by spraying or brushing. Thus such preservatives do not move great distances from their point of application. Besides currently restricted compounds i.e. pentachlorophenol (PCP) and creosote solutions, copper-8-quinolinolate (Cu-8), copper naphthenate, and zinc naphthenate are the most available compound in this category to be used in remedial treatments [2].

Fumigants are applied in liquid or solid form in predrilled holes in wood members of a structure. They then volatilize into a gas that moves much greater distances through the wood than do the diffusible treatments. There are currently three types of fumigants: Liquid, granular and encapsulated. Liquid fumigants contain metham sodium (33% Sodium N-methyldithiocarbamate) and finally decompose to produce the active ingredient methylisothiocyanate (MITC). Chloropicrin fumigant is also available in liquid form. Granular fumigants are placed into drilled holes like liquids. The current formulations use granular Dazomet (98% tetrahydro-3,5-dimethyl- 2-H-1,3,5, thiodazine-6-thione), which decomposes to produce MITC. Encapsulated fumigants are pre-packaged for convenient application. Encapsulated products contain the same granular Dazomet or solid 97% MITC [2].

Lebow and Anthony (2012) have reviewed and classified supplemental boron-based preservatives and their applications as shown below:

Applied as	Active	Supplied as	Dilution	Trade Name*
Liquid	98% DOT	Powder	10-15% in water	Board Defense, Borasol, Timbor, TimberSaver, Armour-guard
Liquid	25-40 DOT	Water-glycol	Dil. with water	Bora care, Bor-Ram, BoraThor, Shell-guard
Liquid	9.1% DOT 0.96% Boric acid 0.6% Cu	Water-based	-	Genics CuB
Rod	100% anhydrous DOT	Solid rod	-	Impel Rod
Rod	93% NaF	Solid rod	-	FluRod
Rod	90.6% DOT 4.7% Boric acid 2.6% Cu	Solid rod	-	Cobra Rod
Paste	43.5% Borax 2% Cu	Paste	-	Cu-Bor
Paste	40% Borax 2% Cu	Paste	-	CuRap 20
Paste	43.7% Borax 0.2% Azole 0.04% Bifen-thrin 0.05% Cu	Paste	-	MP400-EXT
Gel	40% DOT	Gel	-	Jecta

* The use of trade or firm names in this publication is for reader information and does not imply endorsement by Istanbul University, Faculty of Forestry of any product or service.

4 APPLICATIONS OF BORON-BASED REMEDIAL WOOD PRESERVATIVES

Lloyd et al. (1999) have reviewed that for diffusion, borates need moisture in the wood, more than 15% normally [13]. Boron diffusion into wood changes depending on a number of factors such s the concentration of the borate used, formulation, the number of treatments; ambient temperature, age of wood, surface condition of the wood, wood species and moisture content. Fast penetration of borates in wood occurs within the first week of application regardless of initial wood moisture content. However, for significant diffusion after one-week post application a moisture content of 15% or more (preferably 30%) is needed. Turner (2008) states that several studies have found that 40% moisture content is necessary for proper diffusion [14].

There are many other factors that contribute to penetration depth of borates in wood including temperature, solution concentration, and density of wood. In general, the heavier wood, the less penetration in wood. As the concentration of boron compounds increases, retention level in wood increases. On the other hand, borate formulations prepared with ethylene glycol at high concentration levels penetrate faster and deeper in wood when compared to water based formulations. The solubility of borates shows increases with increased temperature affecting also diffusion rates [14].

Powdered borates are generally applied, for remedial purposes, in attics, in wall voids, in subflooring voids, or in cracks and crevices. Boron solutions at 10 or 15% strength are applied as a surface spray, surface foam, or injected under pressure into pest galleries in wood members. Glycol formulations are used either diluted as a surface spray to wood surfaces or injected under pressure into pest galleries in wood, or as a concentrate in place of injectable pastes. Solid boron rods and paste formulations on the other hand, are introduced into exterior or ground contact timbers such as decks, or components in contact with exterior walls or below damp proof course in structures. Such rods and paste formulations also provide a reservoir slow boron release into the wood [13].

In remedial treatments of timber structures, the methods are classified as follows:

(i) Surface treatments (external treatments), and
(ii) Internal treatments.

In external treatments, chemical penetration more than a few millimeters across the grain of the wood is not expected. Even though boron-containing remedial formulations can diffuse more deeply under high moisture conditions, complete protection of the interior of large timbers might be difficult. In case of checks, splits, end-grain, holes etc. available on wood surfaces, liquids in surface treatments can penetrate more efficiently. In order to prevent component leaching from the surfaces, water-repellent finishes can be applied as a second treatment. In external applications, paste surface treatments can provide a larger reservoir of chemicals than do liquids. Paste treatments can result in several centimeters of diffusion across the grain into moist wood over time [2].

Internal treatments generally include applications by drilling holes into the wood; however, some other different practices are available. Application of boron compounds via internal treatments is important to prevent decay to be occurred inside the wood since large wood members are typically too thick to efficiently treat the inner parts of wood with surface treatments. Internal treatments are generally applied to the interior of large wooden members in timber structures. Diffusible chemicals such as borates move through moisture in the wood but do not move in dry wood. The diffusion distance in moist wood is about 5 to 10 cm across the grain and nearly 15 to 30 cm along the grain. Solid rod-based diffusible treatments may provide a longer/slower release of chemicals while liquid-based diffusible treatments result in a more rapid, but less long-lasting dose of chemical. Internal treatments in paste and gel form are somewhere between rods and liquids considering speed of release. Since fumigant treatments move as a gas through the wood, they can move several centimeters along the grain of the wood [2].

Boron retention levels in treated wood for DOT as determined by the EN 117 standard are 5.60 kg/m^3 (1.12% BAE – boric acid equivalent) for protection against termites [4,15]. The AWPA U1-12 standards demand 4.50 kg/m^3 retention levels of inorganic boron compounds for sawn products in above ground, interior construction, and dry and humid conditions against Formosan termites. In case of non-Formosan termites, lower retention levels are advised (~2.70 kg/m^3) [1]. Kartal (2009) states that the European standards generally require 0.76, 0.59, 0.32, and 0.30 kg/m^3 minimum DOT retention levels for protection of wood against wood degrading fungi, *Trametes versicolor*, *Gloeophyllum trabeum*, *Coniophora puteana*, and *Poria placenta*, respectively. Wood to be treated commercially with borates in the United States is in general treated with DOT at a borate retention of 2.70 kg/m^3 BAE based on the AWPA standards to eliminate decay [16]. Freeman et al. (2009) have reviewed that boron treatments are also effective remedial treatments for joinery [8]. Target borate retention levels of 0.8-1.5 kg/m^3 for remediation of window joinery are needed to stop fungal growth [17].

5 CONCLUSION

Remedial preservative treatment of wood provides an alternative solution to replacement or repair methods by extending the service life of wood. Wood preservatives are important to increase the service life of wood and timber structures. In wood protection, chemicals and techniques followed in remedial treatments should comply with design, value, composition, and texture of the structure.

The use of broad-spectrum preservatives to protect wood material and timber structures is being restricted since such chemicals contain components that are toxic to mammals and other non-target organisms in the environment. Boron compounds are considered to be only preservatives capable of acting as both insecticides and fungicides commonly accepted as effective and low toxic. High mobility property of boron elements is another benefit in most applications. Because of increased toxicity and environmental issues and properties as wood-protecting agents, boron compounds have been receiving a lot attention increasing their importance for the wood industry. Since borate preservatives are capable of diffusing from the surface of wood into the internal parts, the process is suitable best for damp lumber (MC > 30%) where the moisture in the wood functions as an instrument for diffusion.

Borate treatments of wood in buildings have been widely accepted and available worldwide. Wood treated with borates is colorless; it may be machined, glued, and painted without corrosion risks. Most borate formulations are water-soluble and remain mobile in wood after treatments. Wood treated with borates is successfully used in many parts of the world where fungi, insects, termites, and other wood-destroying organisms cause major problems. Thus, borate-treated wood shows excellent performance as a building material.

REFERENCES

[1] AWPA, 2012. "Use Category System: User Specification for Treated Wood". American Wood Protection Association Inc., Birmingham, Alabama, USA.

[2] Lebow, S. and Anthony, R.W. 2012. "Guide for use of wood preservatives in historic structures". General Technical Report FPL-GTR-217. Madison, WI: U.S. Department of Agriculture, Forest Service, Forest Products Laboratory. Pp: 59.

[3] Bhatia, T. K. 2002. "Use of borate-treated wood as part of an IPM approach for durable and sustainable construction". Proceedings of the 4th International Conference on Urban Pests. S.C. Jones, J. Zhai, and Wm H. Robinson Editors, Pp:269-276.

[4] Kartal, S. N. and Yoshimura, T. 2016. "ホウ酸塩:木材をシロアリから護るための天然薬剤 (Borates: A natural way to protect wood against termites)". The Japan Termite Control Association, 1. No: 165, Pp:7-10.

[5] Unger, A., Schniewind, A. P. and Unger, W. 2001. "Conservation of wood artifacts a handbook". ISBN: 978-3-540-41580-0.

[6] Kartal, S. N., 2009. "Boron-based wood preservatives and their use". In: Handbook on Bo-rates: Chemistry, Production and Applications. ISBN: 978-1-60741-822-1 Editor: M.P. Chung 2009 Nova Science Publishers, Inc.

[7] Lloyd, J. D. and Pratt, J. E. 1997. "The use of disodium octaborate tetrahydrate to control conifer butt rot caused by *Heterobasidion annosum*". In: Proceedings of the Second International Conference on Wood Protection with Diffusible Preservatives and Pesticides. Forest Products Society, Proceedings No: 7284, ISBN 0-935018-90-5.

[8] Freeman, M. H., McIntyre, C. R., and Jackson, J. 2009. "A critical and comprehensive review of boron in wood preservation". In: Proceedings of American Wood Protection Association, 105, Pp:279-294.

[9] Laks, P. E. and Manning, M. J. 1997. "Update on the use of borates preservatives for wood composites". In: Proceedings of the Second International Conference on Wood Protection with Diffusible Preservatives and Pesticides. Forest Products Society, Proceedings No: 7284, ISBN 0-935018-90-5.

[10] Vinden, P. and Romero, J. 1997. "Developments in the application of organic boron compounds". In: Proceedings of the Second International Conference on Wood Protection with Diffusible Preservatives and Pesticides. Forest Products Society, Madison, WI, USA. Proceedings No. 7284, Pp: 119-126.

[11] Morrell, J. J., Love, C. S. and Freitag, C. M. 1996. "Integrated remedial protection of wood in bridges". Gen. Tech. Rep. FPL–GTR–94. Madison, WI: U.S. Department of Agriculture, Forest Service, Forest Products Laboratory, Pp: 445–454.

[12] Forsyth, P.G., and Morrell, J. J. 1992. "Diffusion of copper and boron from a groundline wrap formulation through Douglas-fir heartwood". *Forest Prod. J.*, 42(11/12), Pp:27-29.

[13] Lloyd, J. D., Schoeman, M. W. and Stanley, R. 1999. "Remedial timber treatment with borates". Proceedings of the 3rd International Conference on Urban Pests. Wm H. Robinson, F. Rettich and G.W. Rambo (editors), Pp: 415-423.

[14] Turner, A. A. 2008. “Penetration Depth of Borates in Historic Wooden Structures in Virginia City, Montana”. Master Thesis - The University of Pennsylvania (Historic Preservation), Pp: 198.

[15] Schoeman, M. W. and Lloyd, J. D. 1998. “International standardisation: a hypothetical case study with stand-alone borate wood preservatives”. International Research Group on Wood Preservation IRG/WP 98-20147. IRG Secretariat, Stockholm Sweden.

[16] Llyod, J. D. 1997. “International status of borate preservative systems”. In: Proc. of the 2 nd İnter. Conf. On Wood Protection with diffusible preservatives and pesticides, Forest Prod. Soc.Proc. No. 7284

[17] Drysdale, J. A. 1994. “Boron treatments for the preservation of wood: A review of efficacy data for fungi and termites”. International Research Group on wood preservation. IRGWP-94-30037.

SHATIS'17
4th International Conference on
Structural Health Assessment of Timber Structures
20-22 September 2017 Istanbul, Turkey

CONSERVATION AND RESTORATION OF BRAZILIAN COLONIAL ARCHITECTURE

Benedito Tadeu de Oliveira[1]**, Vanessa Araujo Braide**[2]

[1] Fundação Oswaldo Cruz – Fiocruz Minas

[2] Instituto Federal de Minas Gerais - IFMG

Keywords: Conservation, Preservation, Intervention, Urban, Cultural, Heritage

Abstract

This paper will deal with the various conservation problems and challenges encountered during the resto-ration of Brazilian colonial buildings built in the period from the country's discovery in 1500 until its in- dependence in 1822.

In Brazil, the Portuguese settlers found indigenous techniques and materials such as wood, clay and palmleaves used in native buildings that were later incorporated into their own constructions. These techniques and materials, lath-and-plaster, adobe, brickwork, stonework and timber structures formed the traditionalconstruction system in the country.

In Minas Gerais, the colonial buildings were made using mainly stonework for the foundations, wood for independent timber structures and lath-and-plaster or adobe for the walls. Hand lath-and-plaster walls ("pau-a-pique", "taipa de mão", or "taipa de sopapo") were made of long wooden lattices and filled with clay. Monuments and stately buildings were generally made of stonework bound with lime. Wooden floors and ceilings predominated indoors. Roofs were built with wooden frameworks and covered with clay tiles. Walls inside and outside were finished in stucco and painted with lime.

This paper will also deal with the following problems and technical solutions applied to the conservation of Brazilian colonial architecture:

- *humidity in old timber structures and ways of treating it;*
- *diversity of xylophagous insects existing in timber structures in Brazil and ways of extermination;*
- *the use of appropriate techniques and materials for consolidating old timber structures.*

As a case study, the difficulty of filling in gaps in lath-and-plaster or adobe walls will be dealt with, taking into account that it is necessary to distinguish a modern intervention from an architectural element or original material. Technical, theoretical and methodological issues will be examined in relation to the challenges of applying modern principles of restoration to Brazilian colonial architecture.

1 INTRODUCTION

During the colonial period, many coastal cities such as Salvador (Bahia), São Luís (Maranhão), Belém (Pará), and Rio de Janeiro sprang up; they were characterized by a regular outline and an urban nuclear development centered on a large square, around which state and religious buildings were arrayed. After the discovery of gold in the state of Minas Gerais in 1698, many cities known as “vilas do ouro” (gold towns) made their appearance, characterized by a particular plan which did not conform to the traditional urban organization found in the other regions of Brazil. According to Sylvio de Vasconcellos, the organic and linear configuration anticipated the type of urban development presently known as conurbation, that is, the creation of a city from the merging of many neighboring areas. Examples of this phenomenon are the cities of Mariana, São João Del Rei, Diamantina, and Ouro Preto, which came into being through the linking of many settlements created by the discovery of gold.

The vast territory of Brazil with its diverse climate and topography imposed the adoption of techniques that varied from region to region. For instance, rammed earth was used in the state of São Paulo, stone and brick masonry in the north and northeast regions, and lath-and-plaster in the state of Minas Gerais. There predominated the use of stone masonry in the foundations, wood for autonomous structures, and lath-and-plaster or adobe for walls. This building system, also known as hand lath-and-plaster (“taipa de mão” or “taipa de sopapo”), employs interwoven wooden sticks or rods, bound with rope or leather strips, and that are filled in with clay. This technique was widely applied to construction in Minas Gerais, due to its appropriateness to the declivities characteristic of the region. Monuments and stately buildings were usually built in stone set with lime. Internally the use of wood in floors, ceilings and frames predominated. Roofs were also made of wooden structures covered with clay tiles. Both interior and exterior walls were finished with lime plaster whitewash. Wood was widely used during 18th and 19th centuries, even in the structures of buildings. In Minas Gerais, these structures are formed with vertical pieces (supports) and horizontal elements (master beams), bound by dividing walls and diagonal pieces (“Saint Andrew’s Cross” or “French quotation marks”). In these cases, walls are made of lath-and-plaster or adobe bricks. Stone or brick masonry set with lime is found in most of the ground floors in houses, forts, religious or stately buildings. These methods also predominate in residential construction in the north and northeast regions of Brazil.

Figure 1. Lath-and-plaster wall, Casa da Baronesa, Ouro Preto - State of Minas Gerais (Source: IPHAN’s collection)

In the following sections, we will examine the main problems and technical solutions in the conservation of the Brazilian colonial architecture:
- humidity and the ways of treating it;
- the diversity of xylophagous insects and fungi and ways of exterminating them;
- the use of techniques and materials compatible with the consolidation of old structures;
- heavy vehicular traffic and suggestions for reducing its impact on the buildings.

We will also examine the difficulties in the filling of cavities in lath-and-plaster or adobe walls, taking into account the recommendations made by the Cartas Patrimoniais (official publication of IPHAN, the National Institute of The Historical and Artistic Heritage of Brazil) in order to distinguish a modern intervention from one involving an original architectural object or element. Technical, theoretical as well as methodological issues will be briefly examined, focusing on the challenges in their application according to the modern principles of restoration of Brazilian colonial buildings.

Figure 2. Rammed earth wall under rebuilt, Casa Cora Coralina, city of Goiás - State of Goiás (Source: IPHAN's collection)

2 HUMIDITY

Brazil is a large country of approximately 8,500,000 square kilometers (5,283,000 square miles), and characterized by a predominantly warm climate, a relative humidity of between 70% and 80%, and seasons of abundant rainfall over most of its territory. These climatic features, together with the materials used in traditional Brazilian architecture, such as wood and clay, make humidity one of the principal factors in the deterioration of buildings. Many types of humidity are found: capillary attraction, when buildings are in direct contact with humid surfaces; water infiltration through leaks in the roof or pipes; condensation through thermal inertia or insufficient thermal and hygroscopic protection.

Interventions with inadequate materials that prevent respiration of traditional materials, the existence of closed and non-ventilated spaces, as well as the use of cooling systems that create significant temperature variation between internal and external surroundings all contribute to the presence of humidity.

The continual action of humidity results in the complete deterioration of the original construction materials. This causes wooden structures to rot, facilitating infestations of xylophagous insects and fungi and resulting in the physical deterioration and consequent instability of the structure. The loss of structural elements in the building leads to new non-distributed forces, generating unanticipated loads that result in collapse. Excessive humidity causes mineral salt crystallization on wall coatings, which fall down and expose the structures to the elements.

Our experience has demonstrated that simple actions, as routine structural checks, as well as the reinforcement of coverings, including roof guttering, flashing and edging, can prevent most of the potential damage that humidity causes to buildings. In addition, appropriate use of the building and interventions made according to criteria that take into account the characteristics of the building are important factors in preservation. For instance, the maintenance of natural ventilation and the use of materials compatible with the original must be considered. In this regard, the use of plaster and lime whitewash or mineral tints, instead of cement and PVA-based or acrylic painting, allows the original materials to breathe and prevents the accumulation of humidity internally.

Figure 3. Air chamber under the floor, Magazine, Fort São José de Macapá - State of Amapá (Source: IPHAN's collection)

Those problems which are hard to solve are related to permanent sources of humidity such as those resulting from the direct contact of old building materials with humid soil. The solution adopted for wooden floors involves the revival of the use of air chambers consisting of a ventilation space between the wooden floor and the soil. This solution, widespread in traditional Brazilian architecture, is usually ignored in inappropriate restorations and interventions that set wooden floors directly onto the pavement, leading to wood-rot and infestation of xylophagous insects in the structure. In the case of structures in direct contact with humid surfaces underground or supporting structures in hilly places, the solution has been to provide natural ventilation, and, on occasion, even separate the floor from the walls in order to reduce effects of humidity.

In the case of humidity in the vaults of São José de Macapá Fort, in the state of Amapá, the slope of the upper earth embankments was altered so as to prevent rainwater accumulation at certain points, and a new covering made of lime whitewash was applied. Due to excessive humidity, the original coating had deteriorated significantly, leaving the brick masonry exposed and subject to the continual actions of humidity from the soil.

3 THE ACTION OF XYLOPHAGOUS INSECTS AND FUNGHI

Xylophagous insects and fungi, which find optimal conditions for reproduction in the warm and humid climate of Brazil, are the major cause of deterioration in wooden structures. The most commonly found are dry-wood termites, soil termites and borers.

Dry-wood termites restrict their nests to the interior of the wooden pieces they have infested, and their presence can be confirmed through the existence of dry flakes of wood nearby. The “underground” or soil termites make their nests in soil or in any permanent source of humidity. Their infestation can be identified through the existence of underground galleries or earth-covered tunnels on the walls. Exterminating this type of termite is quite difficult, as it does not restrict itself to the infested piece, but continually moves its shelter. Borer is the common denomination for xylophagous beetles, whose infestation can be identified through the existence of a fine yellow powder and small holes in the piece of wood. Fungi change the color of the wood; their infestation is characterized by the appearance of mold or mushrooms and the softening of the piece.

The most common immunization methods used in Brazil consist of application of chemical substances with a clorpirifos, permetrine or deltametrine base, by brushing, spraying, dusting, fogging, injecting or immersing. For new pieces, preventative autoclave sterilization is employed.

Applications by brushing or spraying have been more prevalent as they are more economical and easier to apply. However, they offer lower protection since their action is restricted to the surface.

Figure 4. Xylophagous insects in the Church of São Francisco de Paula, Ouro Preto - State of Minas Gerais (Source: IPHAN’s collection)

More efficient methods are the use of chemical barriers and immunization by immersion, but they are highly controversial since they can contaminate soil and freatic groundwater. The chemical barricade method consists of isolating the building from the termite colony with termiticides. Immunization by immersion consists of soaking the pieces in tanks containing the same chemicals.

Another method little used in Brazil is the setting of attractive cellulose traps around the building that are later replaced by bait with delayed-effect insecticide or substances that interfere with growth of the insects and that are taken as food into the colony.

Preventative measures against xylophagous insects and fungi by making wooden parts embedded in walls impermeable include the following:

- surface carbonization, producing a coal layer that repels insects. This technique has been used in the bases of supporting structure directly placed in the earth, as well as in the interior of religious sculptures;
-application of asphalt and bitumen products;
- isolation of the wooden piece by use of another material, such as metal sheeting.

Prior identification, under the supervision of specialists, of the insects and fungi encountered is very important in determining the treatment to be adopted. Unfortunately, in Brazil this practice is not widespread, and in the majority of restorations immunization is made by dusting, failing to undertake any prior study made to identify the focuses of infestation.

4 TECHNIQUES AND MATERIALS COMPATIBLE TO THE CONSOLIDATION OF OLD STRUCTURES

The experience acquired in many restoration works in Brazil has demonstrated that correct analysis of a problem is essential in order to avoid expensive, complex interventions. The consolidation of old structures can only proceed after taking into account the physical features and original materials of the building. An investigation of the causes of structural instability may begin with the identification of physical modifications that may have occurred within the structure, such as the raising of freatic groundwater levels or leaks from public or neighboring drainage networks which may cause changes in soil resistance. As the foundations of buildings built in the Brazilian colonial period were generally made with stone masonry, bricks and lath-and-plaster, the treatment will depend on a correct diagnosis of the problem, in the majority of cases caused by inappropriate use or poor conservation of the buildings.

Figure 5. Lime mortar coating,Fort São José de Macapá - State of Amapá
(Source: IPHAN’s collection)

The ground is usually consolidated and/or stabilized by mixing earth with cement or lime, and then compacted. In foundations and structures made with stone masonry, the wall is rebuilt with the same material, while the joining and filling in of gaps, known as breaches, is sufficient to stabilize the structure. In lath-and-plaster structures, the reconstitution of material, repaired using the same soil together with injections of lime in the layers, has proven adequate in consolidating the structure. Adequate rain-water drainage must also be ensured, as in the case of the restoration of the Matriz de Santo Antônio in Tiradentes, Minas Gerais.

5 VEHICULAR TRAFFIC

Damage to building structures caused by the traffic of heavy vehicles is common in historic Brazilian cities, leading to the instability of buildings, which can be verified by noticeable, long and permanent cracks.

This problem has been solved by projects that organize the traffic, prohibiting heavy vehicles from historic centers; this includes buses outside of peak hours.

Figure 6. Square in front of the Church of São Francisco de Assis, Salvador – State of Bahia (Source: IPHAN’s collection)

The use of squares as parking areas decharacterizes historic places, prioritizing vehicles instead of pedestrians. The solutions usually adopted in Brazilian historic cities, aiming at returning public spaces to pedestrians are as follows:
- Prohibiting the traffic of vehicles in some streets and the creation of parking areas near the historic centers, as in São Luiz (state of Maranhão) and Salvador (state of Bahia);
- Placing curbs in the center of squares, preventing vehicles from parking; a solution to be adopted through the Program Monumenta-BID- in Ouro Preto (state of Minas Gerais).

6 FILLING GAPS

Maintaining both the distinction between old and new materials on the one hand and keeping the unity of the structure on the other is easy in some cases, but difficult in others. Wooden structures are usually restored through immunization and reintegration of the autonomous structure by completing the damaged area with similar materials, after removing those parts which are compromised. To fill in small holes, one uses wood powder with the same color as the original piece and PVA glue or resin; large gaps are filled in with dry wooden pieces similar to the original ones, which are embedded by using pins and glue. In those cases where the structural piece has been completely destroyed, it is usually replaced by one that is new and trimmed to the same dimensions as the original. This technique has become increasingly difficult as the sale of certain types of high-quality wood, compatible with the original materials, is now restricted. For floors and ceilings, one generally uses the original pieces in prominent rooms while employing replacements in rooms of lesser importance.

This approach is frequently not an option when recoating mortar. Therefore a sand-granule type is used for the differentiated new coating, taking care to ensure that this is not noticeable on the surface. In enclosed spaces we usually encounter significant loss of materials due to humidity and xylophagous insects. The filling of cracks and gaps is difficult, as the addition of new materials must take into account their physical properties together with the final appearance of the assemblage.

Figure 7. Reintegration of coating cavities, Centro Cultural da FIEMG, Ouro Preto - state of Minas Gerais (Source: IPHAN's collection)

The restorations in the texture of lath-and-plaster walls use those pieces that are well-preserved, concentrating them in same section of the wall in order to achieve an interpretation of the preserved assemblage. In these cases, the original clay is reused, being mixed with water and reapplying it into the weave. When filling in cage-like structures, it is almost impossible to achieve this distinction, since the mixture must be homogeneous to prevent new clay from shrinking with time.

7 CONCLUSION

Interventions for the conservation of Brazilian colonial architecture have demonstrated that rigorous research into the causes of damage and accurate diagnosis are essential to achieve adequate restoration and the eventual preservation of the objects' cultural authenticity.

The construction materials currently in use in Brazil, like baked-clay bricks, concrete structures, cement mortar, plastic mass, acrylic, latex or PVA-based paints etc., when used in old structures, make them degenerate since these materials are generally incompatible with those originally used in the Brazilian colonial architecture.

In Brazil, there is some resistance to the use of traditional construction materials and building systems. Lath-and-plaster and the use of lime plaster in painting or in coating mortar are perceived as low-quality construction methods, since they are used by poorer, rural populations. We have encountered the replacement of lath-and-plaster by hollow bricks, wooden structures by wooden-covered concrete (aiming at imitating the original), the recovering of stone pillars with concrete and then with regular-cut stones – idiocies aimed at disguising in- correct interventions. Such slap-dash techniques are practiced by professionals who ignore traditional construction techniques and use improvised methods such as covering brick vaults with asphalt, a solution used for paving modern building, that in fact accelerate the degeneration of original materials.

This does not mean a return to the exclusive use of historic techniques, as some technicians opposed to the use of traditional materials and techniques, such as that of hydrated lime mortars in restorations, would imply. In fact, it is a matter of finding adequate, modern materials and techniques appropriate for historic buildings. As an example, we can point to the use of silicate-based mineral painting, instead acrylic or PVA-based paints, which is as beneficial to the original materials as whitewashing with lime plaster.

Our experience has demonstrated that simple and routine actions such as cleaning, roof maintenance, whitewash, systematic inspection for termites, and repairs using construction materials and systems compatible with the original ones have been efficient.

Considering humidity as one of the most serious degeneration agents in old buildings in Brazil, since it attracts xylophagous insects into wooden pieces, especially structural ones, leading to their collapse, we believe that some traditional architectural techniques and solutions may not be forgotten or ignored in order to avoid historical buildings' degeneration. We for instance mentioned the air chambers under the ground floors and the easy-to-make water-drainage systems in places where water runs down, like windowsills. Wood, as a highly hygroscopic material, while under continuously humid conditions, will get rotten, attracting xylophagous insects and leading to a possible infestation throughout the building.

Architectural solutions that reduce humidity in buildings and wooden structures are extremely important to their conservation. Therefore, this conservation depends precisely on the use of techniques and materials from the Brazilian colonial architecture.

With the conservation actions above mentioned, it is frequently possible to avoid certain complex techniques with questionable results, such as chemical barriers, the insertion of superstructures and application of high-technology products without taking into account the original structures or being sure of the real efficacy of those techniques for the old materials.

We have observed that in places where the materials were not affected by weathering or human action, the building system –even those made of earth and, thus, the most vulnerable – remains intact and well preserved.

An exhaustive investigation of damages, with a detailed diagnosis of the causes for degeneration, has resulted in both careful and successful interventions, with no loss of the intrinsic features of the cultural objects.

We finally conclude that knowledge of and respect for the traditional building techniques of Brazilian architecture, combined with the adoption of new materials compatible with the physical/chemical properties of the original and consideration of the final appearance of the complex, may be the fundamental premise underlying the preservation of the Brazilian colonial architecture. Generally traditional building technology does not involve high costs. This is a positive feature since economic aspects are crucial in a context where the financial resources available are insufficient for preserving the invaluable cultural collection of a continental-size country such as Brazil.

REFERENCES

[1] Massari, Ippolito. 1982.Umiditá nei Monumenti Roma: ICCROM.

[2] Mello, Suzy de. 1985. Barroco Mineiro. São Paulo: Editora Brasiliense.

[3] Oliveira, Mário Mendonça de. 1995.Tecnologia da Conservação e da Restauração: roteiro de estudos.Salvador: Mestrado em Arquitetura e Urbanismo da UFBA/PNUD/UNESCO.

[4] Reis Filho, Nestor Goulart. 2004.Quadros da Arquitetura no Brasil. São Paulo: Editora Perspectiva .

[5] Santiago, Cybele Celestino. 1996. O solo como material de construção. Salvador. EDUFBA.

[6] Vasconcellos, Sylvio de. 1977. Vila Rica. São Paulo: Editora Perspectiva.

[7] Vasconcellos, Sylvio de. 1979. Arquitetura no Brasil: sistemas construtivos. Belo Horizonte: Editora Rona.

SHATIS'17
4th International Conference on
Structural Health Assessment of Timber Structures
20-22 September 2017 Istanbul, Turkey

RECONSTRUCTION OF A WOODEN "POLISH MANOR" WITH THE USE OF SOLID WOOD LAYERED FLOORS

Anna Rozanska[1], Anna Policinska-Serwa[2], Wojciech Korycinski[3] and Piotr Beer[1]

[1] Warsaw University of Life Sciences WULS-SGGW, Wood Technology Department, Poland

[2] Building Research Institute, Warsaw, Poland

[3] University of Life Sciences in Lublin, Department of Industrial and Medicinal Plants, Poland

Keywords: reconstruction, manor house, decorative wooden floors, parquet, solid wood layered floors

Abstract

Historical wooden and bricked manor houses built in Poland since the second half of the 16th century until contemporary times are an important part of Polish cultural heritage. Traditional "Polish manors" were inhabited by the most numerous social class in Poland that had a lot of political importance - the gentry. The range of architectural forms of manor houses is quite vast, from little palaces to richer cottage houses and apart from their practical purposes, had also a symbolic function.

This article describes the cultural phenomenon of the so called "Polish manor" in its historical, stylistic, construction-related and functional aspect. The hereby analysis was used in the reconstruction of a wooden manor house, including some missing decorative elements, as the centre of a set of buildings at the Museum of Folk Culture in Kolbuszowa, together with architectural details of the facade and internal furnishing. The reconstruction of buildings is carried out in order to preserve their non-material value as a document or symbol, but most of all to create new value consisting in making it suitable for use. Due to this latter requirement, the restoration specialists need to observe European construction standards when reconstructing buildings, both in terms of their architecture, as well as the structures in their interiors.

Many "Polish Manors" were destroyed during World War II. Therefore, the documentation of preserved buildings is an urgent matter, just like the reconstruction of the ones that have been destroyed, with special attention paid to all the original structures and furnishing. It is a very up to date issue, due to the ongoing degradation of antique buildings.

1 RESEARCH BACKGROUND, AIM AND METHODOLOGY

Historical wooden and bricked manor houses built in Poland since the second half of the 16th century until contemporary times are an important part of Polish cultural heritage. Traditional "Polish manors" were inhabited by the most numerous social class in Poland that had a lot of political importance - the gentry. A Polish manual from 1659 entitled *A Short Treatise on the Construction of Polish Manor Houses, Palaces and Castles* enumerates three types of residential buildings characteristic for those times: manor houses, palaces and castles. In the times of Renaissance, most manors were bricked, while during the Baroque most of them had the form of single-storey wooden buildings.

The range of architectural forms of manor houses is quite vast, from little palaces to richer cottage houses. Independently of the architectural style and the degree of presentability of the building, the so called "Polish manors", apart from their practical purposes, had also a symbolic function, expressing the independence and personal freedom of the owner belonging to a specific Polish middle class living in the country or in a town, but other than the bourgeoisie. Representatives of the gentry together with nobility and magnates had the right to vote, which mattered in elective monarchy. This is why "Polish manors" have to be treated as "cultural substance", which refers to things that are durable and immutable, independently of the changes of certain internal features or external properties.

This article describes the cultural phenomenon of the so called "Polish manor" in its historical, stylistic, construction-related and functional aspect. The hereby analysis was used in the reconstruction of a wooden manor house, including some missing decorative elements, as the centre of a set of buildings at the Museum of Folk Culture in Kolbuszowa, together with architectural details of the facade and internal furnishing.

The reconstruction of buildings is carried out in order to preserve their non-material value as a document or symbol, but most of all to create new value consisting in making it suitable for use. Due to this latter requirement, the restoration specialists need to observe European construction standards when reconstructing buildings, both in terms of their architecture, as well as the structures in their interiors.

The research of design, construction and technologies applied in manor houses preserved in South-Eastern Poland, was preceded by a scientific and historical analysis of those buildings. It was based on scientific literature and other reference publications related to each of the buildings. The age of the manor houses was determined and the style of the buildings was also analysed. The description of patterns was complemented, whenever possible, with information about the structures and technologies of the decorative parquets preserved inside them. The layout and the dimensions of parquet panel elements were determined, the wood types and species were identified, and photographic and drawing documentation of parquet panels was prepared, taking into account wood grain and section type. On the basis of the research, one of the buildings was selected for reconstruction. Documentation was prepared to create a detailed design, taking into account the reconstruction of traditional decorative patterns of the facade and interior architecture, on the basis of new technological solutions compliant with binding European construction standards.

2. RESEARCH RESULTS

2.1 "Polish manors" as a cultural and architectural phenomenon

The manor complex includes the manor itself - the seat of a noble family, as well as an access road, a decorative garden, outbuildings and other residential buildings, auxiliary buildings with ponds and vegetable gardens, pathways and fences. It is a self-sufficient settlement unit fulfilling residential, service-related, economic and productive functions; an independent urbanistic complex with a closed and logical functional layout of mutually linked elements in its composition and space (Fig.1).

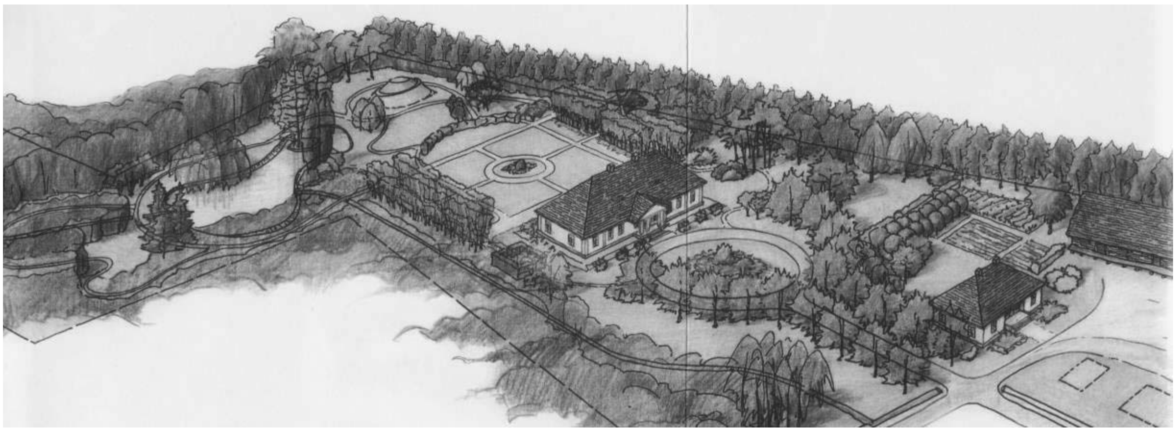

Figure 1: Reconstruction design for the manor complex in Kolbuszowa [1]

In richer homesteads, agricultural functions (related to crops and livestock) were organised in a separate set of buildings, while in poorer ones it was included directly in the group of buildings around the manor house. Therefore, the functional programme of such homesteads was determined by the size, richness, sumptuosity and stately character both of the manor house and the auxiliary buildings.

Some manors can be classified as practical, this type was popular starting from the second half of the 16th century: the manor house was not that dominant in the composition and the entire complex resembled a simple farm homestead; while in other cases a new type was developed under the influence of foreign architecture, with a clearly dominant manor house and axial layout (resulting from secular culture and customs, fashion and the need to make one's social status evident).

During the development of this kind of layouts, the composition axis acquired new elements: an avenue providing access to the manor house and a driveway or a yard in the front, closed with outbuildings on the sides. Due to the fact that there was often a large garden at the back or a park around the front yard, the farm buildings had to be moved further to the side and sometimes even to the transversal axis.

As feudal castles started to disappear since the 17th century, manor houses that implemented some palace solutions at a smaller scale (e.g. only one representational and residential storey) started to dominate in Polish landscape.

Polish baroque nobility manors were defined, to a large extent, by the visions of Tylman von Gameren (1632-1706), a Dutch architect representing mature, classicising baroque, who drew inspiration from the newest French architecture. The above-mentioned manors usually had one storey and a symmetrical, axial layout. The axis was accented by a porch or a central risalit. Two or four protruding corner rooms were situated on the sides, as an echo of the defensive towers of baroque palaces. In the second half of the 17th century, also smaller nobility houses adopted the French layout of residences *entre cour et jardin*. The location, the plan and the shape of the building were inspired by French representative architecture. Manor houses had gambrel roofs: mansard roofs in the French version, but also the so called Polish monitor roofs with two parallel slopes divided by a small wall.

In late 18th century, this model shifted towards a more classicistic manor type for poor and middle-income gentry, with rectangular layout with no corner rooms, high, often monitor-type roof, and a 4-column portico or porch on the axis of the front elevation [2].

After 1900, together with the rising interest in the national style, the classicistic manor model came back under the name of “manor style”. The manor house, as the synonym of the indigenous, became the basic symbol of nobility in the genesis of Polish culture [3]. In romantic literature, it was associated with Poland, although similar buildings exist also in Switzerland, Prussia and Russia.

Since the 19th century, Polish manors turned into a historical, psychological and sociological phenomenon, which became more important than their practical use. They have many symbolic, lifestyle-related, political, social, artistic and literary connotations. Manor houses, as a symbol of peaceful, prosperous life resulting from honest, hard work, were a manifestation of the ethos of the gentry, the ethos of being rooted in local tradition. They were associated with patriotism, conservatism and Catholicism, which made them into an important element of national identity in the times of Partitions of Poland and its loss of independence. This is why their layout was often copied in vicarages, inns, houses and villas, as well as some richer countryside cottages.

The great popularity of the Polish manor house as an architectural model is also related to its universal functionality. The Polish manor is a residential building fit for a wide spectrum of users. It is functional - with one storey, often built of wood on a rectangular plan, easy to make, open to modifications or expansions.

2.2 Wood in the architecture of manor houses

Polish manor houses were often made fully of wood, including interior furnishings. This was due to the abundance and accessibility of this material, resulting in low prices; as well as to the simple technology of manufacture and fast order delivery. For this reason, Polish manor houses apart from a timber roof truss also had wooden wall structure, wooden ceilings and stairs, wooden interior wall panelling and beam floors. The beams supported boarding and, in many cases, also very decorative wooden panel parquets (of the Versailles type), whose patterns developed together with new developments in interior design.

The wood used in buildings had the diameter of about 12 inches and was non-uniform, because some timber elements could even reach 20 inches. It had the form of round or square logs (cut with an axe at the construction site), and only boards were sewn mechanically or manually.

In swampy and waterlogged areas, the corners of the houses were dug deep into the ground in order to place it on more solid, hard base; or alternatively the house was built on oak or pine rootstocks saturated with resin or on stones that served as support for a sill plate that was thicker than the walls and that had to be replaced quite often. Therefore, foundations started to be applied over time, firstly made of loose fieldstones and later of layers of stones and bricks bound with mortar (bigger rocks or locally produced cement blocks were placed under the corners). The foundations could also be made of regular stones with a layer of bricks, and sometimes with horizontal insulation made of tar.

Walls had corner joints with interlocking notches, and in the 19th century dovetail joints without protruding ends started to become more popular, which was convenient for smooth walls required to cover the walls with boarding, which was fashionable at that time. Quite rarely, buildings received stacked log walls with vertical posts (the post had grooves on both sides into which the profiled ends of the horizontal logs fitted), with a similar joint at the jambs of doors and windows. Additionally, wooden rods were introduced vertically into the jambs in order to stabilize elements respect to one another and prevent distortions from the vertical plane. Wooden pegs (dowel pins) were used for the same purpose in stacked log walls with corner notches: to tighten slightly twisted long logs and stabilize them by connecting them to the logs below and above.

Timber roof trusses in modern manor houses (since the Renaissance) usually had the form of collar beam roofs with crown posts - with vertical posts or, sporadically, posts placed diagonally, and later also trusses with purlins and collars (straining beams) with crown posts or diagonal struts.

Windows were also made of wood and had the structure of the so-called Polish windows, based on a frame; and doors made of wooden boards or had the form of frame-and-recess doors used from the times of classicism. Roofs were covered with wooden shingles. Wooden walls were connected with bricked chimney shafts placed in the central part of the house.

The wood species that was most frequently used in wooden constructions in Poland were pine, fir and larch, reserved for more important buildings.

2.3 Scope of the manor house reconstruction

The abundance of wood in the area of Sandomierz Wilderness fostered the use of wood in construction in South-Eastern Poland. In the area of the Sandomierz Wilderness, that is in the powiats: kolbuszowski, leżajski, mielecki, niżański and tarnobrzeski, there were manor complexes in: Bielice, Chorzelów, Dzikowiec, Kiełków, Kolbuszowa, Niwiski, Piskorowice, Sadkowa Góra, Trześnia next to Tarnobrzeg, Trześnia next to Niwiski, Trzęsówka, Wilcza Wola and Brzeziny. Ethnographic publications mention two buildings in the last location, together with their dimensions, while the third one (not mentioned in the documentation, so probably the least architecturally interesting) has been preserved until today. The Museum of Folk Culture in Kolbuszowa bought the above-mentioned building and initiated the procedure of its translocation, to use it as the centre of a reconstructed manor house complex (Fig. 1) and to adapt the manor house for display and cultural functions.

It is a single-storey, rectangular, wooden, stacked log building from the 18th century with corner notches, covered with a gablet roof, with non-habitable attic and bricked foundations (Fig.2). The building dimensions are: 21.75 m x 17.63 m. At the front, it has a covered wooden porch with glass panes, while on the garden side there is a gallery running along the entire width of the elevation, supported by 8 wooden, profiled posts with decorative brackets, enclosed with a low fence. It is a big building with seven axes and two suites of rooms. The entrance is on its axis at the front through a double wing door, and there is the same kind of door on the other side, leading to the garden. There are six double wing windows divided into 6 fields, on the front and on the back elevation. These are the so-called Polish windows with box construction, where one pair of wings opens inwards and the other outwards.

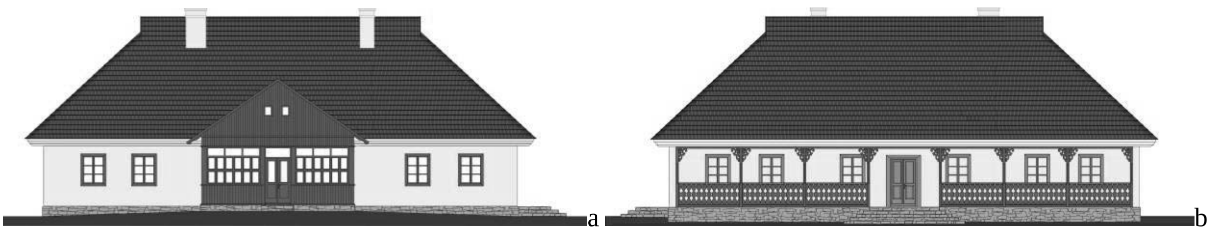

Figure 2: View of the Eastern (a) and Western (b) elevation of the manor house from Brzeziny; based on [4]

Its hip roof was probably covered with shingles. This can be concluded on the basis of densely placed roofing battens, to which the covering was fixed. The rafters have sprockets supported on the protruding ends of roof beams, which slightly breaks the straight line of the roof and makes it wider, providing eaves that protect the walls against water stains. The porch is covered by a saddleback roof and has boarding on the gable, while the gallery is covered by an elongated part of the roof itself, with a small angle comparing to the rest of the roof surface.

Inside (Fig.3) the manor has a bricked, central chimney shaft with two chimneys on top, connected to wooden elements of the partition walls by gradually sliding subsequent logs of the notch. These walls serve as support for the beams of the wooden ceiling, with boarding fixed to the upper side of the ceiling beams and serving as support for multiple crown posts in a two-tier roof truss structure. The type of roof truss resembles historical solutions, but the sections and the number of elements have been calculated in accordance with contemporary methods and in line with the binding construction standards. The attic is non-habitable. Ceiling beams have been decorated with chamfered profiles and are placed in perpendicular to the longer side of the rectangle, supported by a binding joist or made of two elements connected above the point of support on the internal wall. The space on the ground floor, in the highest point, is 3 m high, while in the attic it amounts to 4.75 m, just like in other buildings of this type.

Figure 3: Section of the manor house from Brzeziny; based on [4]

The floors of the manor house have not been preserved and used to have beam structure, with joists lying on a layer of sand and covered with decking made of boards and parquet panels on top. This solution is not acceptable nowadays due to the requirements of construction standards. During the reconstruction, horizontal hydro- and thermal insulation made of construction foil and styrofoam have been introduced and a concrete layer was cast. On top of that layer, frieze and panel parquets will be reconstructed using local, geometric patterns, in compliance with the current European standards for multi-layer parquets.

2.5 Room functionality and parquet patterns

The functional layout of the manor house (Fig.4) is divided into 3 smaller rooms in the front part (hall in the middle connected with the dining room on the axis and two rooms on the sides) and 3 bigger rooms in the garden part (the above-mentioned dining room and two rooms on each side of it on the layout of a vertically placed rectangle). The room functions have been specified in the detailed design, with technical back office in the two rooms on the right-hand side of the hall and the dining room. In accordance with the traditional traffic patterns in the enfilade room suites, each room has two double wing doors, while the hall and the dining room have three of them, which permits smooth circulation of pedestrian traffic in the entire building. Each room is lit by 3 windows, 2 on the front and back walls, and 1 on the side walls.

Potentially, all the rooms could have been heated with stoves or fireplaces connected with chimneys. On both sides of the Hall there are two centrally placed, bricked transverse chimneys. Next to them, in each room, we can find the positions of the stoves. It seems that the Hall was not heated, as it was often the case in manors and palaces. And although the reconstruction design includes underfloor heating, masonry heaters will also be reconstructed.

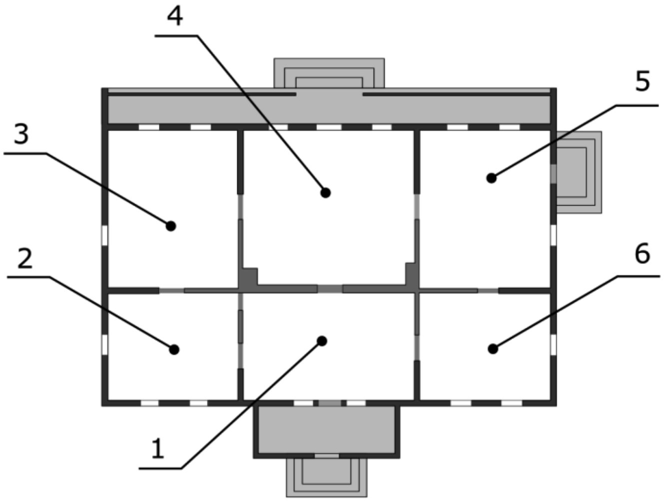

Figure 4: Functional layout of the manor house from Brzeziny: 1- hall, 2- side room in the front suite, 3- side room in the garden suite, 4- representational room on the axis, 5- side room in the garden suite (currently kitchen), 6- side room in the front suite (currently administrative room): based on [4]

Manor house floors were usually manufactured by local craftsmen at different moments: one-two rooms at a time, in order to keep the manor house functional at all times. This is why parquet patterns differ even in adjacent rooms and are usually separated by thresholds. Panels were placed in parallel or in diagonal to the walls, and their dimensions were not adjusted to the size of the room. In 18th-century and early 19th-century manor houses, there were no decorative friezes around the rooms, while rosettes appeared only in highly representational buildings. In such cases, parquet patterns were often designed by eminent architects, together with wall divisions and interior decorations. The manor house in Witkowice designed by Jakub Kubicki and located nearby, has a beautiful rosette that has been preserved in the Banquet Room. The pattern of the rosette resembles *piano nobile* parquets from the Castle in Łańcut, while the parquets that have been preserved in two other rooms of the Witkowice building have a more practical character (Fig.5).

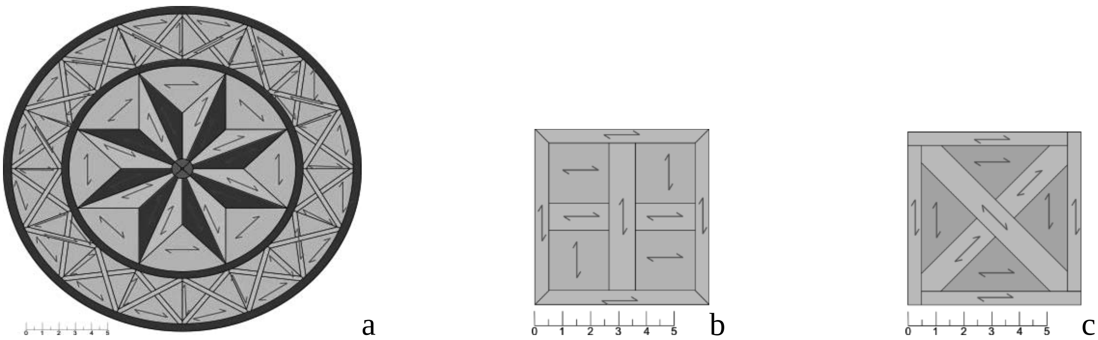

Figure 5: Rosette from the Banquet Room (a) and parquets in the Library (b) and the Dressing Room (c) of the Witkowice manor house

3 GUIDELINES FOR RECONSTRUCTION

- The manor house in Kolbuszowa is a typical, late-baroque wooden manor built in the 18th century.
- It has a baroque shape covered with a gablet roof with characteristic eaves over the gallery on the side of the garden. The porch on the front side was probably enclosed later (probably in the 19th century).

- The functional layout is typical of axis-based manor houses, with a pass-through hall or a hall connected with another representational room on the same axis in the back, and two suites of enfilade rooms on both sides of the central axis.
- The rooms have traditional functions, except for the kitchen that was introduced in late 19th century.
- Parquets still have to be reconstructed, on the basis of patterns typical for the area and preserved in other buildings. The richness of floor patterns must correspond to the room function and location. In representational and residential rooms the parquet patterns should be geometrical. In administrative/auxiliary rooms, floors will be made of planks organised into friezes.

4 RECONSTRUCTION OF WOODEN PARQUETS

4.1 Usage related requirements

The wooden parquets planned for 5 rooms of the manor house from Brzeziny under reconstruction at the Museum of Folk Culture in Kolbuszowa, due to the future display and cultural function of the building, have to meet contemporary requirements defined in European construction standards, as well as the expectations of future users.

The quality of wooden floors and parquets is assessed on the basis of how aesthetically they look after being manufactured and on the basis of their durability in the long run. Durability depends on the wood species and section, type of finish and manner of use, including the microclimate conditions around it. Parquet quality depends, most of all, on the technical and aesthetic properties of wood as a construction material (especially its hardness, elasticity, resistance properties, abrasion resistance and resistance to microbiological corrosion), as well as the quality of its installation, methods of assembly and surface finish. The usage conditions are also very important, because parquets that are properly conserved and used in stable heat and humidity conditions, wear out much slower.

The parquet and the load-bearing structure have to transfer dynamic loads associated with the movement on their top, as well as static loads of the floor itself and the objects standing on it (in residential buildings, concentrated live loads in line with EN 1991-1-1 amount to $Qk=2kN/m^2$, and in case of, for instance, a piano leg: even $3kN/m^2$).

The parquet is the top, wear layer and the external finishing element of the floor. Its wear layer should be resistant to abrasion and humidity, warm to the touch, elastic, noise attenuating, resistant to light, resistant to indentations, electrically insulating or antielectrostatic, easy to keep clean, durable and aesthetic.

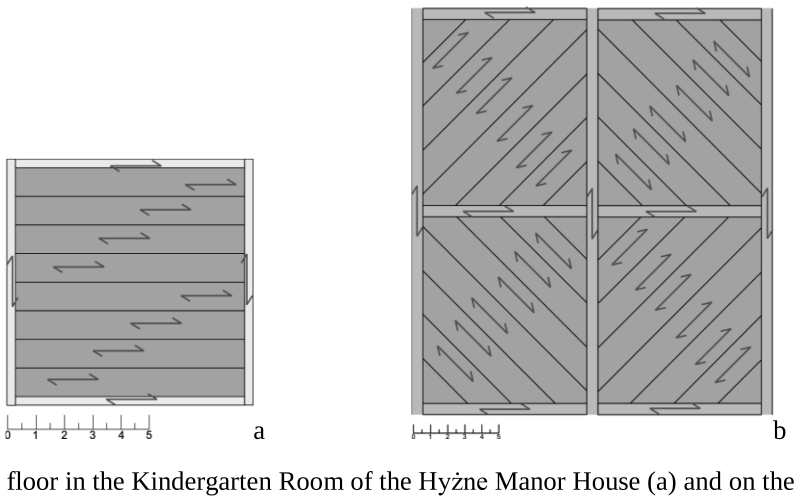

Figure 6: Frieze floor in the Kindergarten Room of the Hyżne Manor House (a) and on the first floor of the Uherce Mineralne Manor House; scale (b) 1:100mm

4.2 Antique parquet patterns

The manor house relocated to Kolbuszowa shall receive wooden plank parquet in the room no. 5 (currently the kitchen), and single-layer panel parquet with geometrical patterns for the representational rooms no. 1-4. The patterns of the plank and panel parquets have been prepared on the basis of the typical antique parquet patterns that can be found in manor houses of South-Eastern Poland (Fig. 6-7).

Among single-layer panel parquet patterns, the most popular ones in this part of the country were simple and included: a cross enclosed within a frame (Fig. 7a) and variants of the French baroque pattern from the Soubise castle (Fig.7b-d).

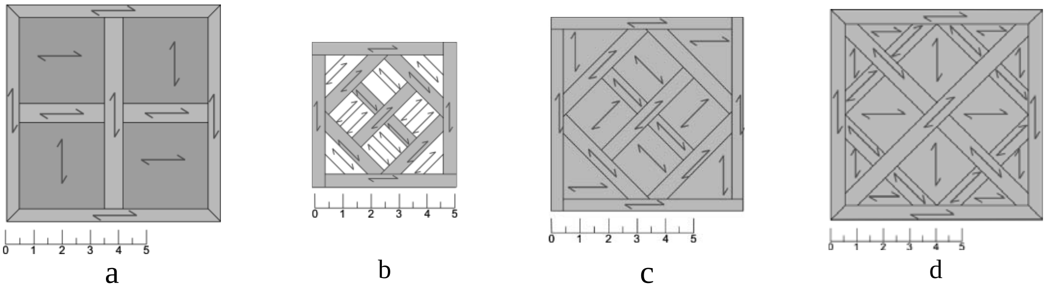

Figure 7: Panels from: Crow Room (a) and Peacock Room (b) of the Niwiski Manor House as well as from Bieździedza (c) and Dydnie (d) manors; scale: 1:100 mm

Panels were made of the wood species that were most common in a given area, in this case: oak combined with wood of slightly worse resistance properties, such as ash, elm, sycamore maple or birch.

4.3 Binding standards

Solid mineral subfloor (made of cement or anhydrite) are made in accordance with EN 13813 and EN 13318, and their declared resistance can be verified, for example, with the use of the test method described in EN13892-2 and EN 13892-1[1].

The joists and the remaining elements - such as binding joists and posts - have to be designed in accordance with the requirements of Eurocode 5 (EC 5). The wood used for joists should be marked with the CE sign and have resistance class C (C24) in accordance with EN 14081:1 and PN-D-094021:2003, confirmed with a declaration of properties. In construction engineering practice, it is recommended that joists be made of waterproof or impregnated ma-

[1]The resistance class of the mineral subfloor, either cast on site or precast, should be appropriate for the type of the floor placed on it. In case of parquets made of wood or engineered wood materials not glued to the subfloor (floating parquets) the usual subfloor resistance is at least C12. C20, C25 and C30 subfloors or subfloors with higher requirements designed individually, e.g. with rebars, are used under wooden floor parquets glued to the subfloor. Subfloor thickness depends on the floor type and parquet element dimensions. It amounts to 40 mm, independently of the kind of subfloor in case of solid wood parquets with elements that are $\leq$500 mm long and $\leq$70 mm wide, glued to the subfloor; as well as for floating multi-layer parquets, laminated panels or panels covered with veneer. Such parquets can transfer concentrated loads up to 1.5 kN/m^2 and are installed on a subfloor cast over thermal and acoustic insulation, whose compressive strength is not lesser than 70 kPa. In case of parquets made of $\leq$ 1500 mm long and $\leq$120 mm wide solid wood elements, whose thickness is equal to at least 1/7 of their width and not lesser than 16 mm, the thickness of the subfloor falls between 45 mm in case of cement and 50 mm for anhydrite. Such parquets can transfer concentrated loads up to 2.0 kN/m^2 and are glued to a subfloor cast over thermal and acoustic insulation, whose compressive strength is not lesser than 100 kPa. Parquets installed on subfloors with water heating or cooling, glued to the base or floating, able to transfer concentrated loads up to 2.0 kN/m^2, require 60 mm thickness in case of both subfloor types, while parquets whose elements are larger than specified above with or without underfloor heating, require individually calculated subfloor thickness.

terials. Usually they are made of solid pine, strips of plywood or OSB panels fixed to the subfloor. Wooden beams, binding joists and other structural elements under the parquet (the floor) should be impregnated with a bioprotective substance.

The blind floor should be made of strength graded coniferous wood planks or OSB/3 or /4. The joints between planks should be made only above the joists, using dowel type fasteners that fulfil the requirements of the EN 14592 standard. The thickness of planks as well as the amount and type of joints have to be specified on the basis of resistance calculations in line with EN 1991-1-1 or tests carried out in accordance with EN 1195 and EN 12871. OSB panels should comply with the EN 13986 standard and have the CE mark and a declaration of usage properties including the application: "roofs, walls, floors".

Multi-layer and solid coniferous or deciduous wood floor elements used currently both for the reconstruction of parquets glued to mineral subfloor and glued (and/or nailed) to a subfloor made of planks or engineered wood materials, have to comply with the standards: PN-EN 14342 and one of the following product standards: EN13226, EN13227; EN13228; EN13488; EN13489, EN 13629, EN 13990; EN 14761.

4.4 Solid wood layered floor usage analysis

The main technological processes related to the manufacture and installation of wooden floors in the manor house under reconstruction consist in preparing the parquet panels in accordance with EU standards for the given subfloor type, subfloor preparation, installation and fixing of the floor elements to the subfloor and parquet surface finishing, protecting it against destructive factors resulting from usage [5]. Parquets made by a craftsman workshop according to traditional technology do not meet the required standards. Traditional single-layer parquets are unstable as far as dimensions are concerned and tend to divert from the horizontal plane by longitudinal curvature deviations. Moreover, they do not guarantee that the shape of the elements will be preserved as required by the EN 13647 standard. The lack of dimension stability of parquet elements results in the creation of stresses and displacements of panel elements and can cause damage in the vertical partitions of the building.

Traditional panel parquets are inadequate for underfloor heating - desirable in antique buildings, as it allows to get rid of radiators that constitute an alien element foreign to the building's cultural context and thus unwanted from the restorers' point of view.

Therefore, it is worthwhile to consider multi-layer parquets for the manor under reconstruction, that would be made of wood and have a 2.5 mm thick wear layer. One of their universally known advantages consists in the optimal wood wear, especially in case of the valuable wood in the wear layers; better quality of surface treatment and joints; easy, fast and durable assembly of parquet elements; rich colours and diversified surface structure; resistance and durability; and the possibility to be renovated.

From the point of view of conservation and restoration, the basic benefit of multi-layer parquets in comparison with single-layer parquets made of solid wood, is better dimensional stability, flatness (preferable nowadays) and less deformations. A controlled production process guarantees a standardised product with stable properties that do not change with time, which is important in public buildings. The product is ecological, its substance emission is known and controlled, it has a specified surface finish and life cycle, including recycling. Floors with multi-layer parquet elements have favourable acoustic parameters, do not boost rumbling or squeaking during use.

Layered parquet elements can be used together with various subfloors: mineral ones both in case of floating parquets and parquets glued to the mineral base, as well as in case of beam floors that can be floating or glued, fixed/nailed to the decking.

Nowadays, multi-layer solid parquet elements successfully replace solid wood planks that used to be universally used in antique manor houses and other buildings in manor complexes, and it is worthwhile to consider their application in the reconstruction of panel parquet patterns.

5 REMARKS AND CONCLUSION

Vernacular art that includes most "Polish Manors" integrates trends from high-profile architecture with a certain delay. It is rather traditionalist in character and there was little variation in the shape of buildings. Only manor interiors followed European fashion and eagerly imitated French styles and, since the 19th century, also English styles. On the outside, manor houses received new elements such as classicistic porticos or porches, while old ones such as corner rooms disappeared. Wooden posts and decorative brackets started to be chamfered in accordance with the baroque or classicistic tradition. Since the 19th century, elevations were very often covered with boarding imitating bricked architecture decorations such as wooden ornaments imitating bricks or pilasters and arcades made of boards. Interior decorations also evolved. Ceiling beams started to be covered with stylish ceilings on their bottom side, walls received panelling and parquet patterns changed. Under the influence of French residential architecture, on the turn of the 18th/19th centuries plank or frieze floors were covered with decorative panels and rosettes started to be designed.

The floors and ceilings of the manor houses served as room decoration, fitted to the style of the interiors, the wall design or the furniture. Parquets served as background to make other objects stand out, sometimes they suggested divisions in the interiors, created illusions of changes in the plan on which they were installed or forced to organise the furniture in a specific manner (decorative frieze bordures or central rosettes). A centrally placed rosette was often a dominant element of interior decoration. Yet sometimes the role of the floor was much bigger in the culture of the nobility. Interior design conveyed a certain message through the aesthetical impression produced in the invited guests. Through such aesthetical impressions, stately buildings communicated something about their owners, their social and financial status, their political affiliation, taste in art or philosophical ideas. Interiors of stately buildings, especially until the times of Rococo, were designed by renowned architects who planned their ceilings, walls and parquets, together with furniture that had to fit the style of the whole. For example, the parquets in Łańcut, created in 1830s, are associated with the artistic taste of Izabella Lubomirska and the time when Christian Piotr Aigner - an outstanding architect of the period of Polish classicism - was active. Moreover, Aigner designed the rosette for Magdalena Morska’s Palace in Zarzecze, and Jakub Kubicki designed the rosette for the Witkowice manor house.

Many "Polish Manors" were destroyed during World War II and in the collectivisation period afterwards. Therefore, the documentation of preserved buildings is an urgent matter, just like the reconstruction of the ones that have been destroyed, with special attention paid to all the original structures and furnishing (Fig.8). It is a very up to date issue, due to the ongoing degradation of antique buildings, especially as far as their interiors and furnishing are concerned, resulting from constant usage, changes of owners or refurbishment works carried out.

ACKOWLEGMENT

The presented research were co-financed by The National Centre for Research and Development (NCBR) under Strategic research and development program „Environment, agriculture and forestry"–BIOSTRATEG, project NR BIOSTRATEG2/298950/1/NCBR/2016

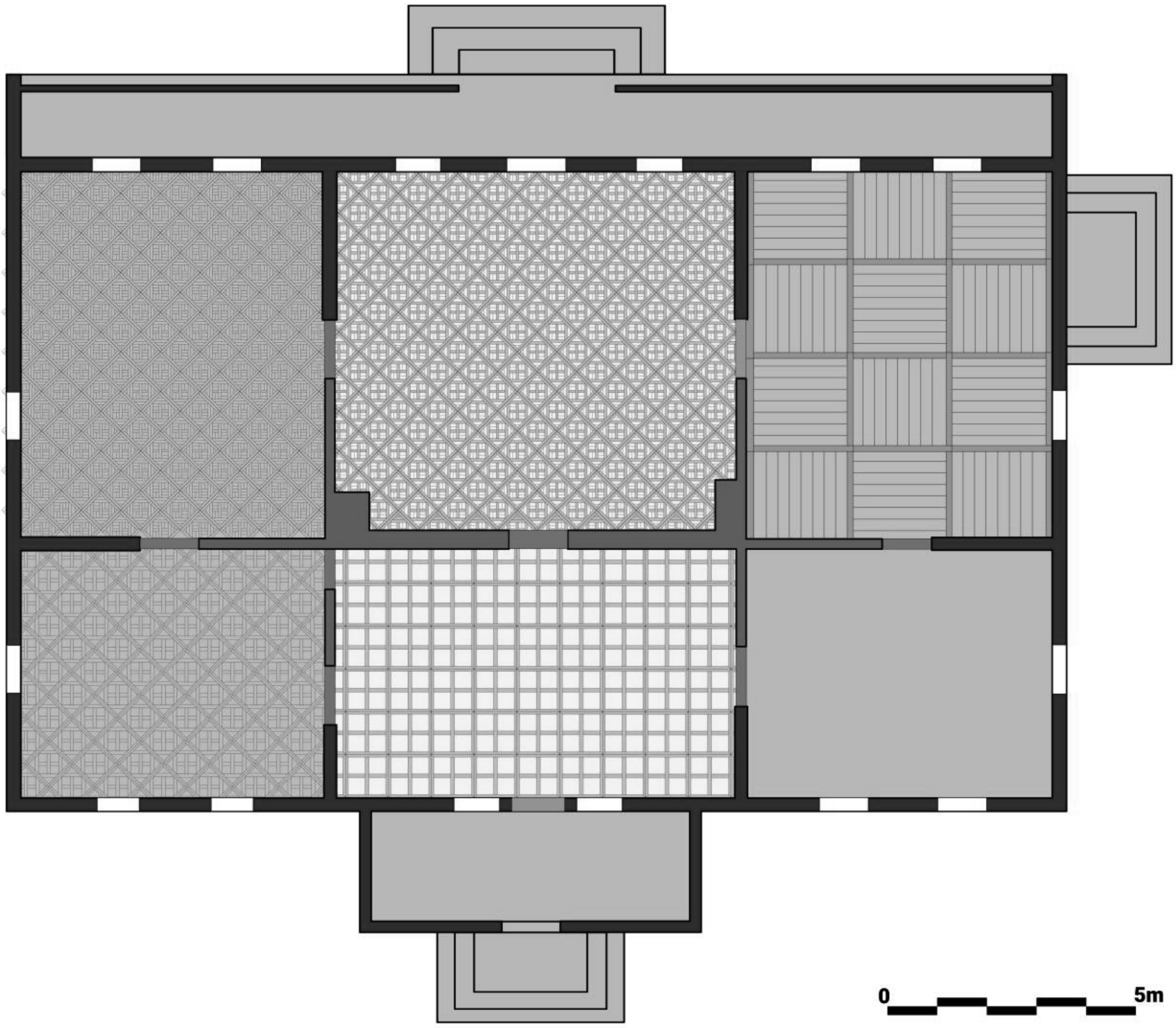

Figure 8: Parquet patterns proposed for the manor house under reconstruction in Kolbuszowa

REFERENCES

[1] Fortuna-Marek A., Gliwa A., Potera B. 2009. Manor Homestead as a Functional Layout and its Realisation in the Ethnographic Park of the Museum of Folk Culture in Kolbuszowa, Biuletyn Muzeum Kultury Ludowej w Kolbuszowej 1, 113-141.

[2] Ruszczyk G. 2007. Wood and Architecture, Warsaw.

[3] Lesniakowska M. 1992. The Manor House- Towards a Retrospective Utopia, "Polish Art Studies".

[4] Sobolewski H., 2014. Detailed Design for a Manor Homestead - Brzeziny Manor House, Rzeszów.

[5] Rozanska A., Policinska-Serwa A. 2016. Usage requirements for antique wooden floors In the context of their conservation, Proc. of the 10th International Conference on Structural Analysis of Historical Constructions-Anamnesis, diagnosis, therapy, controls- Van Balen & Verstynge (Eds), 2016 Taylor & Francis Group, London, 1672-1679.

SHATIS'17
4th International Conference on
Structural Health Assessment of Timber Structures
20-22 September 2017 Istanbul, Turkey

NUMERICAL STUDY ON THE IN-PLANE BEHAVIOUR OF EXISTING TIMBER DIAPHRAGMS STRENGTHENED WITH DIAGONAL SHEATHING

Ermes Rizzi[1], Mirko Capovilla[1], Ivan Giongo[1], Maurizio Piazza[1]

[1] Department of Civil, Environmental and Mechanical Engineering, University of Trento, Italy

Keywords: Timber diaphragms, retrofit, diagonal sheathing, modeling, earthquake

Abstract

The vulnerability assessment of heritage buildings in earthquake prone areas is greatly dependent on the quality of the diaphragms. Inefficient wall-to-diaphragm connection and/or insufficient in-plane strength and stiffness of the diaphragms often lead to extremely ruinous failures characterized by entire building-portions losing their stability (I mode collapses). In traditional buildings, the diaphragms are mostly comprised of flexible wood diaphragms where a layer of floorboards is supported on regularly spaced timber joists spanning perpendicularly to the board direction. The nail couples that fix the floorboards to the underlying framing, determine the in-plane response of such diaphragms which consequently can be inadequate to preventing the out-of-plane collapse of the face-loaded walls in case of strong earthquakes.

The applica-tion of an additional layer of timber planks that are nailed to the original flooring at a 45° inclination to the joists, can significantly improve the in-plane diaphragm behavior by creating strut-and-tie resisting mechanism that engages the timber elements (truss analogy). This retro-fit solution is cost-effective and it is also welcomed by the heritage agencies because of its aesthetic consistency with the original diaphragm condition.

The outcomes of a parametric study mainly based on nonlinear static analyses is presented herein. Among the various aspects included in the study, there are: aspect ratio, scale effect, geometrical and mechanical proper-ties of the sub-components. Two different numerical approaches were considered and validated on experimental data available in literature. Nonlinear dynamic analyses were also conducted in order to evaluate the diaphragm energy dissipation and displacement demand.

1 INTRODUCTION

One of the key aspects in defining seismic vulnerability of unreinforced masonry (URM) buildings is the in-plane behavior of flexible timber floor diaphragms. Under seismic excitation, excessively flexible diaphragms may lead to local collapse of out-of-plane loaded walls and may not be adequate to ensure a box response of the entire building. Therefore, assessment and improvement of the in-plane behavior of such components are crucial, especially in the case of single straight sheathed floors (the most common floor type in traditional URM buildings). In this paper, the effectiveness of an additional diagonal floorboard sheathing is analyzed by means of nonlinear static and nonlinear dynamic numerical modeling.

2 FINITE ELEMENT MODELING DETAILS

The research study presented in this paper is based on finite element modeling of both non-linear static and non-linear dynamic behavior of wooden floors. Two modeling approaches were adopted: a refined model (referred to as M1 in the following) based on the software package TNO DIANA [1] was used to provide reliable data for the validation process of the simplified model (M2 in the following), developed by means of the software package SAP2000 [2]. M2 model was then implemented for the parametric studies presented in section 4. The use of M2 approach facilitates the analysis process, especially for non-linear dynamic simulations that require huge computational efforts. In addition, being SAP2000 a software package well-known to practitioners, modeling details/issues described herein may prove useful also for non-academic purposes.

2.1 Modeling approach 1 (M1)

Use of TNO DIANA enables modeling of floorboard interface phenomena (e.g. contact) by means of interface elements. Timber joists were modeled as linear-elastic frame elements, while curved shell elements and linear elastic orthotropic material properties [3] were adopted for flooring elements of both straight and diagonal floorboard layers. Floorboard interruptions were included in the model by assigning each floorboard to a separate mesh set. Line interface elements, characterized by no-tension behavior (zero stiffness in traction, rigid in compression), were generated at floorboard free edges. Point interface elements were implemented to reproduce nailed connections, whose load-slip response was considered as uncoupled for the two principal directions (i.e. parallel and perpendicular to grain of timber elements). Multiple shear plane fasteners (e.g. nails driven from the retrofit layer to the joists and passing through the original sheathing) were modeled by introducing a point interface element at each shear plane.

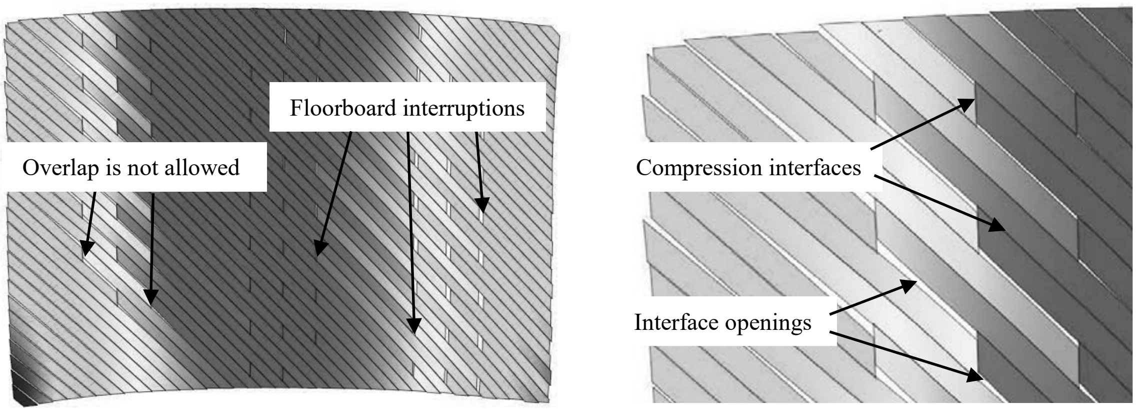

(a) Overall deformed shape *(b) Diaphragm corner close-up*

Figure 1: M1 model details, deformed shapes

2.2 Modeling approach 2 (M2)

Simplified modeling approach (M2) was developed by means of the software package SAP2000. Due to the nature of such finite element analysis tool, floorboard interface phenomena were modeled by adopting an alternative yet effective method. Timber components (joists and floorboards) were modeled as linear elastic orthotropic frame elements, while linear elastic isotropic frame elements were used to represent steel chords. Staggered floorboard layout was reproduced by physically dividing the frame elements. For both straight and diagonal sheathings, contact phenomenon was accounted for by interposing nonlinear *gap-links* between adjacent floorboards and oriented perpendicularly to them. Nailed connections were modeled by means of non-linear links with multilinear elastic behavior. Due to the uncoupled response of multilinear elastic links, the same backbone curve was assigned to each one of the principal shear directions (U2 and U3 Degrees of Freedom, DoFs). Flexural DoFs R2, R3 and U1 were fully restrained, while R1 (torsional) DoF was set free. As for M1, nails passing through multiple shear planes were modeled by means of a connector (multi-linear elastic link) per each shear plane. Eccentricities between fasteners and floorboard axes were reproduced by means of rigid links (6 DoFs fully restrained) connecting the multi-linear links to the frame element representing the floorboards (see **Figure 2**). The stiffening effect of additional nails (inserted to fix diagonal floorboards) on the straight sheathing-to-joist connection was also accounted for by connecting the representative multilinear links to the closest frame element via an additional rigid link.

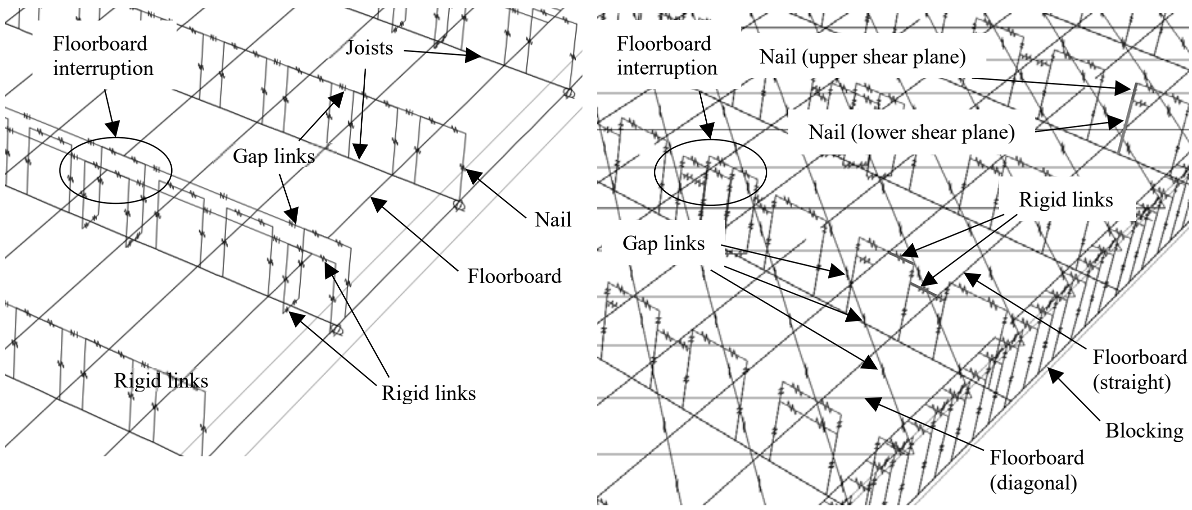

(a) Single straight sheathing *(b) Straight sheathing + diagonal overlay**

*For clarity, some of the elements were removed from view.

Figure 2: M2 model details

3 FINITE ELEMENT MODEL VALIDATION

Experimental tests that are available in literature on single straight sheathed, single diagonal sheathed diaphragms and single straight sheathed diaphragms retrofitted with diagonal board overlay were considered for the validatation of each modeling approach (**Table 1**).

3.1 Modeling approach 1 (M1)

Specimens “1A-PARA”, “1A-PERP”, “Diaphragm I” and “5x4” were reproduced by means of M1 approach (see **Table 1**). Geometrical and mechanical properties of the components were set consistently with the experimental data.

Table 1: Model validation process – reference diaphragm specimens

Reference	Specimen ID	Construction type	Load direction
Wilson et al. (2011) [4]	1A-PARA	Single straight	Parallel to joists
Wilson et al. (2011) [4]	1A-PERP	Single straight	Perpendicular to joists
ABK (1981) [5]	Diaphragm I	Single diagonal	Parallel to joists
Baldessari et al. (2008) [6]	5x4	Straight + diagonal	Parallel to joists
Ni et al. (2007) [7]	Wall 1	Single diagonal*	---
Ni et al. (2007) [7]	Wall 2	Single diagonal*	---
---	6x6	Single straight **	Parallel to joists
---	6x6	Straight + diagonal **	Parallel to joists

*Shear wall specimens **Diaphragm used for the parametric analyses

When available, experimental backbone curves were assigned to the multilinear elastic links representing nailed connections. In case that the experimental curves were not available, the McLain theory as improved by Pellicane [8] was implemented by considering the actual characteristics of both timber elements and fasteners. Validation results are summarized in **Figure 3**. In each case, comparisons between experimental data and model outputs were found to be satisfactory.

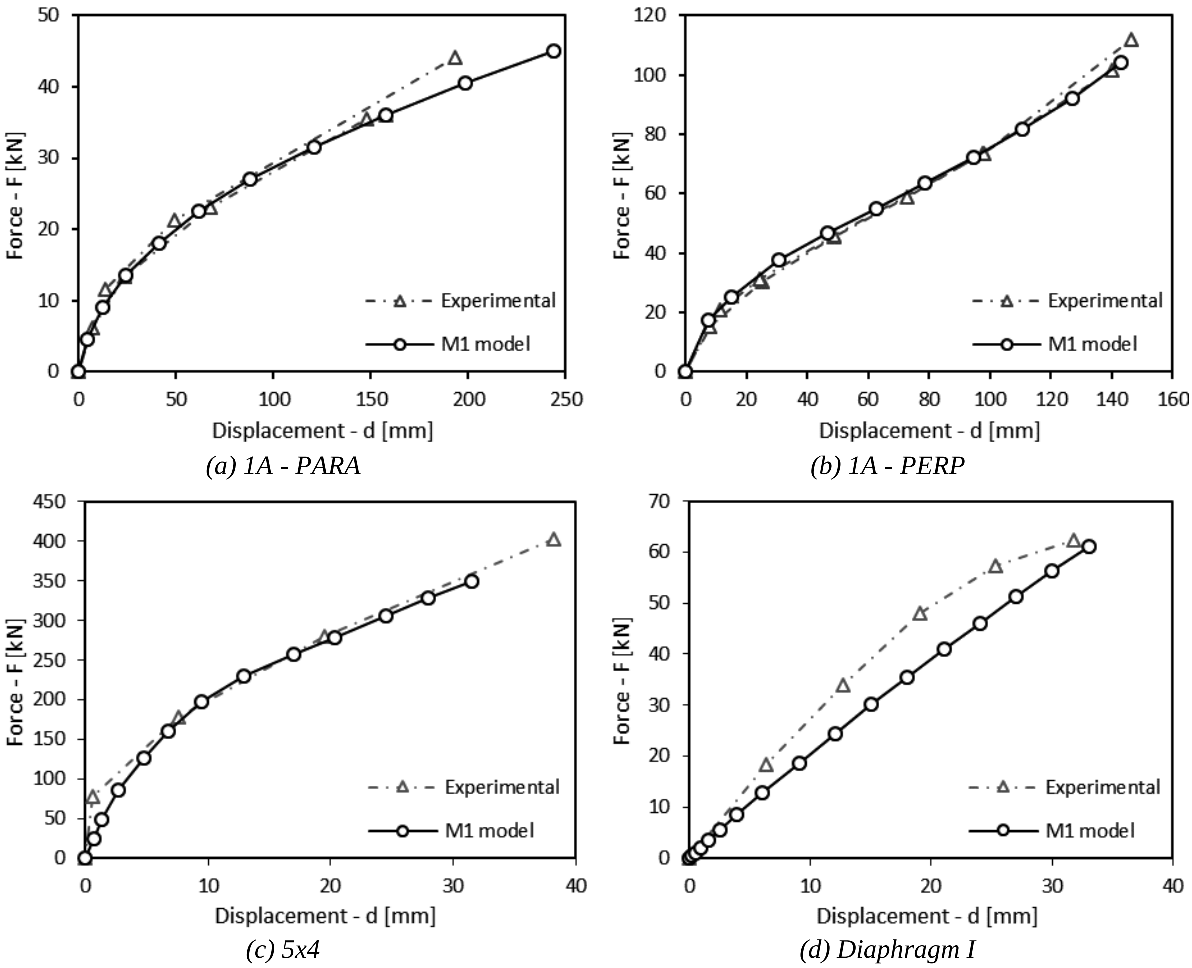

Figure 3: M1 model validation

3.2 Modeling approach 2 (M2)

Regarding M2 model, "1A-PARA", "1A-PERP", "Diaphragm I", "5x4", "Wall 1", "Wall 2" and "6x6" specimens were reproduced in the validation phase (see **Table 1**). As for M1, element geometrical properties were set in accordance with the test reports, while mechanical properties of timber were selected according to the wood species as recommended by [9]. If available, experimental backbone curves were assigned to multilinear elastic links representing nailed connections. If not, the McLain and Pellicane theory was used, as in the previous modelling approach.

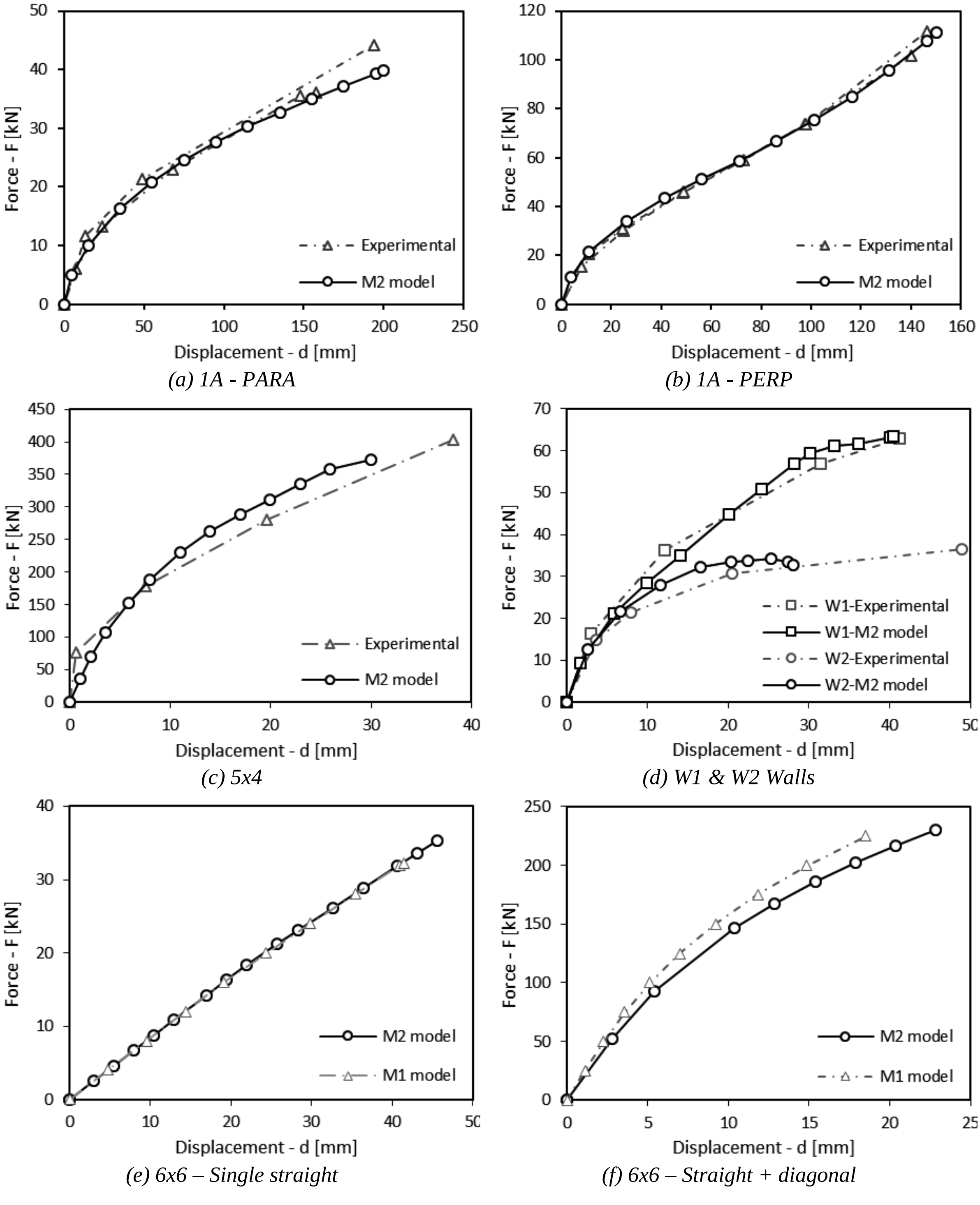

(a) 1A - PARA *(b) 1A - PERP*

(c) 5x4 *(d) W1 & W2 Walls*

(e) 6x6 – Single straight *(f) 6x6 – Straight + diagonal*

Figure 4: M2 model validation

In the case of the 6x6 tests, the same inputs were assigned to both M1 and M2 models. As highlighted in **Figure 4**, M2 model outputs were found to be consistent with experimental data and M1 model predictions for 6x6 diaphragm.

4 PARAMETRIC ANALYSES

4.1 Analyses program

A series of non-linear static and non-linear dynamic (time history) analyses were carried out on a diaphragm selection considered as representative of the European building heritage. Analyzed floors are listed in **Table 2**, where *L* refers to joist length, *B* is diaphragm dimension in the other direction and $\alpha=L/B$ is aspect ratio. Diaphragm penetrations were not considered.

Table 2: Geometrical details of diaphragms

Diaphragm ID	L *[m]*	B *[m]*	α
4x4	4	4	1
4x8	4	8	0.5
6x6	6	6	1
6x12	6	12	0.5

Geometrical and mechanical properties listed in **Table 3** were adopted for the components of every floor. The structural layout shown in **Figure 5** was assumed. Floorboards of the straight sheathing were connected to the joists by means of a nail couple at each floorboard to joist intersection. Diagonal boards were connected to the underlying joists (through the straight sheathing) by means of a nail couple at each intermediate support, while three nails were used at floorboard end supports. Timber blocking elements were interposed between joists at diaphragm ends. Blocking-to-joist connection was modeled as pinned (R2 and R3 DoFs fully released). Tension stiffness of the joist to blocking element connection was assumed equal to 500 *N/mm*. Such low stiffness was intended to reproduce the poor behavior expected from in-situ connections.

Table 3: Common features of FEM models

Feature	Value
Floorboard section	150 x 20 *mm*
Joist section	150 x 200 *mm*
Wood grade	C 24*
Joist spacing	500 *mm*
Nail couple spacing (diagonal)	130 *mm*
Nail couple spacing (straight)	100 *mm*
Seismic mass on diaphragms	230 kg/m^2
Seismic mass of masonry	2200 kg/m

*Timber grade according to [9]

Additional nailing was provided at diaphragm perimeter, connecting each diagonal floorboard to the joist or blocking element below (for the parallel and perpendicular to joists directions respectively). Restraints were assigned at joists level. Global beam-like rotation of diaphragm side ends was allowed. Diaphragm ends perpendicular to the loading direction were restrained in the out of plane direction only. For parallel to joists analyses forces were applied at joist ends and displacements were monitored with reference to the end section of the joist positioned at the diaphragm mid-span. For perpendicular to joists analyses, loads were applied to the side joist and axially rigid rods were added in order to distribute the forces among joists. Displacements were monitored with reference to the mid-span of the side joist. Parabolic load distributions were applied for each load direction, as suggested by [10]. Experimental backbone curve derived by Schiro et al. [11] was assigned to each principal shear direction of the non-linear links in order to reproduce an existing connection behavior. Further analyses were carried out by considering different curves (details are discussed in 4.2.2). For time history analyses, point masses were uniformly distributed on diaphragm surface (at sheathing level) to simulate the effect of seismic loading. Additional masses were placed at diaphragm edges to consider the inertia from the out-of-plane loaded masonry walls. Diaphragms were tested separately for each one of the two principal directions by applying two scaled sets of seven natural accelerograms taken from [12]. Every accelerogram is compatible with the elastic spectrum designated for the set. Two distinct peak ground accelerations were selected: 0.2g for one set and 0.4g for the other. Non-linear plastic pivot behavior was assigned to nail connections and a 5% viscous damping ratio was adopted as suggested by [13]. Results obtained by means of M2 model were then used to calibrate a simpler modeling approach based on linear elastic shell elements.

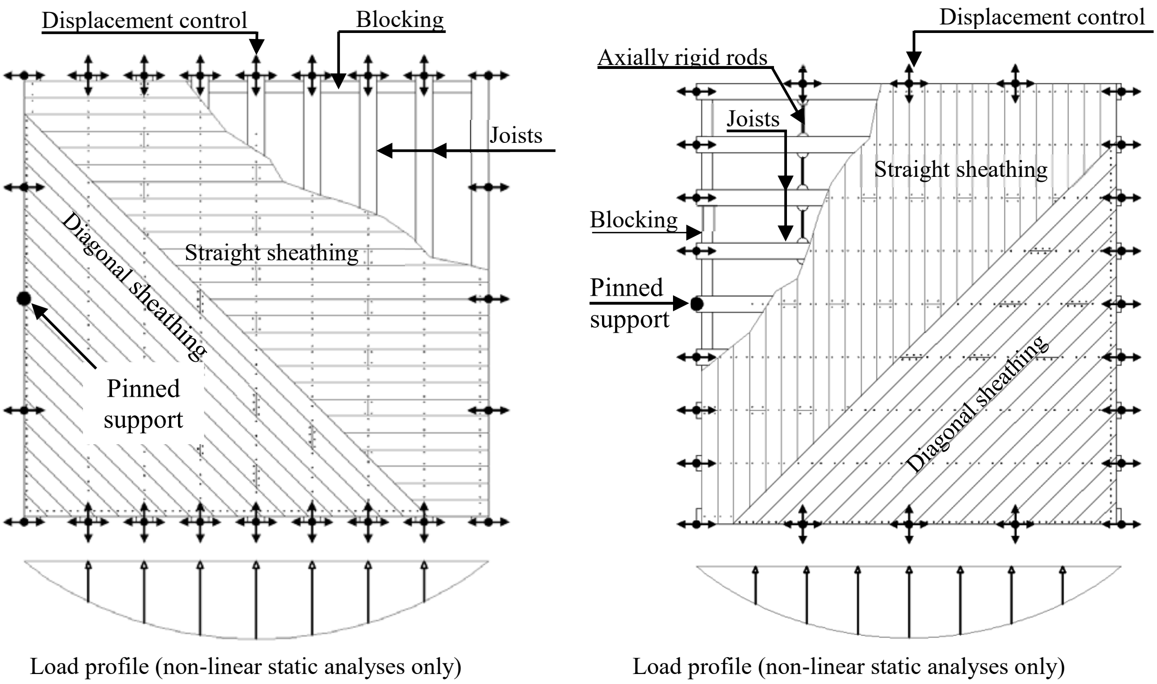

*(a) Parallel to joists** *(b) Perpendicular to joists**

*Arrows represents translational DoFs at the restrained joints.

Figure 5: Boundary conditions and load profiles

4.2 Non-linear static analyses

Non-linear static analyses were carried out on diaphragm specimens listed in **Table 2** by considering both as-built (single straight sheathing) and retrofitted configurations (diagonal sheathing overlay over straight sheathing). It was assumed that diaphragms behave as shear beams under parabolic loading (shear deformation only). Thus, results were compared in terms of equivalent shear stiffness values G_d which, because of the hypotheses, were evaluated via eq.(1). It is worth noting that the G_d values represent the equivalent stiffness of the structural assembly and do not correspond to any specific material property. Analysis results were compared for different levels of the in-plane drift dr, defined by means of eq.(2).

$$G_d = \frac{5 \cdot F \cdot s}{32 \cdot w \cdot \delta} \tag{1}$$

$$dr[\%] = 2 \cdot \frac{\delta}{s} (\cdot 100) \tag{2}$$

Where:

- F is the total load on the diaphragm;
- w and s are, respectively, the diaphragm width and the diaphragm span with respect to the loading direction;
- δ is the diaphragm mid-span displacement under load F;

Because no yield points could be clearly identified on the diaphragm backbone curves, it was decided to compare the results by referring to a 0.25% drift value, which is representative of the initial deformation stage.

4.2.1. Effectiveness of diagonal sheathing overlay

The effectiveness of diagonal sheathing overlays was investigated by comparing equivalent stiffness values of retrofitted units ($G_{d,RF}$) with the ones of as-built diaphragms in the single straight sheathing configuration ($G_{d,AsB}$). Results, obtained at a 0.25% drift level, are listed in **Table 4**.

Table 4: Equivalent stiffness comparison, dr = 0.25%, values in kN/m

	4x4	4x8	6x6	6x12
$G_{d,AsB}$	224.0	96.4	131.4	63.9
$G_{d,RF}$	2055.9	2350.2	2446.3	2357.5
Ratio	**9.2**	**24.4**	**18.6**	**36.9**

(a) Parallel to joists

	4x4	4x8	6x6	6x12
$G_{d,AsB}$	860.5	812.1	403.5	371.1
$G_{d,RF}$	2616.3	2752.3	2513.3	2627.5
Ratio	**3.0**	**3.4**	**6.2**	**7.1**

(b) Perpendicular to joists

It is evident that in each case the retrofit led to a considerable stiffness increment. In addition, stiffness values of retrofitted units do not seem to be significantly influenced by diaphragm geometrical details (e.g. aspect ratio α and scale factor L). Furthermore, retrofitted diaphragms were found to exhibit a substantially isotropic response, while as-built units are characterized by a marked orthotropy. In **Table 5** ratios between equivalent shear stiffness in perpendicular to joists ($G_{d,90}$) and parallel to joists ($G_{d,0}$) directions are listed.

Table 5: Orthotropy ratios $G_{d,90}/G_{d,0}$, dr = 0.25%

	As-built	Retrofitted
4x4	3.84	1.27
4x8	8.42	1.17
6x6	3.07	1.03
6x12	5.80	1.11

High values of orthotropy ratio resulting from as-built units are mainly related to the high in-plane bending stiffness of joists, which participate to diaphragm in-plane deflection with their in-plane (with respect to diaphragm) bending stiffness. If the sole bending stiffness of the joists is considered, the equivalent shear stiffness for perpendicular to joists loading (hereafter referred to as $G_{d,bend}$) can be roughly predicted by means of eq.(3).

$$G_{d,bend} = n_j \cdot 9.84 \cdot \frac{E \cdot J_2}{B \cdot L^2} \tag{3}$$

Where:

- n_j is the number of joists;
- E is the modulus of elasticity of the joists;
- J_2 is the joist moment of inertia about the vertical axis which, in this case, is the weak axis;
- B is the diaphragm width with respect to the loading direction;
- L is the joist length.

In **Table 6** a comparison between numerical stiffness values $G_{d,FEM}$ given by the analyses on as-built diaphragms and the equivalent shear stiffness $G_{d,bend}$ evaluated by means of eq.(3) is given. It is evident that, for each case, the numerically evaluated shear stiffness can be approximated by means of the $G_{d,bend}$ value without significant errors. Results are strictly connected to joist cross section geometry. It is straightforward to predict that for slender joists (e.g. joist sections common in North America and Northern Europe) diaphragm response might become isotropic due to a considerable loss of stiffness in the perpendicular to joists direction.

Table 6: As-built diaphragms - FEM vs bending model

	$G_{d,FEM}$	$G_{d,bend}$
4x4	860.47	856.20
4x8	812.08	808.63
6x6	403.49	366.44
6x12	371.06	352.34

4.2.2. Influence of connection backbone curves

As anticipated in 4.1, results summarized in **Table 4** were obtained by referring to the response of existing nailed connections for all the fasteners. This assumption may lead to stiffness underestimation in cases where existing timber elements are in a good state of preservation. In such a scenario, newly inserted nails would not be affected by timber degradation, responding similarly to new connections. Therefore, further analyses were carried out by modelling the response of newly inserted nails by using different backbone curves. It was decided to adopt the experimental data obtained by Wilson for the New-USA connection specimens [13], being the mechanical and geometrical features of tested specimens consistent with those adopted for the models (in terms of both timber density, component thickness and type of fasteners). Backbone curves thus determined were then assigned to new nails only, while existing connection (straight sheathing to joists) behavior was not modified. Results summarized in **Table 7** highlight the influence of such aspect on diaphragm equivalent shear stiffness in terms of ratios between new and vintage nail response assumptions. An average 37% stiffness increase was observed.

Table 7: Equivalent shear stiffness ratios, new connections/vintage connections

	$G_{d,0}$	$G_{d,90}$
4x4	1.42	1.36
4x8	1.37	1.38
6x6	1.40	1.38
6x12	1.29	1.33

4.3 Non-linear dynamic analyses

4.3.1. Effectiveness of diagonal sheathing overlay

Outcomes from non-linear dynamic analyses were found to be in accordance with what registered for non-linear static analyses. The significant stiffness increments highlighted in **Table 4** resulted in remarkably lower mid-span in-plane displacements and higher seismic loads. Comparisons between maximum mid-span displacements for the as-built ($\delta_{max,AsB}$) and retrofitted ($\delta_{max,RF}$) configurations are given in **Table 8**, while in **Table 9** seismic loads are compared. Being as-built diaphragms stiffness particularly small in parallel to joists direction, it was decided to compare the displacement results just to this load direction.

Table 8: Mean maximum mid-span displacements, parallel to joist analyses, values in mm

	4x4	4x8	6x6	6x12
$\delta_{max,AsB}$	43.4	114.6	95.4	192.5
$\delta_{max,RF}$	4.5	14.4	6.4	30.7
Ratio	**10.3%**	**12.5%**	**6.7%**	**15.9%**

(a) PGA=0.2g

	4x4	4x8	6x6	6x12
$\delta_{max,AsB}$	75.2	194.7	141.5	357.4
$\delta_{max,RF}$	6.5	24.0	9.2	51.9
Ratio	**8.6%**	**12.3%**	**6.5%**	**11.7%**

(b) PGA=0.4g

Table 9: Mean maximum seismic load on diaphragms, parallel to joists analyses, values in kN

	4x4	4x8	6x6	6x12
$F_{max,AsB}$	55.0	29.4	63.3	38.0
$F_{max,RF}$	61.8	110.8	109.6	177.7
Ratio	**1.1**	**3.8**	**1.7**	**4.7**

(a) PGA=0.2g

	4x4	4x8	6x6	6x12
$F_{max,AsB}$	83.6	50.1	88.5	57.3
$F_{max,RF}$	82.4	141.5	145.9	218.4
Ratio	**1.0**	**2.8**	**1.6**	**3.8**

(b) PGA=0.4g

4.3.2. Linear shell-based model calibration

Diaphragms were reproduced by means of linear elastic shell elements, to which the sole in-plane shear stiffness and viscous damping ratio were assigned and calibrated based on M2 model outcomes. Equivalent in-plane shear stiffness was evaluated by means of eq.(1) by considering seismic load and displacement values from M2 model. According to [10] a first attempt 10% value was assigned to viscous damping ratio. In some cases this value was increased up to a maximum of 15% to obtain more consistent results. From comparisons between shell and M2 models (see **Table 10** and **Table 11**) it can be noted that, in each case, results are in good accordance. It is worth noting that analyses times required for shell model are significantly lower compared to the ones of M2 (e.g. minutes vs hours). For such reason, calibrated shell model is particularly suitable for cases where the non-linear dynamic behavior of the entire building is to be modelled.

Table 10: M2 vs linear shell model - mean maximum mid-span displacement comparison (values in [mm])

	4x4		4x8		6x6		6x12	
	PARA	PERP	PARA	PERP	PARA	PERP	PARA	PERP
$\delta_{max,M2}$	4.5	4.5	14.4	2.9	6.4	8.0	30.7	3.4
$\delta_{max,shell}$	4.2	4.1	14.2	2.5	5.6	7.0	29.6	2.9
Error	**6.4%**	**7.2%**	**1.5%**	**13.4%**	**11.1%**	**13.2%**	**3.6%**	**14.8%**

(a) PGA=0.2g

	4x4		4x8		6x6		6x12	
	PARA	PERP	PARA	PERP	PARA	PERP	PARA	PERP
$\delta_{max,M2}$	6.5	6.2	24.0	4.8	9.2	13.2	51.9	5.0
$\delta_{max,shell}$	7.1	6.5	24.9	4.1	10.6	13.1	53.5	4.4
Error	**7.8%**	**5.7%**	**3.8%**	**14.5%**	**15.3%**	**0.8%**	**3.1%**	**10.8%**

(b) PGA=0.4g

Table 11: M2 vs linear shell model – mean maximum seismic load comparison (values in [kN])

	4x4		4x8		6x6		6x12	
	PARA	PERP	PARA	PERP	PARA	PERP	PARA	PERP
$F_{max,M2}$	61.8	61.5	110.8	64.9	109.6	93.1	177.7	142.6
$F_{max,shell}$	53.8	53.6	105.6	68.8	94.1	84.3	158.1	124.8
Error	**13.0%**	**12.9%**	**4.7%**	**6.0%**	**14.1%**	**9.4%**	**11.0%**	**12.5%**

(a) PGA=0.2g

	4x4		4x8		6x6		6x12	
	PARA	PERP	PARA	PERP	PARA	PERP	PARA	PERP
$F_{max,M2}$	82.4	80.4	141.5	101.4	145.9	139.2	218.4	199.9
$F_{max,shell}$	82.5	82.5	155.4	104.9	149.7	144.4	257.9	184.9
Error	**0.2%**	**2.5%**	**9.9%**	**3.4%**	**2.6%**	**3.7%**	**18.1%**	**7.5%**

(b) PGA=0.4g

5 CONCLUSIONS

In this paper two modeling approaches were proposed and validated on a wide number of experimental results found in literature, regarding different diaphragm constructions. Non-linear static and non-linear dynamic analyses were performed on a range of differently sized diaphragms to evaluate the effectiveness of a retrofit intervention based on a diagonal sheathing overlay. Non-linear static analyses highlighted a remarkable stiffness increment associated to the retrofit intervention. Non-linear dynamic analyses confirmed such trend as the significant reduction in the displacement demand was observed for the retrofitted specimens. A simplified model based on linear elastic shell elements was calibrated in terms of in-plane shear stiffness and viscous damping in order to obtain values consistent with the refined model for both seismic force and displacement demands.

ACKNOWLEDGEMENTS

ReWIS is acknowledged for the modelling assistance provided during the research.

REFERENCES

[1] TNO DIANA Release 9.5 “User’s Manual: analysis reference manual”, 2014.
[2] Computers and Structures Inc. (CSI), “CSI Analysis Reference Manual, SAP2000 v17”, Berkeley, California, 2014.
[3] New Zealand Standards, “NZS 3603:1993 - Timber Structures Standard”, Wellington, New Zealand, 1996.
[4] A. W. Wilson, P. J. H. Quenneville, J. M. Ingham, “In-plane orthotropic behavior of timber floor diaphragms in unreinforced masonry buildings” on *Journal of Structural Engineering,* 2013.
[5] M. S. Agbabian, S. B. Barnes, J. C. Kariotis (ABK) “Methodology for mitigation of seismic hazards in existing unreinforced masonry buildings: diaphragm testing”, National Science Foundation, El segundo, California, 1981.
[6] C. Baldessari, M. Piazza, R. Tomasi “The refurbishment of timber floors: characterization of the in-plane behavior” in *PROHITEC International Conference,* Taylor and Francis, Rome, Italy, 2008.
[7] C. Ni, E. Karacabeyli, “Performance of Shear Walls with Diagonal or Transverse Lumber Sheathing” on *Journal of Structural Engineering,* 2007.
[8] P. J. Pellicane, “Generalized Model for Lateral Load Slip of Nailed Joints” on *Journal of Materials in Civil Engineering,* 1991.

[9] European Committee for Standardization "EN338: Structural Timber – Strength Classes", CEN, Brussels, Belgium, 2009.
[10] American Society of Civil Engineers (ASCE), "ASCE/SEI 41-13, Seismic Evaluation and Retrofit of Existing Buildings", Reston, Virginia, 2013.
[11] G. Schiro, I. Giongo, J. M. Ingham, D. Dizhur, "Lateral performance of as-built and retrofitted timber diaphragm fastener connections", Journal of Materials in Civil Engineering, 2017 (submitted).
[12] P.E.E.R. Center, "PEER-NGA-West2 Ground Motion Database", Berkeley, California, USA.
[13] A. W. Wilson, "Seismic Assessment of Timber Floor Diaphragms in Unreinforced Masonry Buildings", PhD dissertation, The University of Auckland, Auckland, New Zealand, 2012.

SHATIS'17
4th International Conference on
Structural Health Assessment of Timber Structures
20-22 September 2017 Istanbul, Turkey

SINGLE STEP JOINT REINFORCED WITH SELF-TAPPING SCREWS: DESIGN MODELS COMPARED TO EXPERIMENTATION

Maxime Verbist[1], Jorge Branco[1], Elisa Poletti[1], Thierry Descamps[2], Paulo Lourenço[1]

[1] ISISE, University of Minho, Campus de Azurém, 4800-058, Guimarães, Portugal

[2] University of Mons, Rue du Joncquois 53, 7000, Mons, Belgium

Keywords: Timber, Single Step Joint, Reinforcement, Self-Tapping Screws, Design, Experimentation

Abstract

In the field of Built Heritage Restoration, Architects and Engineers have to work with old timber carpentry connections including badly preserved Single Step Joints (SSJ). Over time, this traditional connection may be subject to structural damage such as the shear crack or the compressive crushing. These both SSJ failure modes cause high deformation as well as the destabilization of timber elements inside the carpentry. As the Self-Tapping Screws (STS) are widespread used in new timber constructions, this modern intervention technique has then been opted for the reinforcement of damaged Single Step Joints.

Featured by a good workability and reduced visual impact on-site, the STS strengthening is however very limited in Built Heritage Restoration because no European standard details how to design and to reinforce effectively old timber connections with STS. As the Single Step Joint is structurally damaged by both failure modes, several STS strengthening strategies as well as the related design equations have been defined for the SSJ reinforcement with STS, based on recent research and European standards about "Common connections with STS". In order to check the reliability of these design equations, the SSJ specimens damaged by shear crack and by compressive crushing have been reinforced with STS and then tested under monotonic compression.

For each STS strengthening strategy related to both SSJ failure modes, the design equations of Single Step Joint reinforced with STS have been defined and then compared with experimental results. It has been shown that the strengthening strategies R1 and R2 tested are efficient, providing to the reinforced Single Step Joints higher load-bearing capacities than those from initial Single Step Joints before being damaged. Being restrictive, the related design equations should be optimized by taking into account the geometrical recommendations from European standards in order to prevent the shear block in Single Step Joints reinforced with STS.

1 INTRODUCTION

At the foot (also called "step") of old traditional and contemporary timber carpentries, the Single Step Joint (SSJ) has been used so far to connect the rafter with the tie beam, according to Yeomans [1]. As shown in Figure 1, Architects and Engineers may be confronted with this joint structurally damaged by two failure modes due to either poor design of the connection, or normal overloading in the rafter N_{rafter} over time, conform with Verbist et al. [2]. The former called "shear crack" occurs at the heel depth t_v along the shear length l_v in the tie beam, by causing the destabilization of the rafter along with the timber truss. The latter called "crushing" emerges at the front-notch surface inclined under an angle α_{front} to the normal of the tie beam grain, by generating high deformation inside the connection. From Branco et al. [3], traditional and modern intervention techniques exist in order to reinforce the old carpentry connections. For example, metal devices (i.e. stirrup, lateral bolts, binding strip, tension ties) are used to correct the structural disorders in the Single Step Joint [4].

In the last decades, the Self-Tapping Screws (STS) have stood out from other intervention techniques, for strengthening "Common connections" in timber engineering [5], [6]. Therefore, STS have been chosen to reinforce the Single Step Joints damaged by both failure modes, with respect to several strengthening strategies. The present paper then focuses on the determination of design models for the SSJ reinforcements with STS, through recommendations from European standards [7] or scientific reports [8] about timber "Common connections" reinforced with STS. In order to check the reliability of design equations and the efficiency of strengthening strategies, the experimentation on SSJ reinforcements with STS has been performed in the lab. The SSJ specimens previously damaged by the shear crack or the crushing from the experiments of Verbist et al. [2] have been reinforced with STS according to the strengthening strategies, and then tested under monotonic compression.

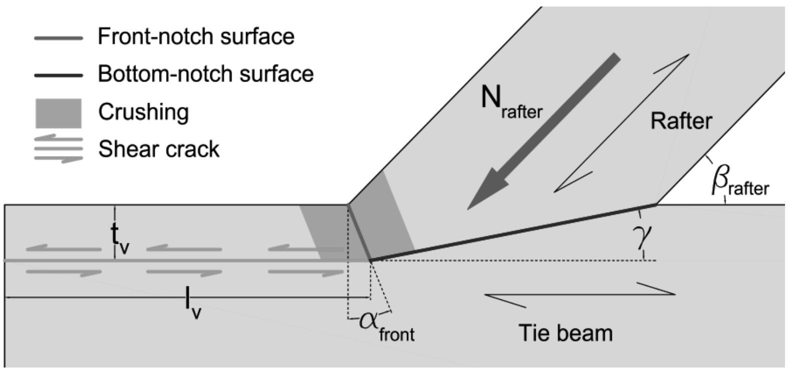

Figure 1: Failure modes and geometrical parameters of the Single Step Joint.

2 DESIGN MODELS

2.1 Self-Tapping Screws

Among the intervention techniques used for the joint strengthening, the Self-Tapping Screws (STS) stand out from the others in timber engineering, featuring many advantages: easy handling on-site, low cost, reduced visual impact, easy visual inspection, and high degree of reversibility. Because wood is an orthotropic material characterized by low tensile, compressive strength perpendicular to the grain as well as low shear strength parallel to the grain, the timber connections must be reinforced with STS in order to enhance their mechanical properties [6]. Thanks to their thread rod, these screws provide to the timber joint elements: lateral shear strength, high tensile strength, and withdrawal strength. Moreover, the reinforcement with STS may induce a ductile failure mode inside the connection according to Tomasi et al. [9], preventing the emergence of brittle failures as the shear crack in the Single Step Joint for example. In addition to the load-bearing capacity, the stiffness of the joint reinforced with STS has also been changed. As it has a direct impact on the internal forces distribution and deformation inside timber connections, the modified stiffness must be taken into account when strengthening traditional joints. Indeed, differential deformation and eccentricity forces may then occur in reinforced carpentry connections due to the modified stiffness, reducing the structural efficiency of the timber truss.

Different STS geometries do exist, varying according to their tip, head, and thread as shown in Figure 2. As these screws are called "self-tapping", the specific shape of the tip and the threaded rod ensure their easy implementation and maintenance time inside timber joint elements, by using only a screwdriver as work tool. Note that the pre-drilling in the connection is not required if the density of timber elements is not too high ($\rho_k \leq$500 kg/m^3) conform with Eurocode 5 [7]. However, the predrilled holes and proper spacing between screws ensure an accurate implementation of inclined STS, by decreasing the risk of timber splitting or shear bock inside timber joint elements at the headside screw [10].

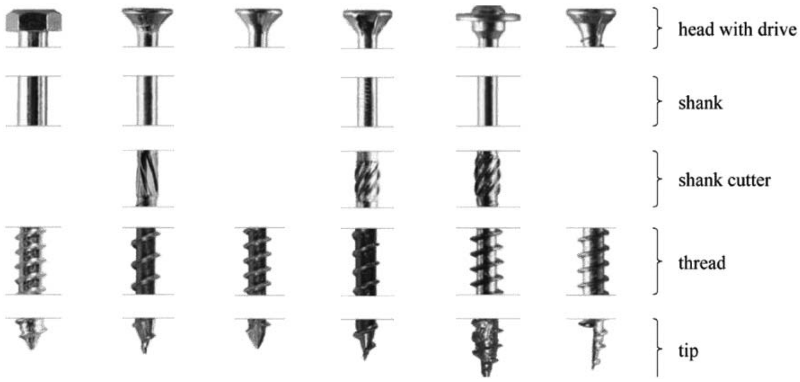

Figure 2: Types of STS with respect to the drill tip, the head and the thread, from Dietsch et al. [6].

2.2 Reinforcement strategies with STS

Because the shear crack splits the tie beam into two parts at the heel depth t_v along the shear length l_v, the upper side of the tie beam moves and causes the collapse of the rafter along with the timber truss, according to Verbist et al. [2]. As shown in Figure 3, the first strengthening strategy against the shear crack consists of positioning VGZ screws inclined under an angle α to the normal of the shear plane in the damaged tie beam. Because they are characterized by a whole threaded rod, these STS provide high withdrawal capacity so that the load-bearing capacity of the tie beam reinforced with VGZ screws increases with their inclination angle α. Because the heel depth t_v is very small in the Single Step Joint, the beneficial effect of the withdrawal capacity is however negligible on the load-bearing capacity from the reinforced tie beam, which depends only on the lateral shear strength of the screws. In order to conciliate the workability on-site with mechanical performances of optimal strengthening, the VGZ screws must be inclined under 45° angle to the normal of the shear plane. As illustrated in Figure 4, the second strengthening strategy against the shear crack deals with the perpendicular positioning of HBS screws to the shear plane in the tie beam. As the HBS screws have a smooth rod on the upper side of the tie beam, the related lateral shear strength is then higher than those from the VGZ screws. Moreover, the positioning of HBS screws in the tie beam is easier and faster because it does not require any guiding for the STS inclination on-site, unlike the VGZ screws. In addition to implement HBS screws perpendicularly to the shear plane in the tie beam, the third strengthening strategy also consists of positioning

VGZ screws at the bottom-notch surface, perpendicularly to the grain in the rafter as shown in Figure 5. Thereby, the load-bearing capacity from this SSJ reinforcement with STS should be higher than those from other two strengthening strategies in the tie beam.

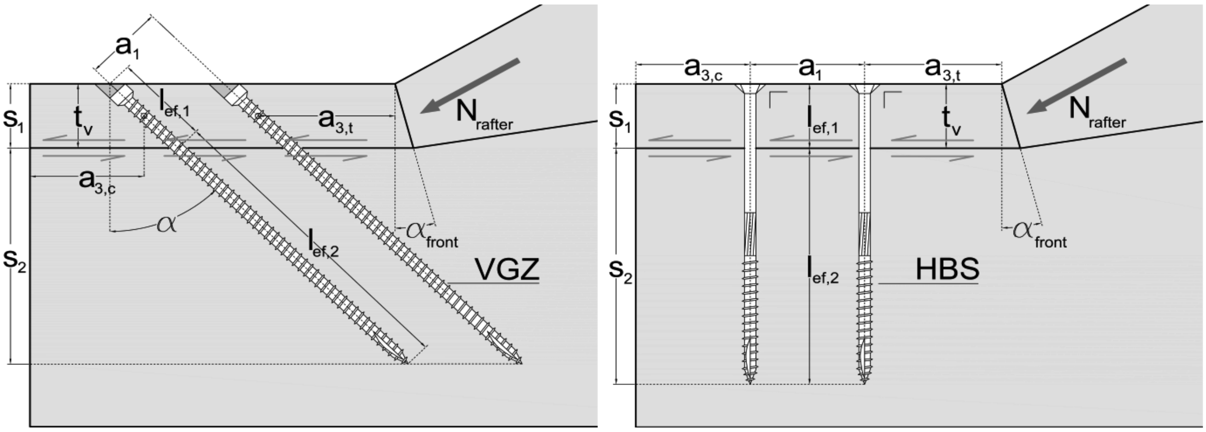

Figures 3 and 4: First reinforcement strategy with VGZ screws inclined under an angle α (left), the second one with HBS screws perpendicularly to the shear plane (right) in the tie beam.

In contrast to the shear crack, the crushing at the front-notch surface inclined under an angle α_{front} to the normal of the tie beam grain is a ductile failure mode causing serious deformation inside the connection, according to Verbist et al. [2]. Therefore, the strengthening strategy against the crushing then consists of positioning VGZ screws at the bottom-notch surface, perpendicularly to the grain in the rafter as shown in Figure 6. Because the shear crack could occur in the tie beam as the finale failure mode of the Single Step Joint, the first two strengthening strategies with STS might also be considered. Because the rafter end is brittle due to the heel geometry, the workers must pay attention not to position the screws too close to the front-notch surface in order to prevent timber splitting and shear block inside the joint. Note that all the geometrical parameters dealing with the distance, spacing, and dimensions of screws (s_1, s_2, $l_{ef,1}$, $l_{ef,2}$, a_1, $a_{3,c}$, $a_{3,t}$) in timber "Common connections" can be given by Eurocode 5 [7], the recommendations from Uibel et al. [10], or the European Technical Approval ETA-11/0030 [11].

2.3 Design equations of SSJ reinforced with STS

2.3.1 Reinforcement against the shear crack

In order to optimize the strengthening of Single Step Joint (SSJ) with Self-Tapping Screws (STS) against the shear crack, the HBS screws must be positioned perpendicularly to the shear plane at the heel depth t_v in the tie beam while the VGZ screws are implemented perpendicularly to the rafter grain at the bottom-notch surface. Nevertheless, the internal forces resolutions related to both reinforced tie beam and rafter make complex the determination of the rafter load-bearing capacity in SSJ, noted $N_{rafterR}$, which is the sum of the load-bearing capacities from the reinforced joints in the tie beam ($N_{rafterR,tb}$) and in the rafter ($N_{rafterR,bott}$). In order to simplify the equations, each connection reinforced with STS can be related to its own internal forces resolution independently to each other, as shown in Figure 5.

Because the high tightening of the Single Step Joint is ensured by the STS positioned in the rafter, the friction coefficient μ or the friction angle φ_{bott} (such as $\mu = \tan(\varphi_{bott})$) at the bottom-notch surface between the rafter and the tie beam must be taken into account in the design equations. With respect to the internal forces resolutions in SSJ, the rafter load-bearing capacity related to the reinforcement of the bottom-notch connection with STS (noted $N_{rafterR,bott}$) and the rafter load-bearing capacity related to the reinforcement of the shear plane with STS in the tie beam (noted $N_{rafterR,tb}$) can be both detailed below by the equations (1) and (2) respectively. Note that both quoted load-bearing capacities mainly depend on the rafter skew angle β_{rafter}.

$$N_{rafterR,bott} = \frac{R_{V,bott,Rk}}{\cos(\beta_{rafter} - \gamma) - \tan\varphi_{bott} . \sin(\beta_{rafter} - \gamma)} \quad (1)$$

$$N_{rafterR,tb} = \frac{R_{V,tb,Rk}}{\cos\beta_{rafter}} \quad (2)$$

As illustrated in Figure 5, the load-bearing capacity of the bottom-notch connection in the rafter ($R_{V,bott,Rk}$) and the load-bearing capacity of the shear plane in the tie beam ($R_{V,tb,Rk}$) both reinforced with STS can be determined either by Johansen's equations from Eurocode 5 [7], or by the modified Johansen's equations proposed by Blass and Bejtka [8]. By comparing both calculation methods with experimental results, Tomasi et al. [9] have concluded that Eurocode 5 underestimates the load-bearing capacity of timber "Common connections" reinforced with inclined STS, subjected to shear-(tension or compression) stress. Therefore, it is better to use the modified Johansen's equations from Blass and Bejtka [8] which are more reliable to design the SSJ reinforcement with inclined STS.

The tie beam and rafter reinforced with STS work together in order to counteract the rafter thrust inside the Single Step Joint. Besides, this SSJ strengthening with STS prevents the movement of the upper side element along the shear plane in the tie beam. Thereby, the design rafter load-bearing capacity for the SSJ reinforcement with STS against the shear crack, noted $N_{rafterR,Rd}$, must be checked by the design equation (3), such as the sum of $N_{rafterR,tb}$ and $N_{rafterR,bott}$, given by the previous equations (1) and (2). Conform with Eurocode 5 [7], the modification factor for duration of loading and moisture content k_{mod}, and the partial coefficient of the material γ_M are both included in the design equations to calculate the design value of timber mechanical properties.

$$N_{rafterR,Rd} \leq \frac{k_{mod}}{\gamma_M} . \left(N_{rafterR,tb} + N_{rafterR,bott}\right) \quad (3)$$

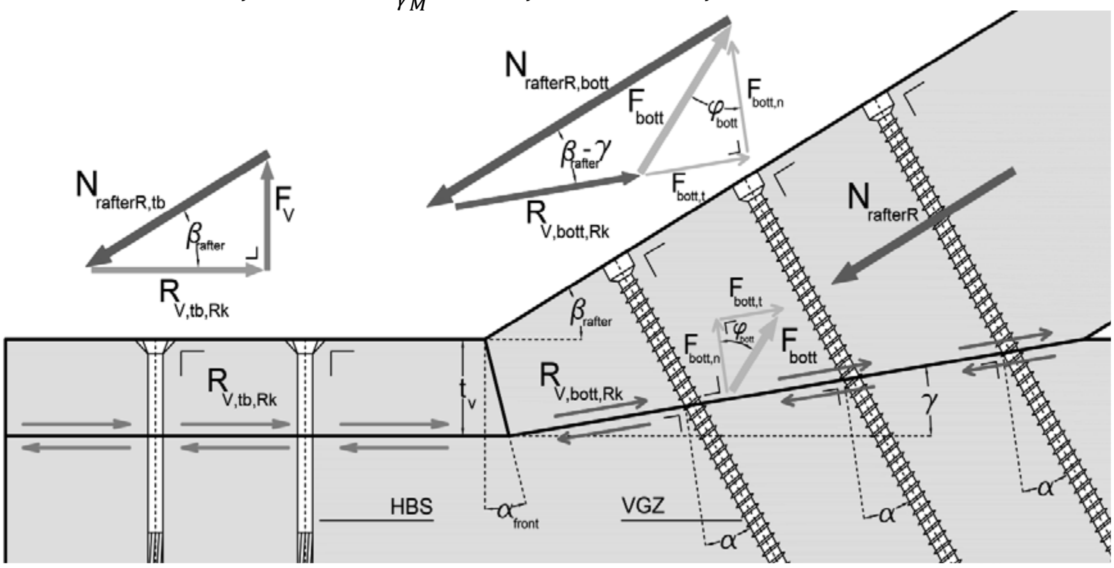

Figure 5: Internal forces resolutions inside the Single Step Joint reinforced with STS perpendicular to the grain in the tie beam (HBS) and in the rafter (VGZ).

2.3.2 Reinforcement against the crushing

The Self-Tapping Screws (STS) are positioned perpendicularly to the rafter edge at the bottom-notch surface, in order to reinforce the Single Step Joint (SSJ) against the crushing at the front-notch surface. As illustrated in Figure 6, the rafter load-bearing capacity related to the reinforcement of the bottom-notch connection ($N_{rafterR,bott}$) can also be calculated by the equation (1). Although most of the internal forces go from the rafter to the tie beam through the STS at the bottom-notch surface, the front-notch surface transfers the remaining forces between both timber SSJ elements. Therefore, the maximal compressive strength against the crushing at the front-notch surface from unreinforced SSJ must be taken into account in the design equations. The design rafter load-bearing capacity against the crushing at the front-notch surface ($N_{rafter,CFN,Rd}$) can be determined by the SSJ design equations from Verbist et al. [2]. Hence, the design rafter load-bearing capacity for the SSJ reinforcement with STS against the compressive crushing at the front-notch surface, noted $N_{rafterR,Rd}$, must be checked by the design equation (4) such as the sum of $N_{rafterR,bott}$ and $N_{rafter,CFN,Rd}$.

$$N_{rafterR,Rd} \leq \frac{k_{mod}}{\gamma_M} \cdot N_{rafterR,bott} + N_{rafter,CFN,Rd} \tag{4}$$

Because the shear crack may occur as the final failure mode of the Single Step Joint [2], the maximal shear strength along the shear length l_v at the heel depth t_v must then be considered in the unreinforced tie beam. The design rafter load-bearing capacity related to the shear crack in the tie beam ($N_{rafter,SC,Rd}$) can be determined by the SSJ design equation from Verbist et al. [2]. Hence, the design rafter load-bearing capacity for the SSJ reinforcement with STS against the crushing at the front-notch surface, noted $N_{rafterR,Rd}$, must be checked by the design equation (5) such as the sum of $N_{rafterR,bott}$ and $N_{rafter,SC,Rd}$. Thereby, the design equation (5) can predict the emergence of the shear crack according to this strengthening strategy when the tie beam is not reinforced with STS beforehand.

$$N_{rafterR,Rd} \leq \frac{k_{mod}}{\gamma_M} \cdot N_{rafterR,bott} + N_{rafter,SC,Rd} \tag{5}$$

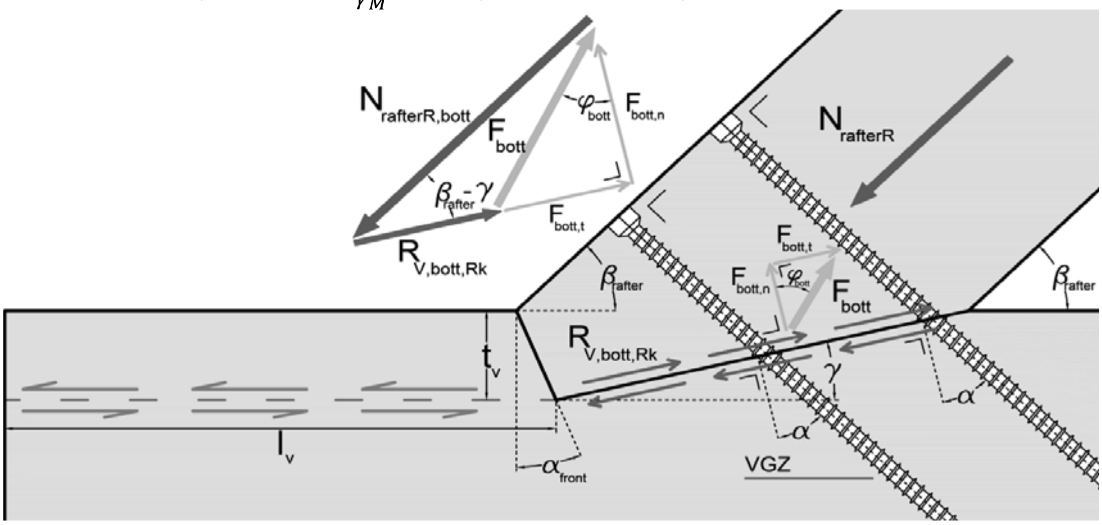

Figure 6 –Internal forces resolution in the Single Step Joint reinforced with STS (VGZ) perpendicular to the grain in the rafter.

3 EXPERIMENTATION

3.1 Experimental process and specimens

The experimentation firstly consists of strengthening with STS all the SSJ specimens which had been damaged by the shear crack in the tie beam or the crushing at the front-notch surface from the work of Verbist et al. [2]. As illustrated in Table 1, four strengthening strategies with STS have then been performed in the lab, under monotonic normal compression in the rafter, to obtain the mechanical behaviour of reinforced Single Step Joints. As shown in Figure 5, the first strengthening strategy labelled R1 consists of reinforcing SSJ specimens damaged by shear crack, with VGZ D9 200L (9 mm diameter and 200 mm length) screws positioned at the bottom-notch surface perpendicularly to the grain in the rafter, and with HBS D8 140L (8 mm diameter and 140 mm length) screws positioned perpendicularly to the grain in the tie beam. As illustrated in Figure 6, the second strengthening strategy labelled R2 deals with the reinforcement of SSJ specimens damaged by the crushing, only with VGZ D9 200L (9 mm diameter and 200 mm length) screws positioned at the bottom-notch surface perpendicularly to the grain in the rafter. To cause the possible emergence of the shear crack during the experimental tests, the tie beam has not been reinforced according to the second strengthening strategy with STS. For some SSJ specimens damaged by the shear crack, two other strengthening strategies with STS have been studied by focusing more in the tie beam. As shown in Figures 3 and 4, the third strengthening strategy labelled R3 consists of positioning VGZ D7 100L (7mm diameter and 100 mm length) screws under 45° angle to the grain in the tie beam while the fourth strengthening strategy labelled R4 is featured by HBS D8 140L (8 mm diameter and 140 mm length) screws positioned perpendicularly to the grain in the tie beam.

The labelling used for the SSJ specimens reinforced with STS can be described by illustrating the following example: GCTB_30^{o}_tv25_240SL_1_R1. The first term deals with the three SSJ families (i.e. GCID, GCPR, and GCPTB) from Verbist et al. [2]. The second term is related to the rafter skew angle β_{rafter} [°]. The third term determines the size of the heel depth t_v [mm] while the fourth one defines the size of the shear length l_v [mm]. The fifth term indicates the number of specimens related to the same SSJ geometrical configuration (i.e. GCTB_30^{o}_tv25_240SL) while the sixth one refers to the labelling of the four reinforcement strategies with STS detailed above.

3.2 Interpretation of results

As illustrated in Figure 7, the maximal normal loads in the rafter from SSJ specimens reinforced with STS only in the tie beam against the shear crack (i.e. the third and fourth strengthening strategies, “R3” and “R4”) are equivalent. Because the positioning of HBS screws makes the SSJ strengthening easier and faster on-site, it is then better to reinforce the tie beam with HBS screws, positioned perpendicularly to the grain, instead of the VGZ screws inclined under 45° to the tie beam grain which require some guiding. As shown in Figure 7, the maximal normal loads in the rafter related to these two strengthening strategies are much inferior to those from the unreinforced SSJ specimens before being damaged by the shear crack. Hence, the reinforcement of the tie beam with STS against the shear crack is not enough efficient to regain entirely the initial rafter load-bearing capacity of the joint. Therefore, the added STS positioning is required in the rafter to optimize the efficiency of the SSJ reinforcement with STS. As illustrated in Figure 7, the maximal normal loads in the rafter from the SSJ specimens reinforced with STS in both tie beam and rafter against the shear crack (i.e. the first strengthening strategy, “R1”) are indeed superior to those from the unreinforced SSJ specimens as well as those from the other two strengthening strategies (i.e. “R3” and “R4”).

As a reminder, the shear crack is a brittle failure mode occurring in the tie beam of unreinforced Single Step Joints [2]. As shown in Figures 7 and 8, the strengthening of both tie beam and rafter (i.e. first reinforcement strategy, “R1”) provides ductile failures to the Single Step Joint reinforced with STS, thanks to the emergence of plastic hinges in HBS and VGZ screws. Featured by high deformation of the joint according to maximal normal loads in the rafter, the ductile failures will always be appreciated for its safety in the strengthening of old timber trusses when the carpentry connections have already entailed some malfunctions. However, the shear block may occur like a timber splitting in the reinforced tie beam along STS rows, as illustrated in Figure 9 and in Table 1. As it causes irreversible damage in the tie beam and the drop of the normal load in the rafter, the shear block must then be prevented carefully by checking the geometrical recommendations about minimum spacing of STS with respect to the minimum thickness of timber joint elements [7], [10], [11]. If they are not checked, the SSJ reinforcement with STS against the shear crack becomes an irreversible intervention technique, by being in conflict with the principles of Built Heritage Restoration.

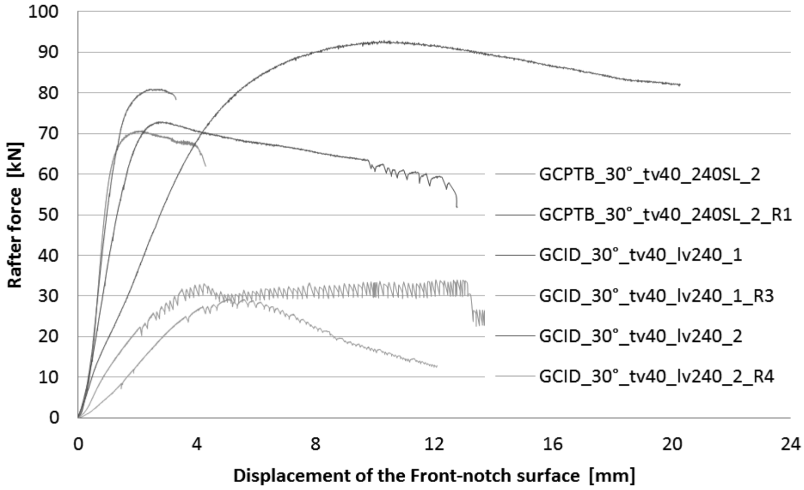

Figure 7: Normal load in the rafter (N_{rafter}) according to the displacement of the front-notch surface. Comparison between the unreinforced SSJ specimens 30°_tv40_240SL and the same ones reinforced against the shear crack with respect to three strengthening strategies (i.e. R1, R3, R4).

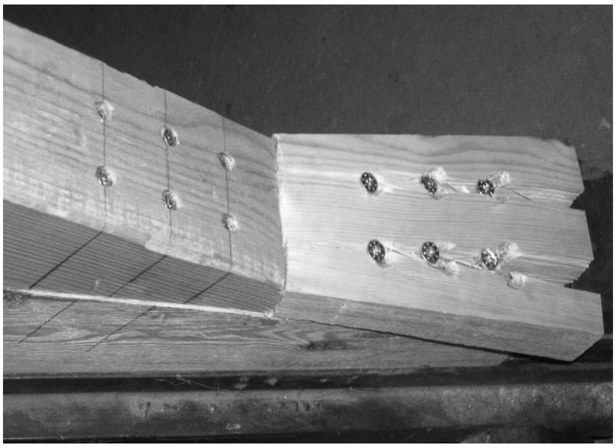

Figures 8 and 9: Plastic hinges in VGZ screws implemented inside the bottom joint between the rafter and the tie beam (left). Shear block in the upper side of the tie beam reinforced with HBS screws (right).

As shown in Figure 10 and in Table 1, the maximal normal loads in the rafter from the SSJ specimens reinforced with STS in the rafter against the crushing at the front-notch surface (i.e. the second strengthening strategy, “R2”) are much superior to those from the unreinforced SSJ specimens. As illustrated in Figure 10 for GCID_45°_tv30_240SL_1_R2, the mechanical behaviour of the reinforced SSJ specimens can ideally be characterized by a bi-linear curve divided into two steps, when the shear crack doesn’t occur as the final failure mode. The first step includes the linear compressive deformation until the maximum normal load in the rafter is reached. The second step is featured by a second linear compressive deformation along which the normal load in the rafter slightly increases according to high displacement of the front-notch surface due to the emergence of double plastic hinges in the VGZ screws (Figure 11). However, this ideal mechanical behaviour could not be encountered if the shear block occurs in the rafter, causing the slightly decrease of the normal load in the rafter according to high displacement of the front-notch surface. Moreover, the shear crack may emerge in the tie beam as the final failure mode in the Single Step Joint, causing the drop of the normal load in the rafter after reaching the maximal value as illustrated in Figure 10 and in Table 1. As shown in Figure 12, the shear crack may occur for the SSJ specimens damaged by the crushing if the tie beam has not been reinforced with STS beforehand.

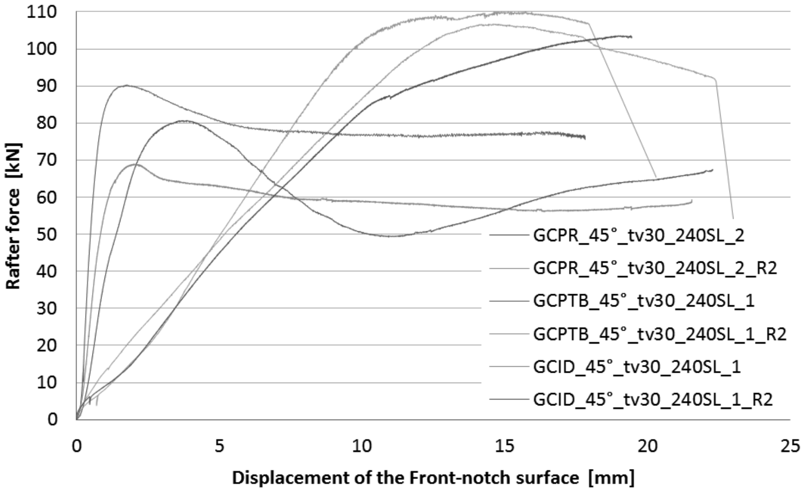

Figure 10 – Normal load in the rafter (N_{rafter}) according to the displacement of the front-notch surface. Comparison between the unreinforced specimens 45°_tv30_240SL, and the same ones reinforced against the crushing at the front-notch surface in respect with the strengthening strategy R2.

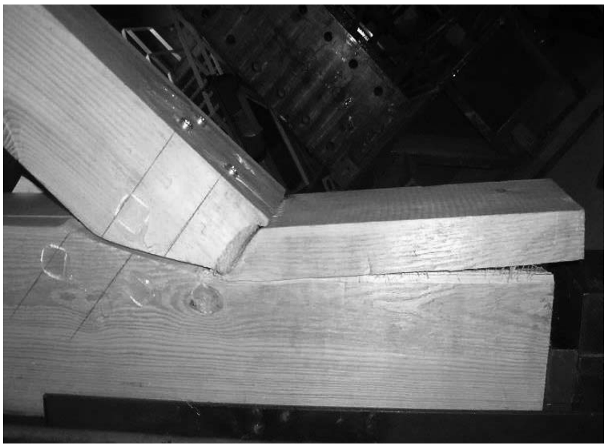

Figures 11 and 12 – Double plastic hinges in the VGZ screws implemented inside the bottom joint between the rafter and the tie beam (left). Shear crack at the heel depth along the grain in the tie beam (right).

3.3 Discussion about design equations

In order to check the reliability of design equations with respect to the strengthening strategies of damaged Single Step Joint (SSJ) with Self-Tapping Screws (STS), all the theoretical and experimental results have been compared to each other. As illustrated in Table 1, the maximum normal load in the rafter **(**$N_{\mathrm{rafterR,exp}}$) measured during the experimental campaign can be compared with the theoretical rafter load-bearing capacity ($N_{\mathrm{rafterR,theo}}$) calculated from the design equations. Concerning the theoretical calculations, the following parameters have been chosen for all the SSJ specimens tested: k_{mod}=0.9, and γ_M=1.3. Besides, the relative variation $\Delta_{\mathrm{rel,rafter}}$ [%] of maximum normal loads in the rafter between the experimental result and the theoretical value is determined for each SSJ specimen reinforced with STS: $\Delta_{\mathrm{rel,rafterR}}=100.(N_{rafterR,exp}-N_{rafterR,theo})/N_{rafterR,theo}$.

For the SSJ reinforcement with STS in the tie beam and in the rafter against the shear crack (i.e. first strengthening strategy, “R1”), the rafter load-bearing capacity predicted by the design equations (1)-(2)-(3) is too restrictive for all the SSJ specimens tested ($40.5\% \leq$

$\Delta_{\mathrm{rel,rafterR}} \leq 112.5\%$). Because the thickness of the headside timber element s_1 (i.e the heel depth t_v) is small in the Single Step Joint as shown in Figures 3 and 4, the geometrical recommendations [7], [10], [11] about the minimum spacing of STS with respect to the minimum thickness of timber joint elements have not been checked when strengthening the tie beam. Therefore, the shear block always occurs by generating irreversible damage in the reinforced tie beam. Because it also causes the drop of the rafter load-bearing capacity, the shear block should then be taken into account in the design equations for the SSJ reinforcement with STS. Note that the same observations and discussion can be made for the SSJ specimens reinforced with STS only in the tie beam against the shear crack (i.e. third and fourth strengthening strategies, “R3” and “R4”).

Table 1: Comparison between the experimental and theoretical results of the rafter load-bearing capacities from the SSJ specimens reinforced with STS.

Specimen labelling	$N_{\mathrm{rafterR,exp}}$ [kN]	$N_{\mathrm{rafterR,theo}}$ [kN]	$\Delta_{\mathrm{rel,rafterR}}$ [%]	Failure modes BR	AR
GCID_30°_tv25_240SL_1_R1	105	53	98	SC	SB
GCID_30°_tv25_240SL_2_R2	130	92	41	CFN	SC
GCID_30°_tv30_160SL_1_R1	102	48	112.5	SC	SB
GCID_30°_tv30_160SL_2_R1	87	48	81	SC	SB
GCID_30°_tv30_240SL_1_R2	120	100	20	CFN	SC
GCID_30°_tv30_240SL_2_R2	130	100	30	CFN	SC
GCID_30°_tv40_240SL_1_R3	29	21	38	SC	SB
GCID_30°_tv40_240SL_2_R4	30	18	66.5	SC	SB
GCID_45°_tv30_240SL_1_R2	100	89	12.5	CFN	CFN
GCID_45°_tv30_240SL_2_R2	92	89	3.5	CFN	CFN
GCPR_30°_tv25_240SL_1_R2	108	89	21.5	CFN	CFN
GCPR_30°_tv25_240SL_2_R2	130	89	46	CFN	CFN
GCPR_30°_tv30_160SL_1_R1	90	49	83.5	SC	SB
GCPR_30°_tv30_160SL_2_R1	74	49	51	SC	SB
GCPR_30°_tv30_240SL_1_R2	126	93	35.5	CFN	CFN
GCPR_30°_tv30_240SL_2_R1	76	54	40.5	SC	SB
GCPR_30°_tv40_240SL_1_R2	133	99	34	CFN	SC
GCPR_30°_tv40_240SL_2_R1	88	54	63	SC	SB
GCPR_45°_tv30_240SL_1_R1	100	53	88.5	SC	SB
GCPR_45°_tv30_240SL_2_R2	106	111	-4.5	CFN	SC
GCPTB_30°_tv25_240SL_1_R1	109	53	105.5	SC	SB
GCPTB_30°_tv25_240SL_2_R1	102	53	92.5	SC	SB
GCPTB_30°_tv30_160SL_1_R1	80	47	70	SC	SB
GCPTB_30°_tv30_160SL_2_R1	85	47	81	SC	SB
GCPTB_30°_tv30_240SL_1_R1	92	52	77	SC	SB
GCPTB_30°_tv30_240SL_2_R3	34	20	70	SC	SB
GCPTB_30°_tv40_240SL_1_R1	90	56	60.5	SC	SB
GCPTB_30°_tv40_240SL_2_R1	92	56	64.5	SC	SB
GCPTB_45°_tv30_240SL_1_R2	109	114	-4.5	CFN	SC
GCPTB_45°_tv30_240SL_2_R2	110	71	55	CFN	CFN

Legend:

BR – Before the Reinforcement; AR – After the Reinforcement; CFN - Crushing at the front-notch surface; SC - Shear crack; SB - Shear Block.

Concerning the SSJ reinforcement with STS in the rafter against the crushing at the front-notch surface (i.e. second strengthening strategy, “R2”), the design equation (4) is high reliable for calculating the rafter load-bearing capacity ($3.5\% \leq \Delta_{\mathrm{rel,rafterR}} \leq 46\%$). Thereby, this reinforcement strategy is optimal for the Single Step Joint damaged by crushing. However, the shear crack may occur as the final failure mode at the heel depth in the tie beam due to high crushing of the grain at the front-notch surface [2]. The design equation (5) is suitable ($-4.5\% \leq \Delta_{\mathrm{rel,rafterR}} \leq 41\%$) to predict the emergence of the shear crack for the SSJ specimens featured by rafter skew angles $\beta_{rafter} \leq 45°$. Hence, both equations (4) and (5) can be considered in determining the value range of rafter load-bearing capacity for the SSJ reinforcement with STS in the rafter against the crushing at the front-notch surface, by preventing the risk of shear crack appearance in the tie beam.

4 CONCLUSION

In the Built Heritage Restoration, the Single Step Joint (SSJ) may be subject to two failure modes (i.e. structural damage): the shear crack in the tie beam, and the crushing at the front-notch surface. Being a recent and attractive technique used in timber engineering, the Self-Tapping Screws (STS) have then been selected to reinforce the damaged Single Step Joint through four strengthening strategies proposed in the present paper. For each one, the geometrical configurations and the design equations of SSJ reinforcements with STS have been defined, based on the recommendations on timber “Common connections” strengthened with STS [7], [8]. The reliability of design equations, the emergence of failure modes as well as the efficiency of SSJ strengthening strategies with STS have then been checked by comparing the theoretical with experimental results.

Concerning the SSJ reinforcement with STS against the shear crack, the HBS screws positioning perpendicularly to the grain in the tie beam is more efficient than the VGZ screws inclined under 45° angle to the grain. Nevertheless, these two reinforcement strategies with STS in the tie beam are inadequate for regaining the initial strength of Single Step Joint. Therefore, the added STS positioning in the rafter is required because it ensures a higher load-bearing capacity than both reinforcement strategies only in the tie beam. The shear block may occur in the rafter and especially in the tie beam because the thickness of the upper part conditioned by the heel depth t_v is always small. As the shear block causes timber splitting inside the Single Step Joint, the reinforcement with STS becomes an irreversible intervention technique, in conflict with the principles of Built Heritage Restoration. To prevent the shear block, a compromise must then be found between the recommended minimum spacing of screws and the optimal load-bearing capacity of reinforced SSJ. The predrilled holes could also be a good alternative to restrain the emergence of shear block. Nevertheless, the design equations are too restrictive according to the experimental results and may be unsuitable to design the reinforcement with STS both in the rafter and tie beam against the shear crack. Further studies should focus on the optimization of these equations with Finite Element Models in order to determine the internal forces resolutions inside the reinforced SSJ.

For the SSJ reinforcement with STS against the crushing at the front-notch surface, the VGZ screws positioning perpendicularly to the rafter edge is very efficient because it provides higher load-bearing capacity than the maximal strength of the unreinforced SSJ specimens. Besides, the design equations are highly reliable to predict the maximal load-bearing capacity for the SSJ reinforcement with STS. Due to high crushing at the front-notch surface, the shear crack may occur as the final failure mode at the heel depth in the unreinforced tie beam. In order to prevent the shear crack, the related design equations are only suitable for SSJ specimens featured by low rafter skew angles $\beta_{rafter} \leq 45°$. Nevertheless, the prediction of the shear crack could be improved by investigating the influence of crushing at the front-notch surface on the shear stress distribution at the heel depth along the grain in the tie beam. Another alternative to prevent the shear crack could be to reinforce the tie beam with HBS perpendicularly to the grain.

Although the strengthening strategies with STS seem very efficient for the SSJ reinforcement, they should be improved by considering better the intervention principles with respect to the Built Heritage Restoration. If future results lead to decisive conclusions, the STS can be used to reinforce the damaged Single Step Joint.

5 REFERENCES

[1] Yeomans, D. (2003). "The Repair of Historic Timber Structures" – Editor, Thomas Telford Ldt, London – Published by ICE Publishing, United Kingdom – October 10, 2003

[2] Verbist, M., Branco, J.M., Poletti, E., Descamps, T., Lourenço, P.B. (2017). "Single Step Joint: overview of European standardized approaches and experimentations" – *Materials and Structures* – DOI 10.1617/s11527-017-1028-4 – March 27, 2017.

[3] Branco, J.M., Descamps, T. (2015). "Analysis and strengthening of carpentry joints" – *Construction and Building Materials* – Special Issue: Reinforcement of Timber Structures – Volume 97, 30 October 2015, Pp: 34-47.

[4] Parisi, M.A., Piazza, M. (2000). "Mechanics of plain and retrofitted traditional timber connections" – *Journal of Structural Engineering* – Asce, 126(12), Pp: 1395-1403.

[5] Bléron, L., Lathuillière, D., Descamps, T., Bocquet, J-F. (2015). "Reinforcement of connections with dowel-type fasteners" – Reinforcement of Timber Structures – A state-of-art report – Edited by Harte A. and Dietsch P. – Shaker Verlag Aachen, 2015..

[6] Dietsch, P., Reinhard, B. (2015). "Reinforcement with self-tapping screws and threaded rods" – Reinforcement of Timber Structures – A state-of-art report – Edited by Harte A. and Dietsch P. – Shaker Verlag Aachen, 2015.

[7] Eurocode 5, NBN EN 1995-1-1 (2004). "Design of timber structures – Part 1-1: General – Common rules and rules for buildings" – *CEN, European Standardization Institute* – Brussels, Belgium, November 2004.

[8] Blass, H. J., Bejtka, I. (2002). "Joints with inclined screws" – *International Council for research and Innovation in Building and Construction – Working Commission W18 – Timber Structures* – CIB W 18/35-7-5 – Kyoto, Japan, September 2002.

[9] Tomasi, R., Crosatti, A., Piazza, M. (2010). "Theoretical and experimental analysis of timber-to-timber joints connected with inclined screws" – *Construction and Building Materials* – Volume 24, Issue 9, Pages 1560-1571 – September 2010.

[10] Uibel,T., Blass, H. J. (2010). "A New Method to Determine Suitable Spacings and Distances for Self-tapping Screws" – *International Council for research and Innovation in Building and Construction – Working Commission W18 – Timber Structures* – New Zealand, August 2010.

[11] ETA-11/0030, European Technical Approval (2012). "Self-tapping screws for use in timber structures" – *EOTA (European Organization for Technical Approval)* – Rotho Blaas Self-tapping Screws, 2012.

AUTHOR INDEX

AUTHOR INDEX